



UNIVERSITAT
POLITÈCNICA
DE VALÈNCIA

CONTRIBUTION TO THE MODELIZATION,
ANALYTICAL AND NUMERICAL, OF
GENERATION AND PROPAGATION OF
VIBRATIONS ORIGINATED BY RAILWAY
TRAFFIC. ANALYSIS OF MITIGATION
PROPOSALS

Author: Julia Irene Real Herráiz

Director: Dra. Clara Zamorano Martín

Tutor: Dr. Joaquín Catalá Alís

Valencia, January 2015

The present Doctoral Thesis is presented as a **compendium** of the following publications:

Analysis of Vibrations in a Modeled Balasted Track Using Measured Rail Defects. J.I. Real, T. Asensio, L. Montalbán, C. Zamorano. Journal of Vibroengineering. June 2012. Volume 14. Issue 2. ISSN 1392-8716.

Study of Wave Barriers Design for the Mitigation of Railway Ground Vibrations. J.I. Real, A. Galisteo, T. Real, C. Zamorano. Journal of Vibroengineering. March 2012. Volume 14. Issue 1. ISSN 1392-8716.

Study of Railway Ground Vibrations caused by Rail Corrugation and Wheel Flat. J.I. Real, A. Galisteo, T. Asensio, L. Montalbán,. Journal of Vibroengineering. December 2012. Volume 14. Issue 4. ISSN 1392-8716.

Clara Zamorano Martín, as Director of the Doctoral Thesis named “Contribution to the modelization, analytical and numerical, of generation and propagation of vibrations originated by railway traffic. Analysis of mitigation proposals”

AUTHORIZES

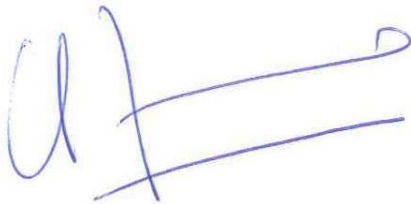
The presentation of de mentioned Thesis as Compendium of the following publications:

Analysis of Vibrations in a Modeled Balasted Track Using Measured Rail Defects. J.I. Real, T. Asensio, L. Montalbán, C. Zamorano. Journal of Vibroengineering. June 2012. Volume 14. Issue 2.

Study of Wave Barriers Design for the Mitigation of Railway Ground Vibrations. J.I. Real, A. Galisteo, T. Real, C. Zamorano. Journal of Vibroengineering. March 2012. Volume 14. Issue 1.

Study of Railway Ground Vibrations caused by Rail Corrugation and Wheel Flat. J.I. Real, A. Galisteo, T. Asensio, L. Montalbán,. Journal of Vibroengineering. December 2012. Volume 14. Issue 4.

In Valencia, January 10th 2014,



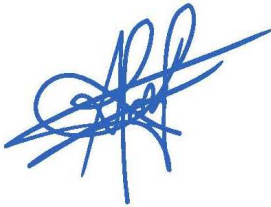
Clara Zamorano Martín

El Prof. Alfredo García García, como Coordinador del Programa de Doctorado en Ingeniería Civil y Urbanismo de la Universidad Politécnica de Valencia,

CERTIFICA:

Que en la reunión de la Comisión Académica del Programa de Doctorado en Ingeniería Civil y Urbanismo del día dieciocho de noviembre de dos mil trece, se acordó autorizar definitivamente a Dña. Julia I. Real la elaboración y presentación de su tesis doctoral como compendio de las tres publicaciones propuestas finalmente.

En Valencia, a 19 de diciembre de 2013

A handwritten signature in blue ink, appearing to be 'A. García', with a long horizontal stroke extending to the right.

Prof. Alfredo García

Dedication

To Clara Zamorano and Joaquín Catalá for their support.

Acknowledgments

To God, for helping me to bear bad times.

To my parents, for instilling in me the value of work.

To my husband and daughters, for enduring my absences.

To my friends (Laura and Teresa), for joining me on such an arduous path.

To all the co-workers who have been, are and will be in our working group, for their enthusiasm and effort.

To my tutor, Joaquín, for his confidence.

To my director, Clara, for EVERYTHING.

RESUMEN

La tesis doctoral recoge el análisis del fenómeno de generación de vibraciones en el contacto rueda-carril, transmisión de las mismas a través del paquete de vía y propagación en el terreno aledaño. Se ha prestado especial atención al tratamiento de distintas tipologías de cargas (carga cuasi-estática y carga debida a imperfecciones), diferentes configuraciones de vía (vía convencional y vía en placa tranviaria) y mecanismos de atenuación de la propagación de vibraciones (zanjas).

La investigación realizada se ha llevado a cabo implementando un modelo analítico y otro numérico. El primero de ellos se basa en la teoría de Timoshenko, para la modelización del carril, y en la ecuación de ondas para la modelización de la transmisión de vibraciones a través del paquete de vía. El segundo modelo se basa en el método de elementos finitos y se ha implementado en un software comercial.

Las modelizaciones realizadas con ambas metodologías han sido calibradas y validadas con datos reales obtenidos de sendas campañas experimentales. Este hecho dota de una gran robustez a los modelos y los configura como herramientas útiles para distinto tipo de simulaciones adicionales.

RESUM

La tesi doctoral recull l'anàlisi del fenomen de generació de vibracions en el contacte roda-carril, transmissió de les mateixes a través del paquet de via i propagació en el terreny limítrof. S'ha prestat especial atenció al tractament de distintes tipologies de càrregues (càrrega quasi-estàtica i càrrega deguda a imperfeccions), diferents configuracions de via (via convencional i via en placa tramviària) i mecanismes d'atenuació de la propagació de vibracions (rases).

La investigació realitzada s'ha dut a terme implementant un model analític i un altre numèric. El primer d'ells es basa en la teoria de Timoshenko, per a la modelització del carril, i en l'equació d'ones per a la modelització de la transmissió de vibracions a través del paquet de via. El segon model es basa en el mètode d'elements finits i s'ha implementat en un software comercial.

Les modelitzacions realitzades amb les dues metodologies han sigut calibrades i validades amb dades reals obtingudes de sengles campanyes experimentals. Aquest fet dota d'una gran robustesa als models i els configura com a ferramentes útils per a distintes tipus de simulacions addicionals.

ABSTRACT

The present PhD Thesis addresses the analysis of the vibration generation phenomenon in the wheel-rail contact, transmission across the track elements and propagation through the adjacent ground. Additionally, particular attention has been paid to the treatment of different types of loads (quasi-static load and load due to imperfections), different track configurations (ballasted track and tram slab track) and mechanisms of attenuation of vibration propagation (wave barriers) as well.

The research has been developed implementing an analytical model and a numerical model. The first one is based on the Timoshenko theory for the rail modeling, and on the wave equation to model the transmission of vibrations through the track. The second model is based on finite element method and has been implemented in a commercial software.

Models performed with both methodologies have been calibrated and validated with real data obtained from experimental campaigns. This fact provides great robustness to the models and configures them as helpful tools for different types of additional simulations.

INDEX

INTRODUCTION	3
OBJECTIVES	23
CHAPTER 1	27
CHAPTER 2	61
CHAPTER 3	95
GENERAL DISCUSSION	117
CONCLUSIONS	165
APPENDIX 1	169
APPENDIX 2	179
APPENDIX 3	189

INTRODUCTION

Introduction is structured in two parts: in the first one, the theoretical framework in which the following chapters are based is established. In the second one, the state of the art which constitutes the theoretical base to prepare the publications (included in the chapters 1-3) that represent the body of the Thesis is summarized.

Regarding the theoretical framework, the concept of rail vibration is certainly an application of the basic concept of mechanical vibration, in this case to the railway field. Despite its simplicity, it has been considered appropriate to outline the basic concepts of vibrations generation in the wheel-rail contact, transmission of the vibratory wave across the track (superstructure and infrastructure) and propagation of the wave through the adjacent ground. Finally, and although it is not part of the present PhD Thesis, it is worth mentioning the phenomenon of vibration reception in nearby buildings.

In relation with the state of the art, the most interesting contributions of scientific literature are collected and then divided in: experimental contributions and contributions related to the modeling (analytical and / or numerical of the phenomenon).

1. Theoretical Foundations of the generation-transmission-propagation phenomena of railway vibrations.

Traditionally, these three phenomena are studied uncoupled and subsequently assembled to provide an overview of the physical fact that happens since a railway vehicle passage generates an overload over the track until the vibration is perceived in nearby buildings.

1.1 Mechanisms of Generation of Railway Vibrations

Railway vibration is generated at the wheel-rail contact. From the contact point, the dynamic overloads transmitted by the train to the track appear in different forms, being the noise and the vibrations the most important.

Focusing on the vibrations, these are caused by different phenomena, either physiological or pathological. Moreover, some of them are connected to the vehicle and other relative to the track. In both cases, they can be grouped as follows:

1.1.1. Physiological causes

These phenomena are related to the train movement. There are two differentiated subgroups:

a. Causes due to Vehicle:

It is traditionally called "quasi-static load" and it is due to the constant movement of the train load along the track.

The characteristics of these vibrations are defined by three parameters: Structure of axles and bogies of the train composition, train speed and load transmitted per axle.

The first two parameters influence the frequency of vibration (specifically they correspond with a lower peak, linked to the distance between bogies; and a higher peak due to the distance between axles). The third parameter has influence in the amplitude of the excitation, being possible to assume that the value of this one is proportional to the value of the load.

b. Causes due to the Track:

In this case, all the "stiffness discontinuities" existing along the trace are taken into account, such as: separation of sleepers (this fact gives rise to the secondary bending of the rail), expansion joints, stiffness transition in infrastructure and / or superstructure and others.

The characteristics of these vibrations are defined by three parameters: train speed, load transmitted per axle and finally, several characteristic distances determined from the separation between sleepers, type and separation of the joints, values of railway stiffness and the variation of all of them along the trace.

Aspects related to the separation of sleepers, joints, stiffness variations and others in addition to the speed are responsible of the vibration frequency. The third, in addition to structural aspects of the first, is the cause of the excitation amplitude.

1.1.2. Pathological Causes:

These are anomalous phenomena associated with railway traffic. Two subgroups are distinguished:

a. Causes due to Vehicle:

These can be continuous wheel defects (which are classified into different groups depending on their wavelength) and discrete defects (such as wheel flats).

In both cases, the excitation frequency depends on the speed of the railway vehicle and on the wavelength of the defect, continuous or discrete. Consequently, if the wavelength decreases maintaining a constant speed, higher frequencies will be obtained. The amplitude of vibration is given by the load transmitted by the axle and the magnitude of the defect.

b. Causes due to the Track:

As in the previous case, these can be continuous defects on the rail (i.e. rail corrugation) or discrete. Continuous defects have been traditionally classified, although there are opposing opinions (Kalousek and Grassie), according to the document UIC 712. This document distinguishes between short wavelength corrugation (less than 80 mm) and long wavelength corrugation (between 200 and 300 mm). On the other hand, discrete rail defects comprise isolated skating, rail joint sinking, exfoliation and squat.

As in the previous case, the excitation frequency depends on the vehicle speed and on the wavelength of the defect (continuous or discrete). Moreover, the amplitude of vibration is given by the load transmitted by the axle and the magnitude of the defect.

Finally, the frequencies associated with pathological causes, are highly variable and complete the full range of the frequency spectrum, even high frequencies up to 2 kHz. The amplitudes are also diverse because as it has been mentioned, they depend on the magnitude of the defect that, indeed, can be very different from one case to another.

In addition, according to Jones et al. (1996, 2000) this type of vibrations can be perceived, not only close to the track, but also at some distance from the track. This author considers that from 10 meters in advance measured from the rail, in a ground type, only the vibration generated by this mechanism is able to be perceived.

1.2. Transmission Mechanisms of vibrations across the track

After the generation of vibrations in the wheel-rail contact, these are transmitted across the railway superstructure and infrastructure to the ground.

In the case of a ballasted track, the transmission of the vibrations follows the following order: rail - elastomer 1 – sleeper -elastomer 2 (optional) - ballast - platform. In the case of a slab track would be: rail – elastomer 1 - sleeper (optional) - elastomer 2 (optional) - concrete slab - elastomer 3 (optional) - platform.

The passage through various elements causes that the amplitude of vibration is steadily attenuated as it moves away from the wheel-rail contact. This fact occurs in most cases, except in those in which resonance phenomena occur.

It is worth noting that this decrease of the vibration amplitude is not homogeneous for all frequencies.

1.3. Propagation of vibrations through the ground

In this point, the necessary assumptions to address the submodel of vibration propagation through the ground are introduced. Firstly, Rayleigh waves will be defined and then the phenomena of wave propagation will be presented.

a. Wave types

Once the disturbance is generated in the wheel-rail contact, this is transmitted through the track elements and propagated through the ground in waves form. Due to its similarity to the seismic phenomenon, the theory of seismic waves is used to adequately explain the phenomenon.

This theory provides two types of waves: the compression waves (P) and shear waves (S), which can be further divided in horizontal shear waves (SH) and vertical shear waves (SV). The combination of P and SV waves on the ground surface originates the known as Rayleigh Waves that, due to its higher energy and its propagation near the free surface, have been usually regarded as the most important in the railway field.

Indeed, as Thompson (2009) demonstrates in *Railway Noise and Vibration. Mechanisms, modeling and means of control*, the maximum vertical displacement caused by the railway vibration is concentrated at a depth equal to 0.15 times the length of the Rayleigh wave. From this point, the vertical displacement clearly decreases until the depth equals the wavelength. This is an important aspect for the analysis of the applications referred in chapter 2 of the Thesis.

Finally, the propagation velocity of Rayleigh waves depends on soil mechanical parameters (density, elastic modulus and Poisson's ratio). This fact will be analyzed in the discussion of the second paper.

b. Propagation phenomena

Previously, it is necessary to define two basic concepts: wavefront and ray. Wavefront is the geometric locus of all points of the medium with the same vibration phase. Rays are understood as the lines perpendicular to the successive wavefronts.

The geometric shape of a wave front depends on the shape of the emitter focus and on the medium through it propagates. If the focus is isolated and the medium is isotropic, the successive wave fronts are concentric spheres whose common center is the source. In the case of considering a two-dimensional medium, wave fronts are concentric circles. If the emission focus has a linear shape, it is obtained a cylindrical wavefront that propagates along the radius of the cylinder axis. If the wave is examined in very remote points of the source, spheres wave fronts will have great radius and could be considered as planes.

Throughout the three introduced publications, the conditions of homogeneous and isotropic media are assumed, as a kind of simplification of the problem. In this assumption two facts are accomplished:

- The propagation velocity is the same at every point and in all directions. Hence, the gap between two wave surfaces must be the same between corresponding points.
- The rays are straight lines.

The concept of propagation was analyzed and characterized by Christian Huygens in the 17th century, and is basically defined as the advance of the wavefront in the medium. When the wave arrives at the surface of separation of two different medium (different propagation velocities), two important phenomena occur: part of the energy carried by the wave crosses to the second medium and part of the energy remains in the same medium. These phenomena are linked with some changes in the direction of propagation known as reflection (the wave does not change of medium) and refraction (the wave changes of medium).

The following diagram shows the parameters involved in the cited reflection and refraction phenomena.

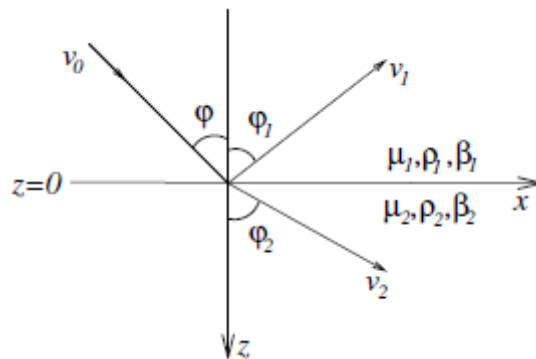


Fig. 1. Reflection and refraction phenomena.

Source: Thompson.

While frequencies remain constant (except specific cases where the critical angle is exceeded or in multilayered medium) the amplitudes of the reflected and refracted waves change with respect to the incident wave. The parameters that relate these amplitudes are respectively known as coefficient of reflection and coefficient of refraction.

One of the characteristics of Rayleigh waves is that a mode conversion may happen when waves incide on an interface between solids (as shown in the figure above). This conversion means that after the incidence of a P wave, the SV waves may appear reflected or refracted. In addition, an SV incident wave may generate P waves after inciding on the interface. The following figure outlines the phenomenon.

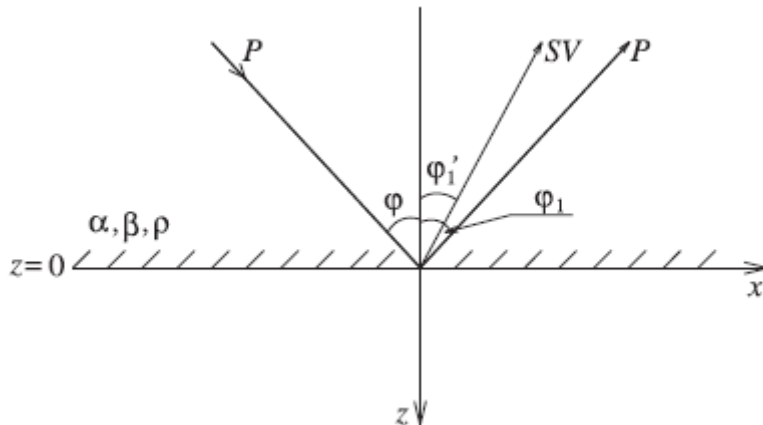


Figure 2. Conversion phenomenon of a P wave.
Source: Thompson.

2. State of Art

When collecting the main researches that have been studied for the development of this PhD Thesis, the contents will be divided in two different thematic blocks: experimental studies and mathematical models (analytical and numerical).

Regarding the experimental results, the main results are shown below in chronological order.

The first studies date from 1863 and were published by South. These studies contained the results of a measurement campaign of railway vibrations in the Watford tunnel (United Kingdom).

In 1901 Mallock carried out a measurements campaign of vibrations in the Central Station of London, and he analyzed how the vibrations were propagated until the houses close to the station.

In 1979, Dawn and Stanworth measured the level of vibrations generated by railway in a structure located about 40 meters away from the track. The data were analyzed trying to understand the effect that the speed and type of train have on the final results. Following these studies, in 1983 Dawn studied the influence of the sleeper separation on the generation of vibrations and how these, related to a particular frequency, propagate through the ground.

In 1983, Melke and Kramer measured in both infrastructure and superstructure the vibrations caused by the passage of a tram.

In 1996, Jones and Block measured the vibrations generated by the circulation of a freight train circulating at a specific speed in determinate elements of the superstructure and other points located at a certain distance from the track.

The development of high-speed trains caused some concern in the railway administrations responsible for the operation caused by the phenomenon of generation-transmission-propagation-reception of vibrations. Thus, in 1998 the Swedish railway administration organized an intensive measurement campaign of displacements, velocities and accelerations at different points of the railway superstructure and at

the surrounding soil during the passage of a conventional train at different speeds. It was demonstrated that at speeds below 70 km/h the response of the ground was similar to the static response, but when the speed exceeded the 200 km/h the characteristic magnitudes of vibration (displacement, velocity and acceleration) experienced an extraordinary increase. The reflections of this work were collected by Adolfson et al. in 1999.

Also in 1998, the Belgian railway company organized a set of tests to certify the high-speed line between Brussels and Paris. The accelerations of vibrations on different elements of the railway superstructure and different ground points were measured, even it was possible to collect data at 72 meters from the trace. The campaign was performed with a Thalys train circulating at speeds between 160 and 300 km/h. The results of the study showed the main track excitation frequencies. Also, the study showed that these frequencies corresponded to different genesis. In this case, as Degrande and Schillemans published in 2001, the vibrations were characterized by the circulation frequency of axles, circulation frequency of bogies and circulation frequency over sleepers.

In 2003 Schillemans studied the influence that the burying of the railway line of Antwerp would have on the neighboring buildings, given that in some cases the distance between the foundations of buildings and the infrastructure was only 4 meters. One of the most interesting results of this study was the recommendation to build a slab track on an elastomeric mat.

In 2005 Xia studied the vibrations generated by a train passage through a viaduct. They recorded data in different points of the ground and checked how the vibration accelerations level increased with the train speed and decreased as the measuring point was moved away from the piles of the infrastructure. Data in two buildings near the track were also collected, showing how the amplitude of vibrations increased with the number of floors of the building.

Finally, Auersch (2005) and (2006) participated in an intense vibration measurement campaign sponsored by the German railway administration. The accelerations of vibration in vehicle, track and ground were measured with different railway trains circulating at

speeds between 100 and 300 k/h. One of the main conclusions drawn is that the effect of the quasi-static load was only important in measurements made on track and in its immediate surroundings.

Regarding the modeling of the phenomenon of generation-transmission-propagation of railway vibrations, the most interesting researches are introduced.

The first models date from 1976 and were performed by Gutowski and Dym. They focused on two specific aspects: to model the train's load, either as a punctual load or as loads train, and to study the ground damping phenomena. They concluded that in the case of modeling the train as a punctual load, the ground damping is due to its own internal damping, being possible to neglect the geometric damping.

The main conclusion of Gutowski and Dym was refuted in 1979 by Verhas, who compared the results obtained using both load models. He concluded that to accurately obtain the vibrations level induced by the passage of a train, it has to be taken into account the two damping mechanisms cited.

In 1979, Kurzweil published an analytical expression to obtain the level of vibration caused by the passage of a train in the vicinity of a metropolitan tunnel.

Since 1995, concurring with the commissioning of various high-speed railway lines, different works about analytical, semi-analytical and numerical modeling of these phenomena began to be published.

One of the most interesting contributions is that from Krylov et al (2000). They focused their work on the characterization of the vibration source. They presented an analytical model to represent the quasi-static part of the force transmitted by the vehicle to the track. Thus, the contribution of potential irregularities related to track and vehicle was ignored. The authors worked with a train which moved at a constant and known speed. In this context, the rail is modeled as an Euler-Bernoulli beam resting on an elastic halfspace.

Dieterman and Metrikine (1996) and Metrikine and Popp (2000) modified the model of Krylov et al. They assume that in the longitudinal direction to the track, the track geometry remains

constant. Hence, the Fourier transform can be performed to rise and solve the problem formulated in frequency domain and wavenumber. Moreover, they carried out two important simplifications. On the one hand, a uniform distribution of normal stresses along the section of track is assumed and, on the other hand, it is only required compatibility of displacements in the midline of the track. One limitation of this approach (as revealed later by Steenbergen and Metrikine, 2007) is that it was only valid for low circulation speeds (below 70 km/h).

In 1996 Jones et al. developed a model of vibration generation that allows distinguishing among vibrations generated by the quasi-static load (similar to the work of Krylov) and vibrations due to the irregularities of rail and / or wheels.

Regarding the study of dynamic overloads, Valerio and Cuéllar (2009) analyzed its influence not only in the generation of vibrations but also, indirectly, in the fatigue of various elements of a high speed railway line with mixed traffic.

In 2004, Jones and Sheng presented a model which included the load treatment method developed by Jones in 1996. In this work, the track was modeled using beam and spring elements coupled to a model that represents the dynamic behavior of a multilayered ground. These authors, in several times, carried out a validation of the proposed model with experimental data thanks to an exhaustive data gathering campaign. One of the main conclusions deals with the relation between the train speed and the Rayleigh waves propagation velocity through the ground: when the train speed is far greater than the velocity of Rayleigh waves through the ground, the vibrations due to the irregularities of rail and wheels are similar, in terms of magnitude, to the vibrations due to the quasi-static load effect. However, when the train speed is similar to the velocity of Rayleigh waves, the predominant vibrations through the ground are those due to the passage of the quasi-static load.

The study of dynamic overloads generated by pathologies such as rail corrugation and complicated points (curves, turnouts, etc.) was analyzed by Egaña et al. (2002), from the point of view of their influence on the genesis of vibrations.

Auersch in 2005 studied the vibratory phenomenon in the Germany high-speed lines, as well as in an experimental manner with a model that assumes the interaction vehicle-track-ground. The vehicle is represented by a multi-body model; the railway superstructure is modeled using the finite element method and the ground is modeled using a boundary element model in frequency and wavenumber domain.

In 2006 Karlström and Boström, presented a numerical model (finite element method) of generation and propagation of vibrations generated by a high-speed train using special boundaries to satisfy the condition of radiation.

Since 2007, Galvín et al. work on the experimental and numerical studies of vibrations caused by the passage of high-speed trains through the ground and nearby structures using boundary element models in time domain. Furthermore, they have also carried out complete 3D finite element models of vehicle-track-ground interaction and, in 2014, a 3D model in time domain based on Green's functions that take into account the ground-structure interaction has been presented.

Koziol et al. (2008 y 2009) analyzes the generation-transmission-propagation of railway vibrations with Wavelet techniques for the analysis of these phenomena, even considering multilayered grounds with high circulation speeds.

Real et al. (2011) developed an analytical model, which is the precursor of one of the articles contained in this PhD Thesis, whose main contribution, in addition to the treatment of loads, is the modeling of the rail as a Timoshenko beam, instead of employing the Euler-Bernoulli model.

In view of the above, this document introduces three publications that present both models, analytical and numerical, and may be useful to explain the whole phenomenon of generation – transmission - propagation of the vibration generated in the wheel-rail contact. In every case, real data have been used, being very useful to calibrate and validate the presented models.

References

Adolfsson, K., Andréasson, B., Bengtson, P. E., Bodare, A., Madshus, C., Massarch, R., y otros. (1999). *High speed lines on soft ground. Evaluation and analyses of measurements from the West Coast Line.* Banverket, Sweden.

Auersch, L. (2006). Ground vibrations due to railway traffic. The calculation of the effects of moving static loads and their experimental verification. *Journal of Sound and Vibration*, 293 (3), 599-610.

Auersch, L. (2008). The effect of critically moving loads on the vibrations of soft soils and isolated railway tracks. *Journal of Sound and Vibration*, 310 (3), 587-607.

Auersch, L. (2005). The excitation of ground vibration by rail traffic: theory of vehicle-track-soil interaction and measurements of high-speed lines. *Journal of Sound and Vibration*, 284 (1), 103-132.

Auersch, L. (2010). Theoretical and experimental excitation force spectra for railway induced ground vibration-vehicle-track soil interaction, irregularities and soil measurements. *Vehicle System Dynamics*, 48 (2), 235-261.

Auersch, L. (2012). Train induced ground vibrations: different amplitude-speed relation for two layered soils. *Proceedings of the Institution of Mechanical Engineers, Part F: Journal of Rail and Rapid Transit*, 226 (5), 469-488.

Auersch, L., & Said, S. (2010). Attenuation of ground vibrations due to the different technical sources. *Earthquake Engineering and Engineering Vibration*, 9 (3), 337-344.

Cámara, J. L., Cuéllar, V., & González, P. (2012). Análisis estadístico de cargas dinámicas para el estudio de la fatiga de una línea de alta velocidad con tráfico mixto. *Ingeniería Civil*, 165, 115-122.

Dawn, T. M. (1983). Ground vibrations from heavy freight trains. *Journal of sound and vibration*, 87 (2), 351-356.

Dawn, T. M., & Stanworth, C. G. (1979). Ground vibrations from passing trains. *Journal of sound and vibration*, 66 (3), 355-362.

- Degrande, G., & Schillemans, L. (2001). Free field vibrations during the passage of a Thalys HST at variable speed. *Journal of Sound and Vibration*, 247 (1), 131-144.
- Dieterman, H. A., & Metrikine, A. (1996). The equivalent stiffness of a halfspace interacting with a beam. Critical velocities of a moving load along the beam. *EUROPEAN JOURNAL OF MECHANICS SERIES A SOLIDS*, 15, 67-90.
- Egaña, J. I., Viñolas, J., & Gil-Negrete, N. (2002). Modelización y estudio del desgaste ondulatorio de carril. *Anales de la ingeniería mecánica*, 14 (1), 223-227.
- Galvín, P., & Romero, A. (2014). A 3D time domain numerical model based on half-space Green's function for soil-structure interaction analysis. *Computational Mechanics*, 53 (5), 1073-1085.
- Galvin, P., François, S., Schevenels, M., Bongini, E., Degrande, G., & Lombaert, G. (2010). A 2.5D coupled FE-BE model for prediction of railway induced vibrations. *Soil Dynamics and Earthquake Engineering*, 30 (12), 1500-1512.
- Galvín, P., Romero, A., & Domínguez, J. (2010). Vibrations induced by HST passage on ballast and non-ballast tracks. *Soil Dynamics and Earthquake Engineering*, 30 (9), 862-873.
- Gutowski, T. G., & Dym, C. L. (1976). Propagation of ground vibration: a review. *Journal of Sound and Vibration*, 49 (2), 179-193.
- Jones, C. J., & Block, J. R. (1996). Prediction of ground vibration from freight trains. *Journal of Sound and Vibration*, 193 (1), 205-213.
- Jones, C. J., Sheng, X., & Petyt, M. (2000). Simulations of ground vibration from a moving harmonic load on a railway track. *Journal of Sound and Vibration*, 231 (3), 739-751.
- Karlström, A., & Boström, A. (2006). An analytical model for train-induced ground vibrations from railways. *Journal of Sound and Vibration*, 292 (1), 221-241.
- Kozioł, P. (2009). Wavelet analysis of multilayered ground vibrations as a result of high speed trains. *Proceedings of the Twelfth*

International Conference on Civil, Structural and Environmental Engineering Computing. Funchal, Madeira.

Koziol, P., Mares, C., & Esat, I. (2008). Wavelet approach to vibratory analysis of surface due to a load moving in the layer. *International Journal of Solids and Structures*, 45 (7), 2140-2159.

Krylov, V. V. (2001). Generation of ground vibration boom by high-speed trains, in Noise and Vibration from High-Speed Trains. *Noise and vibration from high-speed trains* , 251-283.

Krylov, V. V. (1995). Generation of ground vibrations by superfast trains. *Applied Acoustics*, 44 (2), 149-164.

Krylov, V. V. (1994). On the theory of railway-induced ground vibrations. *Le Journal de Physique IV*, 4 (C5), 769-772.

Krylov, V. V. (1996). Vibrational impact of high-speed trains. Effect of track dynamics. *The Journal of the Acoustical Society of America*, 100 (5), 3121-3134.

Krylov, V. V., & Ferguson, C. C. (1995). Recent progress in the theory of railway-generated ground vibrations. *Proceedings of the Institute of Acoustics* .

Krylov, V. V., Dawson, A. R., Heelis, M. E., & Collop, A. C. (2000). Rail movement and ground waves caused by high-speed trains approaching track-soil critical velocities. *Proceedings of the Institution of Mechanical Engineers, Part F: Journal of Rail and Rapid Transit*, 214 (2), 107-116.

Krylov, V., & Ferguson, C. (1994). Calculation of low-frequency ground vibrations from railway trains. *Applied Acoustics*, 42 (3), 199-213.

Kurzweil, L. G. (1979). Ground-borne noise and vibration from underground rail systems. *Journal of sound and vibration*, 66 (3), 363-370.

Lagos, R. F., Alonso, A., Vinolas, J., & Pérez, X. (2012). Rail vehicle passing through a turnout: analysis of different turnout designs and

wheel profiles. *Proceedings of the Institution of Mechanical Engineers, Part F: Journal of Rail and Rapid Transit*.

Lang, J. (1988). Ground-borne vibrations caused by trams, and control measures. *Journal of Sound and Vibration*, 120 (2), 407-412.

Lombaert, G., Degrande, G., Kogut, J., & François, S. (2006). The experimental validation of a numerical model for the prediction of railway induced vibrations. *Journal of Sound and Vibration*, 297 (3), 512-535.

Madshus, C., & Kaynia, A. M. (2000). High-Speed Railway Lines On Soft Ground: Dynamic Behaviour At Critical Train Speed. *Journal of Sound and Vibration*, 231 (3), 689-701.

Madshus, C., Bessason, B., & Hårvik, L. (1996). Prediction model for low frequency vibration from high speed railways on soft ground. *Journal of sound and vibration*, 193 (1), 195-203.

Melke, J. (1988). Noise and vibration from underground railway lines: Proposals for a prediction procedure. *Journal of Sound and Vibration*, 120 (2), 391-406.

Melke, J., & Kramer, S. (1983). Diagnostic methods in the control of railway noise and vibration. *Journal of Sound and Vibration*, 87 (2), 377-386.

Metrikine, A. V., & Popp, K. (2000). Steady-state vibrations of an elastic beam on a viscoelastic layer under moving load. *Archive of Applied Mechanics*, 70 (6), 399-408.

Metrikine, A. V., & Vrouwenvelder, A. C. (2000). Surface ground vibration due to a moving train in a tunnel: two-dimensional model. *Journal of Sound and vibration*, 234 (1), 43-66.

Real, J., Martínez, P., Montalbán, L., & Villanueva, A. (2011). Modelling vibrations caused by tram movement on slab track line. *Mathematical and Computer Modelling*, 54 (1), 280-291.

Romero, A., Galvin, P., & Dominguez, J. (2012). A time domain analysis of train induced vibration. *Earthquake and Structures*, 3 (3-4), 297-313.

- Salvador, P., Real, J., Zamorano, C., & Villanueva, A. (2011). A procedure for the evaluation of vibrations induced by the passing of a train and its application to real railway traffic. *Mathematical and Computer Modelling*, 53 (1), 42-54.
- Schillemans, L. (2003). Impact of sound and vibration of the North-South high-speed railway connection through the city of Antwerp Belgium. *Journal of sound and vibration*, 267 (3), 637-649.
- Sheng, X., Jones, C. J., & Petyt, M. (1999). Ground vibration generated by a harmonic load acting on a railway track. *Journal of Sound and Vibration*, 225 (1), 3-28.
- Sheng, X., Jones, C. J., & Petyt, M. (1999). Ground vibration generated by a load moving along a railway track. *Journal of sound and vibration*, 228 (1), 129-156.
- Sheng, X., Jones, C. J., & Thompson, D. J. (2003). A comparison of a theoretical model for quasi-statically and dynamically induced environmental vibration from trains with measurements. *Journal of Sound and Vibration*, 267 (3), 621-635.
- Sheng, X., Jones, C. J., & Thompson, D. J. (2004). A theoretical study on the influence of the track on train-induced ground vibration. *Journal of Sound and Vibration*, 272 (3), 909-936.
- South, J. (1863). Experiments, Made at Watford, on the Vibrations Occasioned by Railway Trains Passing through a Tunnel. *Proceedings of the Royal Society of London*, 13, 65-83.
- Steenbergen, M. J., & Metrikine, A. V. (2007). The effect of the interface conditions on the dynamic response of a beam on a half-space to a moving load. *European Journal of Mechanics-A/Solids*, 26 (1), 33-54.
- Takemiya, H. (2001). Ground vibrations alongside tracks induced by high-speed trains: prediction and mitigation, in Noise and Vibration from High-Speed Trains. *Noise and vibration from high-speed trains* , 347.
- Thompson, D. (2009). *Railway noise and vibration: mechanisms, modelling and means of control*.

Udías, V. A. (1999). *Principles of Seismology*. Cambridge, United Kingdom: Cambridge University Press.

Valerio, J., & Cuellar, V. (2000). Análisis de las vibraciones producidas por el tráfico ferroviario en medios urbanos. *Ingeniería Civil*, 118.

Verhas, H. P. (1979). Prediction of the propagation of train-induced ground vibration. *Journal of Sound and Vibration*, 66 (3), 371-376.

Xia, H., De Roeck, G., Zhang, N., & Maeck, J. (2003). Experimental analysis of high speed railway bridge under Thalys trains. *Journal of Sound and Vibration*, 268 (1), 103-113.

Xia, H., Zhang, N., & Cao, Y. M. (2005). Experimental study of train-induced vibrations of environments and buildings. *Journal of Sound and Vibration*, 280 (3), 1017-1029.

Xia, H., Zhang, N., & Gao, R. (2005). Experimental analysis of railway bridge under high-speed trains. *Journal of Sound and Vibration*, 282 (1), 517-528.

Yang, Y. B., & Hung, H. H. (1997). A parametric study of wave barriers for reduction of train-induced vibrations. *International Journal for Numerical Methods in Engineering*, 40 (20), 3729-3747.

Zhai, W. M., Wang, K. Y., & Lin, J. H. (2004). Modelling and experiment of railway ballast vibrations. *Journal of sound and vibration*, 270 (4), 673-683.

OBJECTIVES

General Purpose

To go more deeply into the knowledge of vibrations generation phenomenon in the wheel-rail contact, its transmission across the track and its propagation through the adjacent ground to the track. In this regard, it is important to identify which are the generator causes of these vibrations, in which operation regimes predominate one or other vibration frequencies, which are the physical phenomena that justify the transmission of these vibrations across the track and its propagation through the adjacent ground and which are the tools (methods or materials) available to minimize the vibrations generated in the wheel-rail contact, as in new tracks as in tracks in operation.

Specific Objectives

To develop, calibrate and validate an analytical model capable to predict the generation and transmission of railway vibrations. The application of this model to a real case has been essential to evaluate the validity its accuracy. In this regard, it has been important to discern in the formulation between the different track typologies (ballasted track versus concrete slab track), different railway operations and railway vehicles in operation, level of detail required to the modeling (regarding the grouping of elements in layers), adjustment of the boundary conditions and compatibility with the real circumstances of the studied case.

Formulate, calibrate and validate a numerical model able to predict the generation, transmission and propagation of railway vibrations. The application of this model to a real case has been essential to evaluate its suitability. In this context it will be necessary to establish basic modeling assumptions leading to find the balance between the accuracy of the results provided by the model and computation time. Furthermore, heterogeneity of the different elements that constitute the track has obliged to find easier geometries capable of simulate mechanically the behavior of the original element.

To confirm the existing results in the scientific literature about the effectiveness of the different types of wave barriers in the mitigation of railway vibrations propagation. Certainly, this is one of the easiest solutions to implement in a railway infrastructure in operation, but it is necessary to analyze the relevant factors (depth, width, in-filled

material, etc) for its implementation in an urban environment. In this context, the type of terrain in which this solution is implemented plays a key role. Hence, the results must be circumscribed to the specific study case.

To go more deeply into the modeling of certain pathologies inherent to the railway traffic (specifically, wheel flats and rail corrugation) from the perspective of its potential for generate vibrations. In this regard, it has been necessary to quantify the accelerations due to these phenomena and the frequency ranges in which they occur, all in the finite element method context.

CHAPTER 1

ANALYSIS OF VIBRATIONS IN A MODELED BALASTED TRACK USING MEASURED RAIL DEFECTS

J. I. Real, T. Asensio, L. Montalbán, C. Zamorano

*Vibroengineering. Journal of Vibroengineering, June 2012. Volume14,
Issue 2. ISSN 1292-8716*

Abstract.

Vibrations generated by trains and transmitted to the ground and nearby structures are a known source of problems associated with railway transport. Therefore this phenomenon should be studied in detail to avoid a negative impact on the environment. Within this framework, the article develops an improved version of a previously published analytical model capable of predicting ground vibrations caused by the passing of railway vehicles. The new features include a new formulation of the models with five layers of material and an enhanced load input process that takes into account actual rail defects data as well as the Hertz theory for the rail-wheel contact. The model is adapted to a conventional ballasted track in Solares (Spain) as well as calibrated and validated with data collected on site. Hence the model is proved to be able to properly reproduce vibrations for the case of varying track typologies, constituting a useful research and design tool.

Keywords: ground vibrations, ballasted track, rail defects, Hertz contact.

Nomenclature

a	Track gauge
A	Rail cross-sectional area
A_k	Rail shear cross-sectional area
c_2	Train primary damping coefficient
c_{Lj}	Rail pad/sleeper/ballast/ground 1/ground 2 longitudinal wave velocity ($j=1,2,3,4,5$)
c_{Tj}	Rail pad/sleeper/ballast/ground 1/ground 2 shear wave velocity ($j=1,2,3,4,5$)
C	Equivalent ballast coefficient
E	Rail and wheel Young's modulus
E_j	Rail pad/sleeper/ballast/ground 1/ground 2 Young modulus ($j=1, 2, 3,4,5$)
E'	Hertz equivalent elastic modulus
G	Rail shear modulus
h_j	Layer thickness ($j=1, 2, 3,4,5$)
I	Rail inertia in y-axis direction
k_1	Equivalent track spring constant

k_2	Train primary spring constant
K_H	Hertz contact stiffness
m_1	Unsprung mass per axle
m_2	Sprung mass per axle
P_i	Harmonic load magnitude
Q	Static load per axle
R_0	Hertz effective radius of curvature
R_R	Rail longitudinal radius of contact
R_{RT}	Rail transverse radius of contact
R_W	Wheel longitudinal radius of contact
R_{WT}	Wheel transverse radius of contact
V	Train velocity
y_1	Unsprung mass vertical displacement
y_2	Sprung mass vertical displacement
z_r	Rail vertical profile
α_1	First semi-axis of elliptical contact area
α_2	Second semi-axis of elliptical contact area
ε	Wheel roughness

λ_j	First Lamé parameter (j=1, 2, 3, 4, 5)
λ_j^*	First damping coefficient (j=1, 2, 3, 4, 5)
μ_j	Second Lamé parameter (j=1, 2, 3, 4, 5)
μ_j^*	Second damping coefficient (j=1, 2, 3, 4, 5)
θ	Angle between planes containing R_w and R_R
ρ	Rail mass density
ρ_j	Rail pad/sleeper/ballast/ground1 ground2 mass density (j=1, 2, 3, 4, 5)
ν	Rail and wheel Poisson coefficient
ν_j	Rail pad/sleeper/ballast/ground 1/ground 2 Poisson coefficient (j=1,2,3,4,5)
$\bar{\omega}_i$	Harmonic load frequency
ξ	Hertz parameter

Introduction

The increasing development of both urban and interurban railway lines across the world is a consequence of growing mobility needs as well as rising environmental concerns among the citizenry. Railways present many advantages such as high capacity and low CO₂ emissions compared to other transport means. However, they also present certain potential problems which should be addressed in order to make this transport mean a truly beneficial choice.

Within this context, vibrations caused by the passing of trains arise as one of the main sources of potential disturbance for the environment near railway lines. The generation and transmission of mechanical waves through the track and the ground is a phenomenon widely studied and yet not fully modeled, therefore representing a challenge for track designers.

In order to better understand this process, Salvador et al. [1] and Real et al. [2] developed an analytical model of the wave generation and transmission through the track infrastructure. This model was calibrated and validated with real data for both a high-speed ballasted track and a tram slab track, hence proving to be a useful tool for further research.

The main objective of this paper is to improve certain important aspects of its formulation and adapt the model to a conventional ballasted. The most important improvement is the implementation of the model constituted by five layers of materials. Moreover the load modeling is further enhanced from previous versions as it now takes into account the actual rail defects measured on-site.

The paper is structured as follows: first of all a brief literature review is exposed. Then the model development is explained, focusing mainly on all the modified aspects from previous published versions. A brief explanation of the data collection is then described, and finally the model is calibrated and validated with acceleration data measured on the Santander-Liérganes line operated by FEVE (Ferrocarriles Españoles de Vía Estrecha) in the north of Spain.

Modeling vibrations associated with railways has been a subject of study for many years. From a theoretical point of view, it is worth mentioning the work of Thompson [3], which deals with both vibration and noise. More practical studies have been carried out by authors such as [4] and [5], focusing on different aspects of the phenomenon.

In terms of modeling, there are two main approaches: analytical and numerical. Several works regarding both modeling schemes are reviewed in [1] and [2] as a background for the model presented in this paper. Among them the reader may consult [6] and [4] as an example of numerical formulations [7] and [8] as an example of analytical approaches.

The way loads are defined as an input for a vibration model has been widely addressed for numerical models ([9]) but it is still an issue when choosing an analytical formulation. The model defined in [2] presented an improvement in this aspect by formulating both harmonic and static loads and defining a set of loads so as to represent the train axle configuration. However, that approach showed certain limitations as there was no actual data available to define wheel and rail defects and the disused Zimmermann formulation to calculate the static component of railway vibrations. Moreover, the auxiliary quarter-car model adopted to calculate input forces relied on a parameter

representing the “track stiffness” which was only roughly calibrated along with the main model damping parameters.

The modeling of the loads induced at the track-wheel contact has been widely studied for many years. One of the seminal works regarding this issue is that of Hertz, who defined a general theory of contact of elastic solids. This theory has been extensively applied to the wheel-rail contact problem with some variations ([3] and [11]), and its soundness has been widely assessed [12]. Nowadays, numerical formulations are used in several investigations ([13] and [14]). However, the non-linear Hertz theory developed in [3] has been implemented in this paper due to its better fit to the analytical formulation presented.

Analytical model

The model presented in this paper follows the same formulation developed in [1] and [2]. The model considers a two dimensional cut (length and depth) consisting of the track and the ground underneath. It provides both vertical and longitudinal displacements and stresses induced by the applied loads.

The section studied in this paper is a conventional ballasted track with wooden sleepers, screw spikes and UIC 45 rails. This typology is adapted to the model domain as shown in Fig. 1.

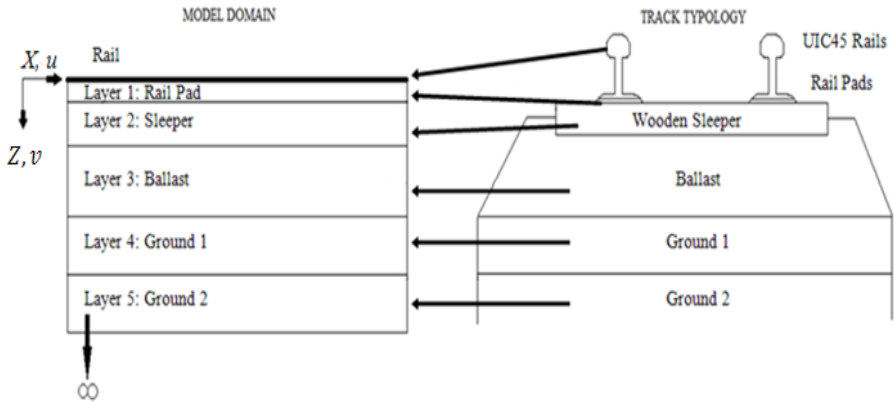


Fig. 1. Main model scheme.

The new version of the model considers five layers to represent track behavior accurately. Layer 1 and layer 2 represent the rail pads and the sleepers respectively. These elements, which are discontinuous elements in the track, are made equivalent to the first and second layer by modifying its thickness so as to ensure a similar vertical behavior. The thicknesses of the layers in the model are calculated setting the vertical stiffness of the layer equal to the real stiffness of the elements. As a result, discrete elements will be transformed to continuous material layers.

This assumption may not work properly for horizontal displacements but it does for vertical ones and is accepted because vibrations in that direction are the most interesting for this study. As for the rails, they are modeled as a single Timoshenko beam of negligible thickness resting over the top layer.

The model core equation is the wave equation, expressed in vectorial terms:

$$(\hat{\lambda} + \hat{\mu})\nabla_{x,z}(\nabla_{x,z}\mathbf{d}) + \hat{\mu}\nabla_{x,z}^2\mathbf{d} = \rho\frac{\partial^2\mathbf{d}}{\partial t^2} \quad (1)$$

Where \mathbf{d} is the displacement vector, ρ is the density of the material and $\hat{\lambda}$ and $\hat{\mu}$ are operators describing the viscoelasticity of the ground:

$$\begin{aligned} \hat{\lambda} &= \lambda + \lambda^* \frac{\partial}{\partial t} \\ \hat{\mu} &= \mu + \mu^* \frac{\partial}{\partial t} \end{aligned} \quad (2)$$

Where λ and μ are Lamé parameters and λ^* and μ^* are damping coefficients which must be calibrated using experimental data.

Load modeling

The load modeling is provided in order to obtain the forces, which applied to the model are made of a static component and some dynamic harmonic components. The objective is to generalize the inputs in the model. For this reason, both static and dynamic loads are modeled using harmonic loads with different amplitudes and frequencies:

$$F_i(t) = P_i \cos(\bar{\omega}_i t) \quad (3)$$

where P_i represents the amplitude and $\bar{\omega}_i$ the harmonic load frequency of the i -th load F_i . The static load is considered as harmonic function with $\bar{\omega} = 0$ and P equal to the load applied by a single train axle, to represent that the static load is a permanent action. Each

harmonic which represents dynamic loads is caused by certain rail or wheel defect such as rail joints, rail corrugations, wear and tear, etc.

In order to obtain the different pairs of amplitude and frequency to define the dynamic loads, an auxiliary quarter car model is used, as defined by Melis [15]. The model layout, which represents a single train axle, is shown in Fig. 2.

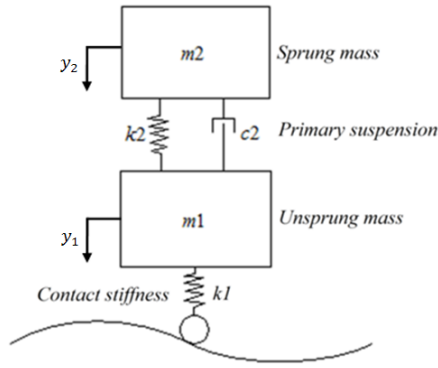


Fig. 2. Quarter car model scheme.

The equations that describe the movement of the two masses are as follows:

$$m_2 \frac{\partial^2 y_2}{\partial t_2^2} + c_2 \left(\frac{\partial y_2}{\partial t} - \frac{\partial y_1}{\partial t} \right) + k_2 (y_2 - y_1) = 0 \quad (4)$$

$$m_1 \frac{\partial^2 y_1}{\partial t_1^2} - c_2 \frac{\partial y_2}{\partial t} + c_2 \frac{\partial y_1}{\partial t} - k_2 y_2 + (k_1 + k_2) y_1 - k_1 z_r = 0 \quad (5)$$

where z_r is the rail vertical profile, y_1 and y_2 are the vertical displacements of the unsprung and sprung masses respectively.

All the parameters in this quarter car model are known except for the track equivalent spring constant k_1 . This parameter is calculated as the equivalent track stiffness, taking into account the wheel-rail contact stiffness.

$$\frac{1}{k_1} = \frac{1}{k_H} + \frac{1}{k_{rail}} + \frac{1}{k_{railpad}} + \frac{1}{k_{sleeper}} + \frac{1}{k_{ballast}} + \frac{1}{k_{ground}} \quad (6)$$

According to [3], the wheel-rail contact stiffness is due to local elastic deformation of both elements. As the contact area (which is assumed to be elliptical) depends on the load, this stiffness is not linear. The contact stiffness, K_{rt} , depends on the geometry of the two bodies in contact, i.e. the rail and wheel. Curvature radii in both the longitudinal and transverse direction are required, as show in Fig. 3.

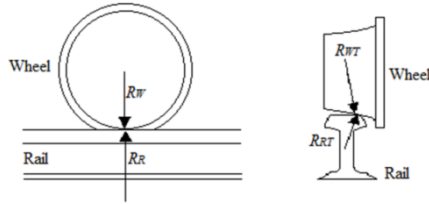


Fig. 3. Geometry parameters for the Hertz theory.

These variables are used to define the following effective radius of curvature.

$$\frac{1}{R_0} = \frac{1}{2} \left(\frac{1}{R_W} + \frac{1}{R_{WT}} + \frac{1}{R_R} + \frac{1}{R_{RT}} \right) \quad (7)$$

Stiffness also depends on the material properties. Both wheel and rail are assumed to be made of the same steel, hence defining the following strain elastic modulus:

$$E' = \frac{E}{(1 - \nu^2)} \quad (8)$$

The angle between the planes containing R_W and R_R is defined as follows:

$$\cos \theta = -\frac{R_0}{2} \left(\frac{1}{R_W} - \frac{1}{R_{WT}} + \frac{1}{R_R} - \frac{1}{R_{RT}} \right) \quad (9)$$

Depending on the value of θ , non-dimensional parameter (ξ) is calculated. Its value was taken from a chart in [3] for the purpose of this paper. The reader may consult that reference for the precise mathematical definition of the parameters.

Now it is possible to calculate the Hertzian contact stiffness:

$$K_H = \frac{2E' \sqrt{R_0}}{3} \left(\frac{2}{\xi} \right)^{3/2} \quad (10)$$

The rest of values to calculate k_1 , are obtained from [16].

Then, we can solve (4) and (5) and obtain the displacements y_1 and y_2 by means of a finite differences algorithm according to [15]. The expressions of the first and second order derivative in terms of finite differences are:

$$y' = \frac{y_{t+1} - y_t}{\Delta t} \quad (11)$$

$$y'' = \frac{y_{t+1} - 2y_t + y_{t-1}}{\Delta^2 t} \quad (12)$$

Introducing (11) and (12) in (4) and (5) and reorganizing:

$$y_{2,t+\Delta t} = \left(\frac{2m_2 - c_2\Delta t - k_2\Delta^2 t}{m_2} \right) y_{2,t} + \left(\frac{-m_2 + c_2\Delta t}{m_2} \right) y_{2,t-\Delta t} + \left(\frac{c_2\Delta t + k_2\Delta^2 t}{m_2} \right) y_{1,t} - \frac{c_2\Delta t}{m_2} y_{1,t-\Delta t} \quad (13)$$

$$y_{1,t+\Delta t} = \left(\frac{2m_1 - c_2\Delta t - (k_1 + k_2)\Delta^2 t}{m_1} \right) y_{1,t} + \left(\frac{-m_1 + c_2\Delta t}{m_1} \right) y_{1,t-\Delta t} + \left(\frac{c_2\Delta t + k_2\Delta^2 t}{m_1} \right) y_{2,t} - \frac{c_2\Delta t}{m_1} y_{2,t-\Delta t} + \frac{k_1\Delta^2 t}{m_1} z_t \quad (14)$$

This equation system may be solved iteratively using time increments from initial conditions, which does not affect to the final results due to the quick disappearance of its influence.

Once y_t and k_t are known, it is possible to calculate the forces at each point of the rail:

$$F_i = k_i (y_i - z_i) \quad (15)$$

The force function defined at Eq. (15) is plotted, yielding the force profile caused by rail defects. From this profile the main amplitudes and frequencies are taken, considering the train velocity, and feed the main model as different harmonic forces according to Eq. (3).

Model solution

Once the model equations and loads are defined, the following boundary conditions must be set. The horizontal displacement is u , v is the vertical displacement, σ_{xx} is the horizontal stress and σ_{xz} is the vertical stress. Note that these parameters depend on x , z and t and the sub-index number express the layer where they are defined. According to [8], initial conditions are not required as only the stationary solution is to be calculated:

$$u_1(x, 0, t) = 0 \quad (16a)$$

$$v_1(x, 0, t) = w(x, t) \quad (16b)$$

$$u_1(x, h_1, t) = u_2(x, h_1, t) \quad (16c)$$

$$v_1(x, h_1, t) = v_2(x, h_1, t) \quad (16d)$$

$$\sigma_{zz_1}(x, h_1, t) = \sigma_{zz_2}(x, h_1, t) \quad (16e)$$

$$\sigma_{xz_1}(x, h_1, t) = \sigma_{xz_2}(x, h_1, t) \quad (16f)$$

$$u_2(x, h_1 + h_2, t) = u_3(x, h_1 + h_2, t) \quad (16g)$$

$$v_2(x, h_1 + h_2, t) = v_3(x, h_1 + h_2, t) \quad (16h)$$

$$\sigma_{zz_2}(x, h_1 + h_2, t) = \sigma_{zz_3}(x, h_1 + h_2, t) \quad (16i)$$

$$\sigma_{xz_2}(x, h_1 + h_2, t) = \sigma_{xz_3}(x, h_1 + h_2, t) \quad (16j)$$

$$u_3(x, h_1 + h_2 + h_3, t) = u_4(x, h_1 + h_2 + h_3, t) \quad (16k)$$

$$v_3(x, h_1 + h_2 + h_3, t) = v_4(x, h_1 + h_2 + h_3, t) \quad (16l)$$

$$\sigma_{zz_3}(x, h_1 + h_2 + h_3, t) = \sigma_{zz_4}(x, h_1 + h_2 + h_3, t) \quad (16m)$$

$$\sigma_{xz_3}(x, h_1 + h_2 + h_3, t) = \sigma_{xz_4}(x, h_1 + h_2 + h_3, t) \quad (16n)$$

$$u_4(x, h_1 + h_2 + h_3 + h_4, t) = u_5(x, h_1 + h_2 + h_3 + h_4, t) \quad (16o)$$

$$u_4(x, h_1 + h_2 + h_3 + h_4, t) = u_5(x, h_1 + h_2 + h_3 + h_4, t) \quad (16p)$$

$$\sigma_{zz_4}(x, h_1 + h_2 + h_3 + h_4, t) = \sigma_{zz_5}(x, h_1 + h_2 + h_3 + h_4, t) \quad (16q)$$

$$\sigma_{xz_4}(x, h_1 + h_2 + h_3 + h_4, t) = \sigma_{xz_5}(x, h_1 + h_2 + h_3 + h_4, t) \quad (16r)$$

$$u_5(x, \infty, t) = v_5(x, \infty, t) = \sigma_{zz_5}(x, \infty, t) = \sigma_{xz_5}(x, \infty, t) = 0 \quad (16s)$$

Additionally, Eq. (1) is expressed in terms of the Lamé potentials so that vertical and horizontal displacements and stresses are as follows:

$$\begin{aligned} u &= \frac{\partial \varphi}{\partial x} + \frac{\partial \psi}{\partial z} \\ v &= \frac{\partial \varphi}{\partial z} - \frac{\partial \psi}{\partial x} \end{aligned} \quad (17)$$

$$\begin{aligned} \sigma_{zz} &= \lambda \left(\frac{\partial^2 \varphi}{\partial x^2} + \frac{\partial^2 \psi}{\partial z^2} \right) + 2\mu \left(\frac{\partial^2 \varphi}{\partial z^2} - \frac{\partial^2 \psi}{\partial x \partial z} \right) \\ \sigma_{xz} &= \mu \left(2 \frac{\partial^2 \varphi}{\partial x \partial z} - \frac{\partial^2 \psi}{\partial x^2} + \frac{\partial^2 \psi}{\partial z^2} \right) \end{aligned} \quad (18)$$

Eq.(1) can be transformed in two scalar equations applying the Fourier Transform, as defined in Eq. (19).

$$\tilde{f}(k, z, \omega) = \int_{-\infty}^{\infty} \int_{-\infty}^{\infty} f(x, z, t) e^{i(\omega t - kx)} dx dt \quad (19)$$

This yields the following system of ordinary differential equations, which is expressed in the frequency and circular wave number domain (represented by \approx):

$$\left. \begin{aligned} \frac{d^2 \tilde{\varphi}}{dz^2} - R_L^2 \tilde{\varphi} &= 0 \\ \frac{d^2 \tilde{\psi}}{dz^2} - R_T^2 \tilde{\psi} &= 0 \end{aligned} \right\} \quad (20)$$

Once solved Eq. (20), the Lamé potentials in frequency-wave number domain for each j layer can be expressed as:

$$\begin{aligned}\tilde{\varphi}_j &= A_{j1}(k, \omega)e^{R_{Lj}z} + A_{j2}(k, \omega)e^{-R_{Lj}z} \\ \tilde{\varphi}_j &= A_{j3}(k, \omega)e^{R_{Tj}z} + A_{j4}(k, \omega)e^{-R_{Tj}z}\end{aligned}\quad (21)$$

And the displacements and stresses in terms of (k, z, ω) are therefore as follows:

$$\tilde{u}_j(k, z, \omega) = ik(A_{j1}(k, \omega)e^{R_{Lj}z} + A_{j2}(k, \omega)e^{-R_{Lj}z}) + R_{Tj}(A_{j3}(k, \omega)e^{R_{Tj}z} - A_{j4}(k, \omega)e^{-R_{Tj}z}) \quad (22a)$$

$$\tilde{v}_j(k, z, \omega) = R_{Lj}(A_{j1}(k, \omega)e^{R_{Lj}z} - A_{j2}(k, \omega)e^{-R_{Lj}z}) - ik(A_{j3}(k, \omega)e^{R_{Tj}z} + A_{j4}(k, \omega)e^{-R_{Tj}z}) \quad (22b)$$

$$\tilde{\sigma}_{zj}(k, z, \omega) = C_{j1}(A_{j1}(k, \omega)e^{R_{Lj}z} + A_{j2}(k, \omega)e^{-R_{Lj}z}) + C_{j2}(A_{j3}(k, \omega)e^{R_{Tj}z} - A_{j4}(k, \omega)e^{-R_{Tj}z}) \quad (22c)$$

$$\tilde{\sigma}_{xj}(k, z, \omega) = D_{j1}(A_{j1}(k, \omega)e^{R_{Lj}z} - A_{j2}(k, \omega)e^{-R_{Lj}z}) + D_{j2}(A_{j3}(k, \omega)e^{R_{Tj}z} + A_{j4}(k, \omega)e^{-R_{Tj}z}) \quad (22d)$$

Where:

$$\begin{aligned}C_{j1} &= (\tilde{\lambda}_j + 2\tilde{\mu}_j)R_{Lj}^2 - \tilde{\lambda}_j k \\ C_{j2} &= -2ik\tilde{\mu}_j R_{Tj} \\ D_{j1} &= 2ik\tilde{\mu}_j R_{Lj} \\ D_{j2} &= \tilde{\mu}_j(k^2 + R_{Tj}^2)\end{aligned}\quad (23)$$

Boundary conditions in Eq. (15) can be also transformed to frequency and wave number domains using (19). Once converted to (k, ω) domain, they are taken into account to obtain an algebraic system

whose variables are the different A_j coefficients. After solving, displacements and stresses for each layer are known in the frequency domain. The last step is to apply the inverse transform to obtain those variables in the time domain. This step is performed numerically as explained in [2]. The resulting vertical displacement is derived twice to obtain vertical accelerations. The resulting acceleration is shifted accordingly to the axles' configuration to obtain the full accelerogram at a specific point of the model domain caused by the passing of the whole train.

Both the main model and auxiliary quarter car model were implemented in Mathematica[®] 7.0 (Wolfram Research Inc.)

Model calibration

The formulated model is now calibrated with actual data collected from the railway track located in Solares (Cantabria, Spain). In this way, damping coefficients for each layer (λ_j^* , μ_j^*) are obtained. Calibration is carried out by the root mean square difference method between the actual and modeled accelerations as defined by [17]. The RMSD between the real accelerogram $a_{z_r}(t)$ and the modeled accelerogram $a_{z_m}(t)$ is obtained as:

$$RMSD = \sqrt{\frac{\sum_T (a_{z_r}(t) - a_{z_m}(t))^2}{\sum_T (a_{z_r}(t))^2}} \quad (24)$$

The value of RMSD represents the mean error between the actual and the modeled accelerations. In our calibration, the criterion to accept a solution is a mean error of 5%.

Acceleration data collection

Data gathered for model calibration and validation was measured on-site in a rather straight track stretch of the Santander-Liérganes line in Cantabria, Spain. This line is operated by FEVE and consists on a conventional ballasted track with UIC 45 rails and wooden sleepers. The track gauge is 1 meter.

Three Sequoia FastTracer[®] triaxial accelerometers based on MEMS technology were used to measure accelerations on the track. Two were placed on the top surface of two non-consecutive sleepers and one on the rail foot. The characteristics of the sensors are shown in Table 1.

Table 1. Accelerometers characteristics

	Sensors on sleepers	Sensor on rail
Scope	<i>±5g</i>	<i>±18g</i>
Bandwidth (Hz)	<i>0-2500</i>	<i>0-2500</i>
Resolution (m/s²)	<i>0.041</i>	<i>0.13</i>
Noise (m/s²)	<i>0.075</i>	<i>0.093</i>
Sampling rate (Hz)	<i>8192</i>	<i>8192</i>

Acceleration at those three points was registered for several trains passing through the studied section within a week. The data obtained was exported to Mathematica[®] 7.0 (Wolfram Research Inc.) in order to process and compare them with the model output for calibration and validation.

As for the rail profile, it was measured by means of a ballast tamping and lining machine provided by ACCISA. Measurements were carried out at night to avoid any interruption of the train regular service. Fig. 4 shows the rail profile along a 60-meter track stretch.

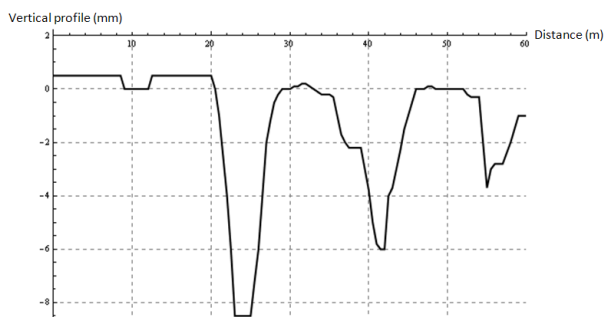


Fig. 4. Measured rail profile.

The line is operated by a single vehicle class: the CAF S/3800 consisting on three carriages and six bogies. Technical data including masses, damping and geometry was provided by FEVE. Velocity at the monitored section was recorded by the drivers and provided afterwards, giving a mean speed of 25 km/h.

Discussion of results

In this section the results given by the model are discussed. First of all, Fig. 5 shows the comparison between modeled and measured

accelerations on the surface (i.e. over the sleeper) after calibration. Calibrated parameters are shown in Table 2.

Table 2. Model parameters after calibration.

Parameter (Pa)	Layer 1	Layer 2	Layer 3
λ_j^*	No influence		
μ_j^*	450 000	400 000	525 000

From the figure it is clear that the model gives a good approximation of the measured accelerogram. Consecutive peaks of acceleration due to the passing of the train axles are reproduced, and the time of growing and decay of the signal is also similar. Therefore, calibration criteria are met (values are shown in Table 3) and the model is successfully calibrated.

Table 3. Calibration criteria.

Criteria	Model	Data	Difference
Maximum peak (m/s^2)	75	74	1
Absolute minimum peak (m/s^2)	78	63	15

Growth (s)	0.5	0.9	0.4
Decay (s)	1.7	1.5	0.2

From Fig. 5 it is clear that the modeled accelerogram is much 'cleaner' than the measured one. This is due to the fact that measurements include vibrations caused by several rail and wheel defects as well as certain resonance components (e.g. the rail pad or the fastening screws) that the model does not consider. This is particularly clear when looking at the growing part of the accelerogram, as the measured one takes more time of growth and shows many small, secondary peaks not reproduced by the model. The main reason for this difference is that only a few harmonics were obtained from the rail profile shown in Fig. 4 (mainly those due to rail joints) and fed to the main model, and thus there are many other defects not considered including those of the wheels. Transient effects are also not reproduced as the model only yields a stationary solution

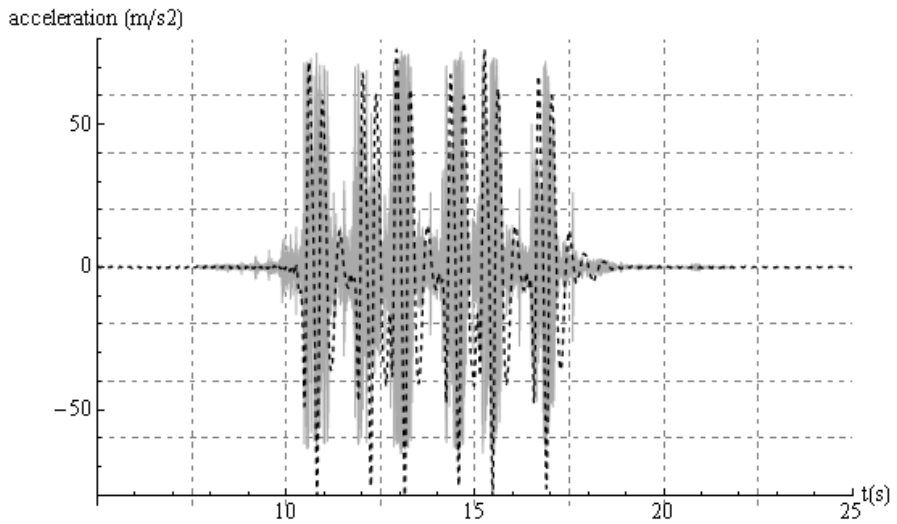


Fig. 5. Model calibration. Model in dashed black, data in gray.

However, despite this limitation, the model reproduces the main trends of the measured accelerogram because the response due to the quasi-static load is dominant compared to dynamic ones for the velocity considered (i.e. about 25 km/h). A better reproduction of the dynamic components of the vibration wave (which would be more important for greater velocities) only requires more comprehensive data of the wheel and rail defects so as to feed the model with more harmonic loads.

Another noteworthy issue is the difference of concordance between model and data for positive and negative peaks. The model as formulated is fairly symmetrical and yields rather similar maximum and minimum values. The data, on the other hand, is quite asymmetrical as there is a difference of about 10 m/s^2 between peaks. It is unclear why the measurements show such trend, and thus the model has been calibrated to fit higher peaks despite overestimating lower ones so as to be on the safer side.

Regarding the calibrated parameters, damping coefficient λ_j was found to be irrelevant when modeling vertical displacements, a result which confirms the observation made in [2]. This parameter has influence on horizontal displacements, but those are not considered for the purpose of this paper because of the lack of data and the assumed hypothesis of continuous sleepers previously described.

Damping coefficient μ_j^* , on the other hand, has a great influence in the model output. As the data for calibration was only measured in the sleepers, only the first parameter μ_1^* is fully calibrated. However, the other two parameters do have an impact in the vibration wave modeled and thus are also calibrated to certain extent. This difference from the behavior shown in [2] is due to the different track typology studied. This ballasted track is far less rigid than the slab track studied in the previous paper (note the damping coefficients are two orders of magnitude lower than those obtained in [2]) and the behavior of each layer affects the others to a greater extent.

The calibrated model was then validated with a different set of data. The results are shown in Fig. 6 and the validation criteria are exposed in Table 4.

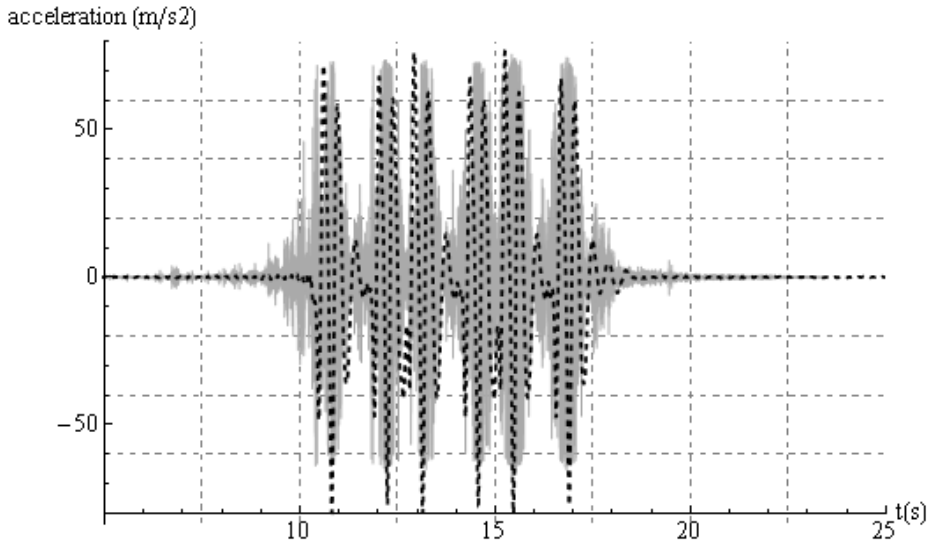


Fig. 6. Model validation. Model in dashed black, data in gray.

Table 4. Validation criteria.

Criteria	Model	Data	Difference
Maximum peak (m/s^2)	76	72	4
Absolute minimum peak (m/s^2)	79	63	16
Growth (s)	0.6	1.5	0.9
Decay (s)	1.7	2.2	0.5

Once again the model overestimates negative peaks but reproduces quite well the positive ones. This is an acceptable result as was explained previously. The wave main traits are correctly predicted and thus the model is properly validated.

Finally, in order to test the model performance across the entire domain, Fig. 7a and Fig.7b shows modeled accelerations in the ballast layer (Fig. 7a) and the ground 1 (Fig. 7b) at 0.2 and 0.5 meters of depth respectively. When compared with the accelerogram modeled at the surface (Fig. 5 and Fig. 6), a clear alleviation of the wave with depth can be pointed out. Peaks of acceleration are reduced from 76 to 30 m/s^2 (60%) when the wave moves from the sleeper to the ballast and drop to 1.5 m/s^2 (98%) when it reaches the ground. This behavior shows that the model is capable of simulate vibration mitigation within its domain and thus it can be used to study wave propagation through different track elements.

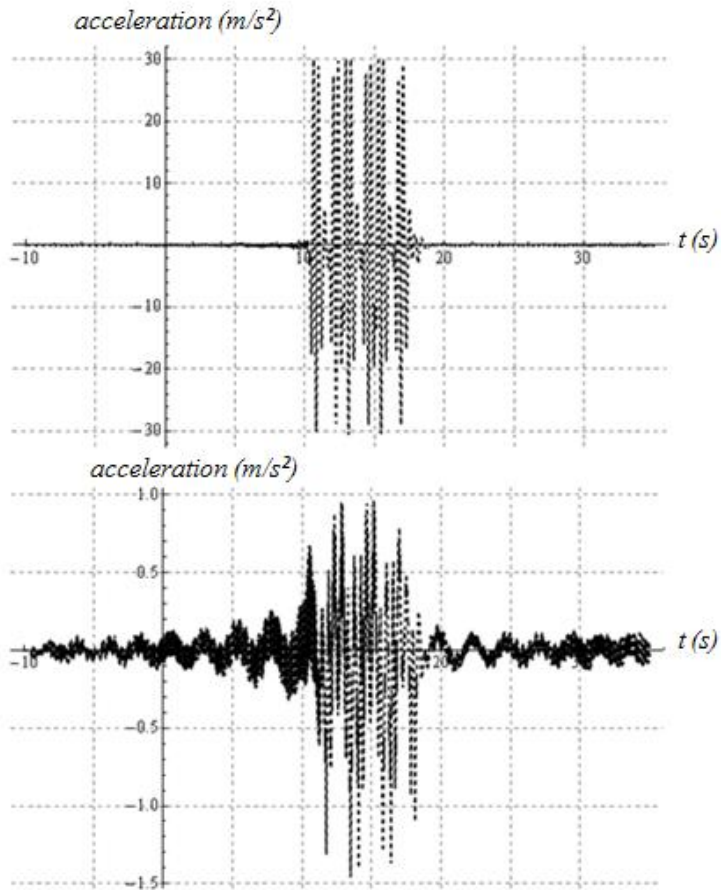


Fig. 7. Modeled accelerations. 7a: at the ballast layer (Depth: 0.2 m).
7b: at the ground layer (depth: 0.5m)

Conclusions

The paper has presented and improved version of the previously developed and reported analytical model and has applied it to a

conventional ballasted track in Solares, Spain. The model has been calibrated and validated using actual data measured on site.

The five-layer model has been implemented and it has been proven to more accurately represent the track behavior. The improvements made regarding load modeling have proved to work properly as the model reproduces the measured wave fairly accurately. In addition, the inclusion of the non-linear Hertz theory provides the model a sounder theoretical base and simplifies the calibration process by reducing the number of parameters to be adjusted.

The model still has certain limitations that should be taken into account. The actual phenomenon of vibration transmission through a track infrastructure is made of several static and dynamic components and the model is only capable of reproducing a portion of them. Transient phenomena and resonance of singular elements such as rail pads or fastening systems are not included in the model formulation. Heterogeneity of the ground and ballast layer is not considered, and singular track features cannot be studied. On the other hand, the improved load modeling allows including virtually every dynamic load due to wheel and rail defects providing there is accurate data available.

This may be another limitation as accurate data is not always available or easy to obtain. However, as the results have proven, for the velocity considered the main features of the wave are properly reproduced with only a few components (i.e. pairs of frequency/amplitude) of measured rail defects. Therefore, the model can yield a good approximation of the phenomenon even with a reduced source of data.

Considering the results obtained in this paper as well as those shown in [1] and [2], the model developed represents a useful tool to study vibration propagation through different track infrastructures, from conventional and high-speed ballasted tracks to urban slab tracks. Therefore, it can be use for designers to assess the vibration performance of new and existing tracks as well as to model the first stage of vibration transmission within wider research projects related to the effects of train-induced vibrations in the environment.

Acknowledgements

The authors would like to thank FEVE (Ferrocarriles Españoles de Vía Estrecha) for their permission to measure in the Santander-Liérganes Line and for providing their vehicle's technical data. We wish also to express our gratitude to ACCISA for their support during the measurement campaign.

Appendix. Values of the parameters used in the study

Table 5. Values of the parameters used in the study.

Parameter	Value
m_1	3.445 Tn
m_2	7.305 Tn
k_2	47.48 kN/mm
c_2	26000 N/m·s-1

k_{rail}	$7.35 \cdot 10^6$ kN/m
$k_{railpad}$	$6.56 \cdot 10^5$ kN/m
$k_{sleeper}$	$6.5 \cdot 10^5$ kN/m
$k_{ballast}$	$2 \cdot 10^5$ kN/m
k_{ground}	$1 \cdot 10^5$ kN/m
R_w	0.425 m
R_{wT}	0.6 m
R_R	∞
R_{RT}	0.305 m

References

- [1] Salvador P., Real J., Zamorano C. and Villanueva A. A procedure for the evaluation of vibrations induced by the passing of a train and its application to real railway traffic. *Mathematical and Computer Modelling*, Vol. 53, Issue 1-2, 2010, p. 42-54.
- [2] Real J. et al. Modelling vibrations caused by tram movement on slab track line. *Mathematical and Computer Modelling*, Vol. 54, Issue 1-2, 2011, p. 280-291.
- [3] Thompson D. *J.Railway Noise and Vibration: Mechanisms, Modelling and Means*. Oxford (UK): Elsevier, 2009.
- [4] Sheng X. et al. Prediction of ground vibration from trains using the wavenumber finite and boundary element methods. *Journal of Sound and Vibration*, Vol. 293, Issue 3-5, 2006, p. 575–586.
- [5] Jones C. J. C. et al. Simulations of ground vibration from a moving harmonic load on a railway track. *Journal of Sound and Vibration*, Vol. 231, Issue 3, 2000, p. 739-751.
- [6] Yang Y. B. and Hung HH. Soil vibrations caused by underground moving trains. *Journal of Geotechnical and Geoenvironmental Engineering*, Vol. 135, Issue 3, 2008, p. 455-458.
- [7] Koziol P. et al. Wavelet approach to vibratory analysis of surface due to a load moving in the layer. *International Journal of Solids and Structures*, Vol. 45, Issue 7-8, 2008, p. 2140–2159.
- [8] Metrikine A.V. and Vrouwenvelder ACWM. Surface ground vibration due to a moving train in a tunnel: two-dimensional model. *Journal of Sound and Vibration*, Vol. 234, Issue 1, 2000, p. 43–66.

- [9] Auersch L. The excitation of ground vibration by rail traffic: theory of vehicle–track–soil interaction and measurements on high-speed lines. *Journal of Sound and Vibration*, Vol. 284 Issue 1-2, 2005, p.103–132.
- [10] Hertz H. *Contact of Elastic Solids. Miscellaneous Papers*. London (UK): Macmillan & Co. Ltd. (1896).
- [11] Otero J. Study of rail vehicle dynamics in curved tracks. Part I: Wheel-rail contact analysis. *Revista Colombiana de Tecnologías de Avanzada*, Vol. 14, Issue 2, 2009, p. 48-53.
- [12] Yan W. and Fischer F. D. Applicability of the Hertz contact theory to rail-wheel contact problems. *Archive of Applied Mathematics*, Vol 70, Issue 4, 2000, p. 255-268.
- [13] Kalker J. J. *Three dimensional elastic bodies in rolling contact*. Dordrecht (Netherlands): Kluwer Academic 1990.
- [14] Polach O. A fast wheel-rail forces calculation computer code. *Vehicle System Dynamics*, Vol. 33(supplement), 1999, p. 728-739.
- [15] Melis M. *Introducción a la dinámica vertical de la vía y señales digitales en ferrocarriles*. Madrid (Spain): Escuela de Ingenieros de Caminos Canales y Puertos, 2008.
- [16] López A. *Infraestructuras ferroviarias*. Barcelona: Cenit, 2006.
- [17] Arslan Y. Z. et al. Prediction of externally applied forces to human hands using frequency content of surface EMG signals. *Computer Methods and Programs in Biomedicine*, Vol. 98, Issue 1, 2010, p.36-44.

CHAPTER 2

STUDY OF WAVE BARRIERS DESIGN FOR THE MITIGATION OF RAILWAY GROUND VIBRATIONS

J. I. Real, A. Galisteo, T. Real, C. Zamorano

Vibroengineering. Journal of Vibroengineering, March 2012.

Volume14, Issue 1. ISSN 1392-8716

Abstract.

Nowadays, the consolidation of the rail in high populated areas has become a reality. Foundations, buildings, high accurate devices and people are susceptible to suffer from vibrations induced by running trains. Therefore, models for predicting ground vibration are required in order determine new mitigation measures. Rectangular open or in-filled trenches are a suitable solution to be used near constructed railway lines. Their installation is fast, easy and economic since no intrusion in the track is needed. In this work, the influence of the trench design in its effectiveness is analyzed considering a train moving with subsonic speed. A finite element model of the track has been developed and validated with real data registered along the tram network in Alicante (Spain). The analysis is carried out in the time domain considering the quasi-static movement of the vehicles. The results demonstrate that, in ascending order, the most relevant parameters in a trench are its width, depth and in-filled material or trench typology. However, it is also concluded that other conditions such as the stratification of soil are essential in order to determine an optimal design of a wave barrier.

Keywords: ground vibration; finite element method; isolation; reflection; wave barrier.

Nomenclature

H	Trench depth
L_R	Rayleigh wavelength
c_{ij}	Refraction barrier coefficient
ρ_i	Soil density
μ_i	Soil shear wave velocity
ρ_j	In-filled material density
μ_j	In-filled material shear wave velocity
θ_i	Incident wave angle
θ_j	Refracted wave angle
\mathbf{F}_{ext}	Applied external forces vector
\mathbf{F}_{int}	Internal forces vector
$\{\mathbf{u}\}$	Nodal displacements
$\{\dot{\mathbf{u}}\}$	Nodal velocities
$\{\ddot{\mathbf{u}}\}$	Nodal accelerations
$[M]$	Mass matrix
$[C]$	Damping matrix
$[K]$	Stiffness matrix

$\{F^a(t)\}$	Time-dependent vector of applied forces
α	Mass-controlling Rayleigh coefficient
β	Stiffness-controlling Rayleigh coefficient
$[\Phi]$	Mass normalized eigen vector matrix
$[c]$	Diagonalized damping matrix
ω_i	natural system frequency
ξ_i	Modal damping ratio
P_{frec}	Main frequency spectrum peak
d	Distance between consecutive nodes
v	Tram velocity
E	Young modulus

1. Introduction

In the last decades of scientific railway research, the necessity of establishing a methodology to calculate and control traffic-induced ground vibration has grown up.

On the one hand, the increase in the standard of living in society has prompted the requirement of high quality transportation services. Therefore, a more accurate study of railway internalities and externalities has to be performed.

On the other hand, it is well known that ground vibrations from railways may produce problems in nearby foundations and as a consequence, the stability of buildings and people health can be affected. To prevent these problems, trenches and buried walls, as a type of mitigation measure, may provide an important reduction of vibration amplitude after their location. Although this mitigation measure is still in research process, it is a highly recommended solution because of its characteristics. Firstly, its construction does not present any complexity. And secondly, its onsite installation is very economic because for an existing railway line it is not needed to modify its structure.

in this paper, two main objectives have been achieved. The first goal was to create a model based on the finite element methodology for the prediction of ground vibration propagation. This model has been calibrated and validated with real measurements taken along the tram network of Alicante (Spain). The second effort was to apply this methodology to study the influence of some hypothetical designs of open and in-filled trenches located in the same soil where the above measurements were taken.

In order to create this model, the most relevant publications on the subject have been reviewed. The first models to predict the ground vibration level produced by the railway appeared during the decade of the 70s. In [1] and [2], the dissipation mechanisms of vibrations that have to be taken into account to perform an accurate model were discussed. Some years later, [3] and [4] focused their work on the urban railways. The first one completed an analytical study of the vibrations induced by the metropolitan trains in nearby tunnel structures. Later, [4] presented a methodology to obtain the amplitude of vibration considering all the subsystems which take part in the phenomenon: generation-transmission-reception.

Nowadays, in the study of railway induced-ground vibrations two main tendencies are acknowledged, namely, the analytical and the numerical one. In contrast to the numerical methodology, the analytical one provides a continuous solution in all the domains in which the problem is studied. Some of the analytical researches that may be cited include works such as [5] and [6]. However, these analytical studies have an important limitation since their solution is only possible for simple geometries and idealized conditions. Hence, it is essential to use numerical models in order to predict the ground vibration propagation from railways and to investigate new measures for attenuating the vibration [7]. Therefore, the Finite Element method (FEM) has been the methodology selected in this paper. Several authors have also chosen this method in order to study railway vibrations. [8] studied with the FEM the dynamic response of an embedded rail track reaching that vibrations increase with the load speed. In 2009, [9] constructed a two-dimensional FE model to study how the wave propagation was influenced by buried walls. However, a 2D model cannot take into account the wave propagation and geometrical and material dissipation in the longitudinal direction of the

railway. That is why, in this paper, a 3D model has been proposed. In contrast, FEM presents a basic disadvantage for reproducing the wave propagation phenomenon. This method pretends to represent a semi-infinite soil by a finite size model. In consequence, several authors use non-reflecting boundaries in order to prevent this problem [10-13]. However, it ends up being a complicated remedy which is sometimes applicable only when the layered soil is supported on a rigid bedrock base [14]. In this paper, the radiation condition has been achieved by dimensioning the model so that the biggest required Rayleigh wavelength can be developed in all directions (section 2).

Related to the second scope of the paper, the reduction of the ground vibration amplitude due to the influence of active trenches has been studied. Specifically, the most important parameters on a trench design have been taken into account in the analysis, i.e., width, depth and in-filled material or trench typology.

This kind of vibration dissipation measures have been studied for more than 40 years. Firstly, [15] and [16] carried out some field works. They both reached similar conclusions: the reduction of ground vibration is possible only when the depth of the trench is comparable to the Rayleigh wavelength. Moreover, [16] revealed that a 75% of amplitude reduction is possible when the quotient H/L_R is higher than 0.6 for active isolation and for a homogeneous soil, where H denotes the depth and L_R the Rayleigh wavelength. In addition, later theoretical researches such as [14] and [17] agreed with the idea that the most relevant geometrical parameter on the effectiveness of a trench is its normalized depth. Consequently, it is well known that for a homogeneous soil, the isolation of ground vibration by trenches is effective only for medium and high frequency vibrations, so it can be thought that for a homogeneous soil and low wavelengths, trenches

could not be very effective. However, from that, several authors such as [14], [16] and [18] suggest that it would be necessary to study the influence of barriers in a layered ground since it is expected to find a greater effect than in a homogenous soil. The soil in the study site of this paper is a layered one. In section 4, the interaction among this fact and the depth of the trench is analyzed. Moreover, there is not a great agreement by the main works on the influence of the trench width. Some authors such as [11] and [19] found this parameter to be significant on the trench effectiveness while [12], [16] and [20] reached the opposite conclusion. In order to come to a clear idea, the trench width is also studied in this paper.

Related to the in-filled trench material, the mitigation phenomenon is produced by the impedance discontinuity in the propagation medium since arriving waves are refracted and reflected. In accordance with [21], the refraction coefficient c_{ij} for a determined in-filled trench is defined as follows:

$$c_{ij} = \frac{2\rho_i\mu_i\cos\theta_i}{\rho_i\mu_i\cos\theta_i + \rho_j\mu_j\cos\theta_j} \quad (1)$$

where ρ_i and μ_i are, respectively, the density and the velocity of the elastic shear waves for the soil and ρ_j and μ_j are the same parameters for the in-filled trench material. In addition, θ_i and θ_j are, respectively, the incident and refracted wave angle. From that, the denser and the stiffer the in-filled material is, the bigger reflection coefficient the trench will have, obtaining a better effective isolation. All this is related to the reflection mechanism, but theoretically, the absorption mechanism could also make the amplitude of vibration reduce in soil

after the trench. In section 4, the influence of the in-filled material density and stiffness over trench effectiveness will be analyzed by proposing concrete and polyurethane as in-filled materials. However, in spite of everything, it is well known that, ideally, an open trench will always be better than an in-filled trench since no waves are transmitted at a solid to void interface. This fact has also been studied in the next analysis as two open trench typologies have been proposed: an open trench and a sheet piling trench.

2. Development of the 3D FE model

In this section, a description of the methodology followed in the development of the FE model is presented.

As it will be seen below, a three-dimensional finite element method has been used for the study of the induced-train ground vibration waves in the time domain. The geometry and material characteristics of the track and soil elements have been taken from a specific point of the tram network of Alicante where the real data were measured. Consequently, the analysis of barriers presented in section 4 will be applicable in the future.

With this methodology, both quasi-static and dynamic mechanisms of train vibration generation can be implemented. However, when creating the model no dynamic components have been taken into account until the calibration and validation process.

2.1 Rayleigh damping theory

For the FEM analysis, the software ANSYS LAUNCHER has been used. In order to resolve the numerical dynamic problem, a global

mass matrix $[M]$, damping matrix $[C]$ and stiffness matrix $[K]$ are generated. Then, the equilibrium is proposed by equation (2):

$$\mathbf{F}_{\text{ext}} = \mathbf{F}_{\text{int}} \quad (2)$$

where \mathbf{F}_{ext} and \mathbf{F}_{int} are, respectively, the applied forces and the internal forces vector. Therefore, based on the values of the state fields (displacements u , velocities \dot{u} , and accelerations \ddot{u}), internal forces are calculated resolving numerically the equation of motion (3):

$$[M]\{\ddot{\mathbf{u}}\} + [C]\{\dot{\mathbf{u}}\} + [K]\{\mathbf{u}\} = \{\mathbf{F}^a(\mathbf{t})\} \quad (3)$$

being $\{\mathbf{F}^a(\mathbf{t})\}$ the external applied forces vector which is time-dependent.

Although the generation of mass and stiffness matrices is performed directly from the system properties, Rayleigh damping theory is considered so as to generate the damping matrix. According to this theory, $[C]$ can be denoted by (4):

$$[C] = \alpha[M] + \beta[K] \quad (4)$$

in which α and β are the so-called Rayleigh coefficients which are required for the dynamic analysis and have a global influence in the phenomenon.

By orthogonal transformation, equation (4) is modified as (5):

$$\begin{aligned}
[\emptyset]^T [C] [\emptyset] &= \alpha [\emptyset]^T [M] [\emptyset] + \beta [\emptyset]^T [K] [\emptyset] = [c] \\
&= \begin{bmatrix} \alpha + \beta \omega_1^2 & \cdots & 0 \\ \vdots & \ddots & \vdots \\ 0 & \cdots & \alpha + \beta \omega_n^2 \end{bmatrix}
\end{aligned} \tag{5}$$

being $[\emptyset]$ the normalized eigenvector mass matrix of the system, $[c]$ is the diagonalized damping matrix and ω_i is the i -natural modal frequency of the system.

From analogy to single-degree-of-freedom systems, it is known that:

$$c_i = 2\xi_i \omega_i \tag{6}$$

where ξ_i is the modal damping ratio. Then, matching (5) and (6), equation (7) is obtained:

$$2\xi_i \omega_i = \alpha + \beta \omega_i^2 \tag{7}$$

and this reduces to (8):

$$\xi_i = \frac{\alpha}{2\omega_i} + \frac{\beta \omega_i}{2} \tag{8}$$

A hypothetical plot of equation (8), considering typical values of α and β coefficients is shown in figure 1.

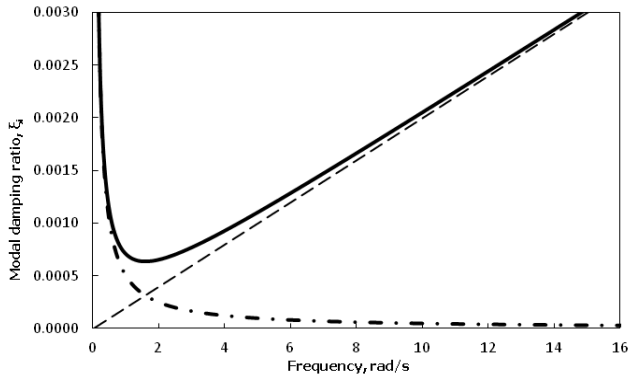


Fig. 1. Graphical representation of expression (8).

—, ξ_i ; - - - , mass component $\left(\frac{\alpha}{2\omega_i}\right)$; - . - . , stiffness component $\left(\frac{\beta\omega_i}{2}\right)$

As can be seen, the modal damping ratio is non-linear frequency-dependent. Moreover, both mass and stiffness components have been plotted. In this way, it can be observed that the mass component, dominated by coefficient α , is only notable for a frequency range from 0 to 6 rad/sec. In contrast, the stiffness component, dominated by coefficient β , is always notable and proportional to the natural frequency of the system. In a large number of civil problems, the natural frequency values of a system are located in the linear tract of the expression because of the large structures stiffness, see equation (8). Therefore, in these cases it can be assumed that the mass component is not influential in the phenomenon and expression (8) can be written as (9):

$$\xi_i = \frac{\beta\omega_i}{2} \quad (9)$$

Clearing the β coefficient from (9), it can be obtained by equation (10):

$$\beta = \frac{2\xi_i}{\omega_i} \quad (10)$$

As an exception, it can be considered the case of a system where a harmonic force or a set of harmonic forces are applied. For the determination of damping Rayleigh properties, ω_i is to be supposed as the most dominant harmonic force frequency since the system is going to vibrate in accordance with this time-dependent action.

2.2 Modeling the railway cross section

Regarding the railway structure modeling, a simplified reproduction of the elements has been determined. Considered actions are vertical, i.e. train weight and hypothetical induced dynamic actions from wheel and rail defects. Consequently, mechanical properties and geometry are modified so that inertia and vertical rigidity are equal to the real ones. A cross section of the studied track is shown in figure 2.

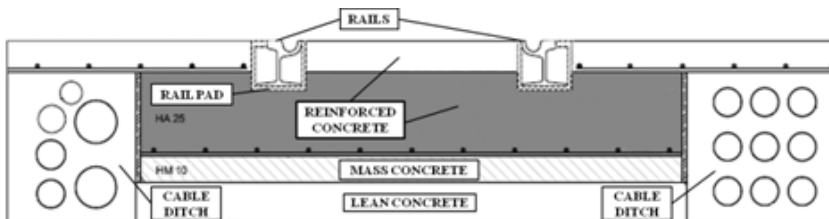


Fig. 2. Cross section of the railway provided by GTP (Management Entity of Transport Network and Ports of the Generalitat)

As can be observed, the studied structure is a slab track with embedded Phoenix rails and three different concrete layers, i.e. reinforced, mass and lean ones. Rails have been modeled as a rectangle which has the same width as the real foot rail but different height so that the horizontal axle inertia is the same as the real one.

Rail pad thickness has been increased since its actual dimension is too small compared to the other elements. In consequence, Young's modulus has been modified so that the element has the same vertical rigidity as in reality. The same geometry as shown in figure 2 has been modeled for the concrete elements. From geotechnical tests it is known that the soil is formed by a 2 meters thick sand layer supported on a calcarenite bedrock base. However, the sand elastic parameters are still unknown. Material characteristics are summarized in table 1.

Table 1. Material properties

Material	E (Pa)	ν	ρ (kg/m³)
Rail	2.1e11	0.30	7830
Rail pad	2.67e7	0.48	900
Reinforced concrete	2.72e10	0.25	2400
Mass concrete	2.25e10	0.20	2300
Lean concrete	2.25e10	0.20	2300
Cable ditch	1.13e10	0.20	2300
Sand	unknown	unknown	unknown
Calcarenite	4.6e9	0.26	1830

2.3 Defining the entire FE model

In order to perform a thorough analysis, wave propagation criterion has to be respected. Hence, no artificial boundaries have to interfere on the vibration transmission by creating wrong reflecting and refracting effects. It has been decided to study a frequency range from 2 to 50 Hz, which includes large part of the frequency interval relevant to the whole body perception. Since ground surface vibration is studied, Rayleigh waves are to be considered in the assumptions. Consequently, for calculating the transversal and longitudinal dimension of the model, the largest Rayleigh wavelength at the lower considered frequency has to fit on the model in all directions. Considering the elastic vibration theory, this wavelength corresponds to approximately 50 m. Similarly, the length of the elements is determined so that 6 nodes are present per wavelength of the Rayleigh waves at the higher frequency [22]. In this way, the length of elements is up to 0.5 m.

The vehicle self-weight is applied to the rail as a punctual force. However, the force magnitude has been modified depending on its position since the vertical rigidity of the modeled track is lower near the frontiers. Consequently, track deflections under a unitary force have been analyzed as can be seen in figure 3. In this way, the train weight has been pondered so that the vertical deflection keeps constant along the full movement.

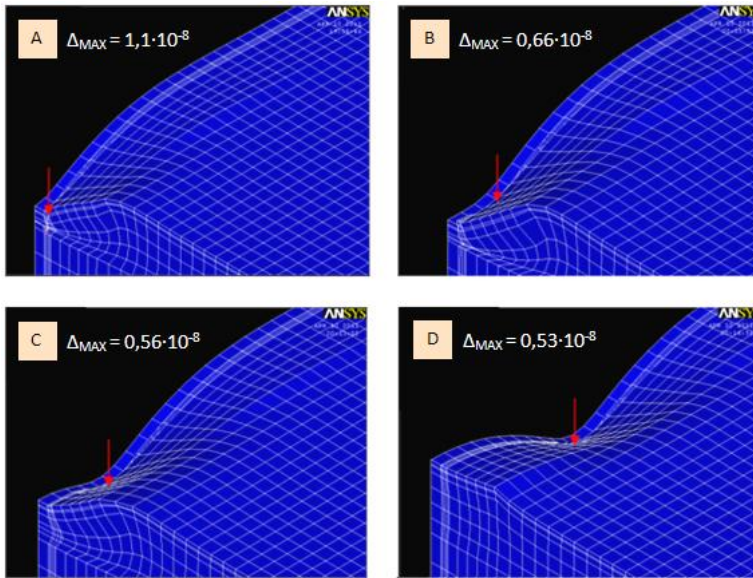


Fig. 3 Study of vertical track displacements under a unitary force

Surface soil accelerations are obtained in a track transversal line located in the half of the model, i.e. as far as possible of the beginning and ending model boundaries, see figure 4.

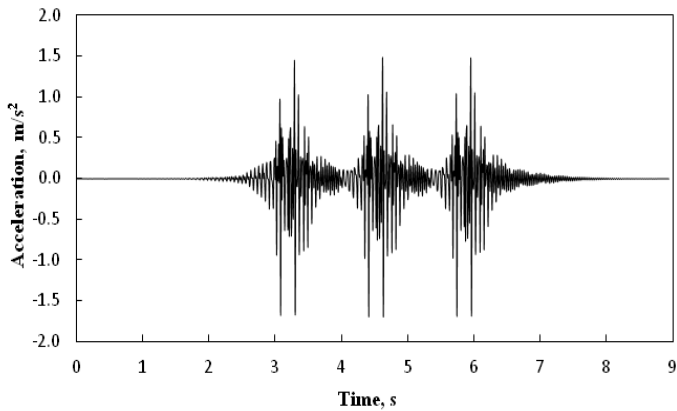


Fig. 4. Rail vertical acceleration

Attending to figure 4, the three different vehicle bogies can be distinguished as three maximum accelerations are registered. In addition, three principal peaks in acceleration spectrums have been recognized: bogies and wheels quasi-static frequencies, which are not too dominant, and the main frequency spectrum peak, i.e. $P_{\text{frec}} = 16.67$ Hz, which is induced by discretized progress of the load since the distance between nodes is $d=0.5$ m and the considered train velocity is $v=30$ km/h:

$$P_{\text{frec}} = \frac{v}{d} = \frac{30/3.6}{0.5} = 16.67 \text{ Hz} \quad (11)$$

To conclude the modeling, different comparisons between initial and simplified model results have been performed and the half part of the structure has been removed since it does not involve any modification on results. This fact has provided a relevant structure simplification since the mesh has become much more economic in terms of computational time.

2.4 Sensibility analysis

It is necessary to establish which parameters that take part in the process are influential in the results and which of them are not. This analysis provides help when carrying out future settings and results comparisons with collected real data, i.e. calibration and validation processes. However, there are some known parameters whose sensibility analysis would not make sense since their magnitude is already established. Unknown parameters are the global β Rayleigh coefficient and the elastic sand properties.

In figure 5, the influence of Young modulus on accelerations results for a point located 1.20 m far from the rail is indicated. As can be observed, this parameter is quite influential since vibration amplitude decreases for higher values of it. Regarding the β Rayleigh coefficient, its effect on the dynamic response is provided in figure 6. It is determined that the higher the β coefficient is, the more attenuated the soil response is since the acceleration amplitude and the time-response after peak are lower. This fact can be explained from equations (9) and (10) as the modal damping ratio is proportional to the β Raileigh coefficient. Moreover, in order to propose some appropriate values of coefficient β for the sensibility analysis, equation (10) has been used. Other sand elastic parameters such as the Poisson's ratio and density have been found not to be so much influential on the results.

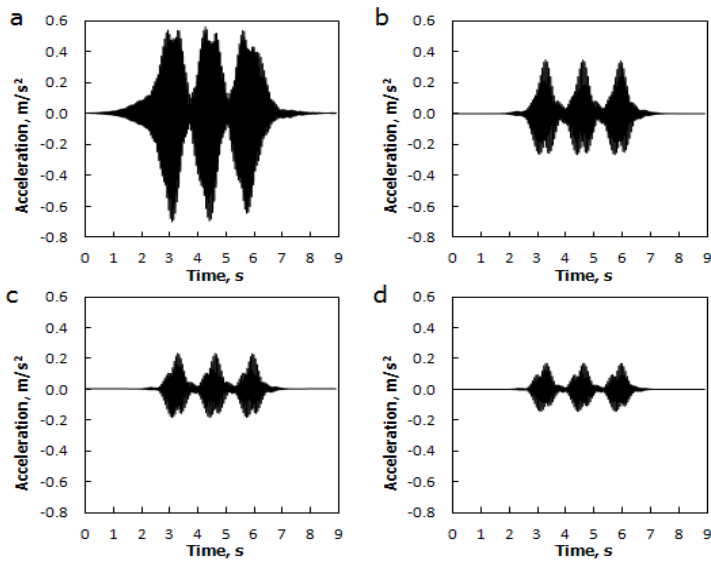


Fig. 5. Acceleration response in a point located 1.20 m far from the rail for different sand Young's modulus values (E). a, $E_1=1.7 \cdot 10^7$ Pa; b, $E_2=7 \cdot 10^7$ Pa; c, $E_3=12.3 \cdot 10^7$ Pa; d, $E_4=17.5 \cdot 10^7$ Pa

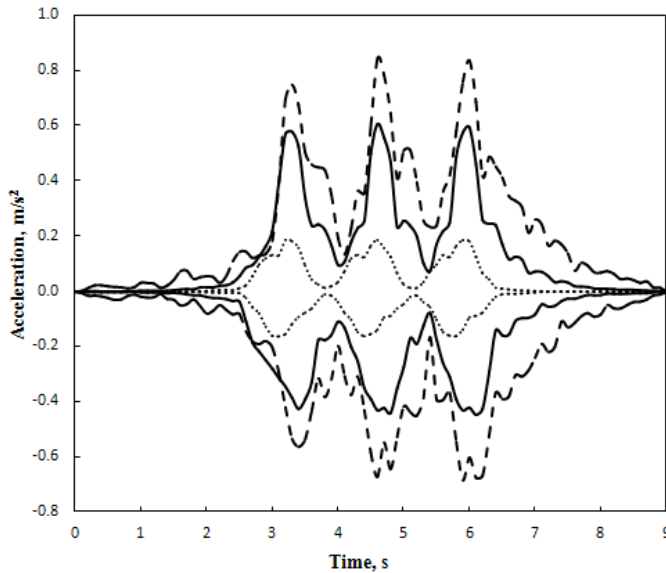


Fig. 6. Schematic acceleration response in a point located 1,20 m far from the rail for different β Rayleigh coefficient. - - -, $\beta_1=0.0001$; —, $\beta_3=0.001$; , $\beta_4=0.01$

Thus, the only two parameters which have been chosen to take part in the calibration and validation processes are the Young's Modulus and the β Rayleigh coefficient.

3. Calibration and validation

Once the model has been developed, it has been calibrated and validated from the measurements registered on Line 4 of the Alicante tram network. The measurements were taken when the vehicle passed by using some FiberSensing™ tri-axial accelerometers. The data was recorded in two points located 0.3 and 1.20 m far from the rail and only data gathered from trains which speed was approximately 30 km/h have been considered. Hence, the effect of velocity has not taken part in the analysis. The average of all registered accelerations has been obtained and used for doing the

comparison since the variability of results has been checked to be acceptable.

As deduced in section 2, the only two parameters considered in the calibration and validation process are those which are influential in results and yet unknown. The rest of the parameters have been provided by GTP or obtained from simple calculus. Both unknown parameters have been calibrated by comparing the model results with data gathered 0.3 m from the rail. The dynamic component has been taken into account by increasing model accelerations in a 33% [23] as, since this point, only quasi-static generation mechanism had been considered.

The calibration process has been rigorously performed by comparing the following criteria between real data and model results:

- Value of the maximum and minimum acceleration peaks.
- Time the signal takes to grow to the first peak.
- Attenuation time from the last peak.

After that, it has been achieved to validate the model with the suitable chosen parameters by making another comparison. It has been checked that model results accurately fit with real data collected 1.20 m from the rail. The resulting parameters from the calibration process are listed in Table 2.

Table 2. Resulting parameter values from calibration process

Parameter	Calibrated value
β Rayleigh coefficient	0.001
Sand Young modulus	70 MPa

The validation process allows the model to study the effectiveness of barriers on wave transmission isolation for the analyzed soil.

4. Study of barriers influence in wave soil propagation

in the present analysis, the main influential parameters in a wave barrier design are studied. According to the reviewed literature, it is well known that factors such as the trench geometry, i.e. depth and width and the in-filled material may have a determined effect on the trench effectiveness. However, this effect has not been entirely established for a layered soil yet, but it is thought that trench effectiveness may be modified. As has been seen, the analyzed railway track is over a stratified soil so the layering effect has been analyzed. The characteristics of the soil materials are shown in Table 3.

Table 3. Soil material mechanical characteristics

	Material	Thickness (m)	E (MPa)	ν	ρ (kg/m ³)
Upper layer	Sand	2	70	0.3	1800
Substratum	Calcarenite	indefinite	4600	0.26	1830

A quasi-static load is applied along the rail at a constant velocity of 30 km/h. The acceleration amplitude after different proposed active trenches is computed. Thus, the influence of trenches characteristics is studied.

4.1 Influence of trench width

According to [24], the isolation improvement of a wave barrier is only appreciable for a width below a quarter of the Rayleigh wavelength. In this model, the main propagation frequency is 16.67 Hz and the Rayleigh wave velocity for the upper layer is about 106 m/s. From that, a quarter of the main wavelength is up to 1.6 m which is not a reasonable dimension for a trench. Hence, widths below this value are studied.

For the present analysis, the effectiveness of three open trenches has been compared. The following widths for each one of them have been considered: 0.45 m, 0.6 m and 0.75 m which are common backhoe bucket sizes and sensible dimensions to be used in urban areas. The trenches depth has always been kept constant and equal to 1.5 m so the calcarenite substratum has not been penetrated. Figure 7 shows the vertical acceleration response in a node located 1.3 m from the trench for each considered width.

Since the main wavelength in the model is lower than the quarter Rayleigh wavelength, the vibration isolation after the open trench grows as the width is larger, which agrees with [24]. However, this dynamic reduction is not so relevant considering that the vibration amplitude for each studied solution has the same order of magnitude. From that, it can be concluded that the slight alteration produced by the increase of the studied parameter cannot justify the choice of the barrier width in the design process. There are some more important

design criteria such as the availability of urban space or the construction budget.

4.2 Influence of trench depth and typology in a layered soil

The previous analysis suggests that a practical solution should be chosen in order to establish the trench width as no dynamic criteria is to be considered. Hence, in this section, a width of 0.45 m is selected for the study. The following trench depths and typologies are considered:

- 1 m depth, which is the shorter trench studied.
- 1.5 m depth, which base is 0.5 m from the calcarenite layer surface.
- 2 m depth, which base is in contact with the calcarenite layer surface.
- 2.5 m depth, which penetrates the calcarenite layer 0.5 m.
- In-filled concrete barrier, see Table 4.
- In-filled polyurethane barrier, which is a relatively soft material, see table 4.
- Open trench.
- Sheet piling trench.

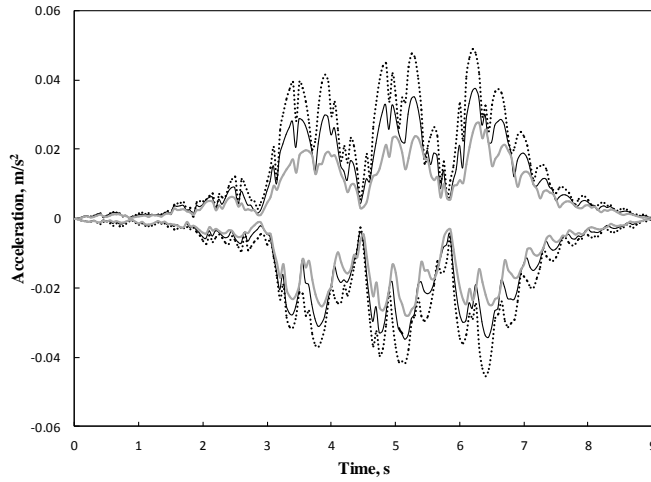


Fig. 7. Schematic acceleration response in a node located 1.3 m far from the trench.

..... , 0.45 m width; ———, 0.6 m width; ———, 0.75 m width

Table 4. In-filled material characteristics and in-filled trenches refraction coefficient

	E (MPa)	ν	ρ (kg/m³)	c_{ij}
Concrete	30000	0.25	2400	0.08
Polyurethane	20	0.45	500	1.58

The influence of depth in the isolation vibration is computed in terms of acceleration registered in the soil after the trench. This analysis is firstly made for each trench typology separately. The results are computed in figures 8, 9, 10 and 11.

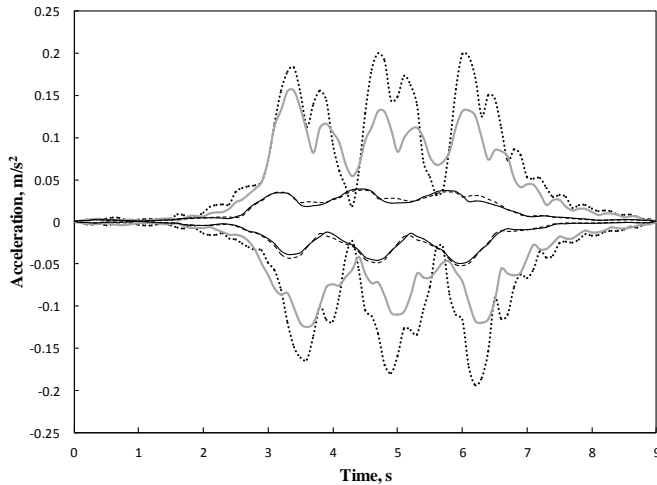


Fig. 8. Schematic acceleration response in a node located 2 m far from an in-filled concrete trench.

....., 0.5 m deep; —, 1 m deep; - - -, 1.5 m deep; ———, 2 m deep

Generally, with the exception of the polyurethane trench, it can be said that an increase of the trench depth induces better vibration isolation only for depths within the sand layer thickness. As can be seen, both depths 1.5 m and 2 m produce the same effect. So, according to this model, a penetration in the bedrock base is not necessary since no remarkable improvements have been registered and in general, the optimum depth will be considered the sand layer thickness. In contrast, according to figure 11, the maximum vibration reduction for a sheet piling trench is given by the 1.5 m depth trench so this would make possible to save 0.5 meters of sand excavation.

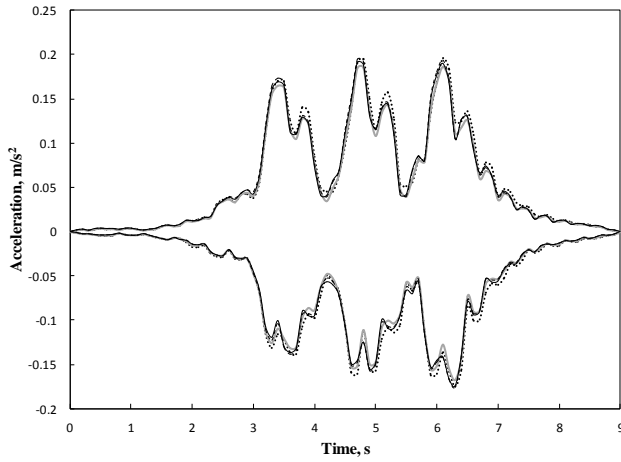


Fig. 9. Schematic acceleration response in a node located 2 m far from an in-filled polyurethane trench.

....., 0.5 m deep; —, 1 m deep; - - -, 1.5 m deep; ———, 2 m deep

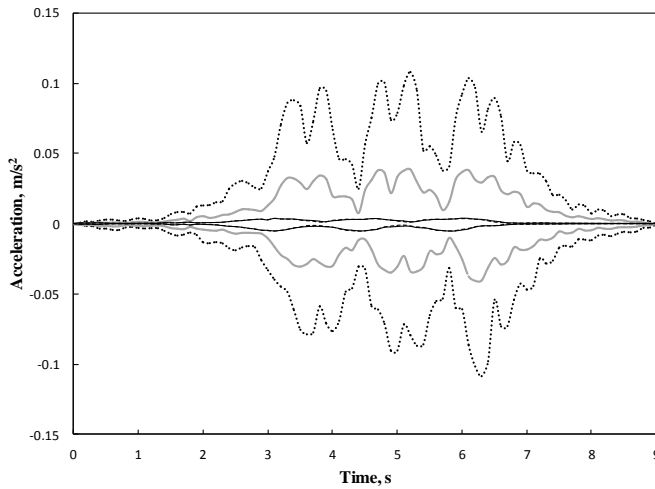


Fig. 10. Schematic acceleration response in a node located 2 m far from an open trench.

....., 0.5 m deep; —, 1 m deep; - - -, 1.5 m deep; ———, 2 m deep

At the same time, however, for the in-filled polyurethane trench, no improvements have been found with depth increment.

To sum up, it has been established that, mainly, the whole vibration energy is propagated by the softer substratum when the soil is stratified. This fact provides a huge advantage for trenches since it is not necessary to reach big depths to achieve a notable vibration reduction level. In addition, it has been seen that the depth is not highly influential for in-filled trenches which material has a big refraction coefficient, i.e. polyurethane.

The above results provide a clear idea about the influence of depth in the trench effectiveness. However, in figure 12 the difference between the four considered trench typologies is compared. The maximum acceleration peak for the time acceleration response of a node located 2 m far from the trench is represented.

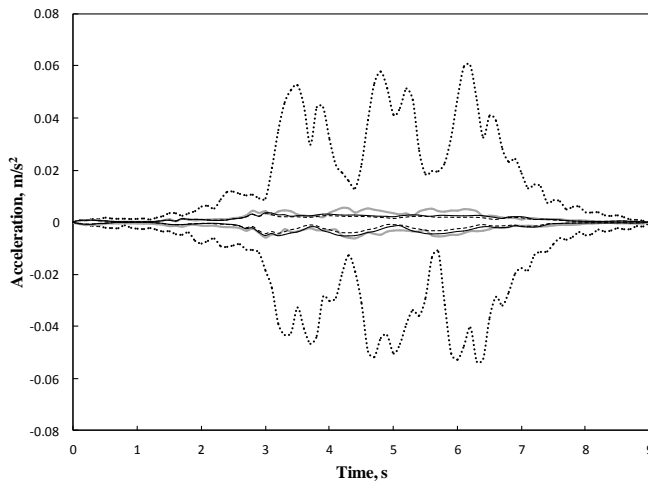


Fig. 11. Schematic acceleration response in a node located 2 m far from a sheet piling trench., 0.5 m deep; —, 1 m deep; - - -, 1.5 m deep; ———, 2 m deep

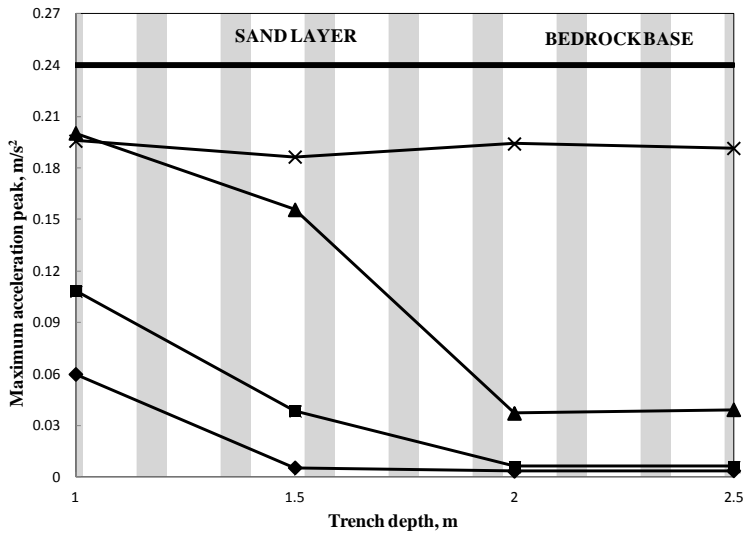


Fig. 12. Maximum acceleration peaks on a node located 2 m far from the trench.

—, no trench located; X, polyurethane in-filled trench; ▲, concrete in-filled trench; ■, open trench; ◆, sheet piling trench

Results in figure 12 imply the following:

- Generally speaking, all the considered trenches have achieved some kind of vibration reduction level since all of them provide a mechanical discontinuity in the soil. Additionally, in every case vibration reduction keeps constant for depths above the sand thickness.
- Void trenches are the better ones since for every depth their vibration reduction is higher than for the in-filled barriers.
- Between void trenches, the most effective ones are those which vertical walls are held up by a sheet pile because it is a more stable structure. However, for a depth equal to the sand layer thickness the vibration reduction provided by both of them is

almost the same. Moreover, as mentioned before, for trench depths bigger than 1.5 m the isolation level of the sheet piling trench keeps constant.

- Since its refraction coefficient is smaller (see Table 4), a concrete in-filled trench is much more efficient than a polyurethane one. In contrast, for low depths, their effectiveness is similar. In fact, the concrete in-filled trenches isolation level has resulted to be very sensitive to depth.

From these ideas, two main conclusions have been reached:

- It has been clarified that void trenches are more effective than in-filled ones. It has been seen that for a depth equal to the sand layer thickness, the reduction level for both of them is similar. However, the sheet piling trench presents a better structural stability and a depth of 1.5 meters may be a suitable solution for the problem.
- It has been confirmed that the refraction coefficient is highly influent in the effectiveness of an in-filled trench. However, from figure 12 the next situations can be considered:
 - If $c_{ij} < 1$, i.e. the material trench is stiffer than soil. Vibration reduction is achieved and a big reduction is provided if the coefficient is near zero.
 - If $c_{ij} > 1$, i.e. the material trench is softer than soil. Vibration reduction is also given but not so much as in the previous situation since in the present case reflection phenomenon does not occur.
 - If $c_{ij} = 1$, no vibration reduction is given since no discontinuity is located in the soil structure.

From that, it is well known that the best materials to be used for in-filled trenches are the stiffer ones as concrete is. In contrast, short

concrete in-filled trenches have to be disposable. Their reduction level is similar to the polyurethane one which has the same magnitude order as the reference situation. With that, a 2 meters deep concrete in-filled trench may also be a suitable solution for the analyzed cross section since it provides an adequate vibration reduction and it has a very stable structure.

5. Conclusions

A finite element model for the prediction of railway ground vibration has been developed and validated with real data. For the analysis, the Rayleigh damping approach has been adopted. Wave transmission condition has been respected and the results are valid for a frequency range from 2 to 50 Hz. The modeled track has been subjected to quasi-static load and applied for the analysis of different configurations of wave soil barriers. From the presented results, the following conclusions can be drawn:

- Regarding the characteristics of a wave barrier and in ascending order of their influence on its effectiveness, the parameters which have been studied are: width, depth and barrier typology.
- The increase of the barrier width within sensible values for urban areas does not affect excessively the vibration isolation provided by a trench. In consequence, non dynamic but practical design criteria have been proposed to choose the trench width in this paper.
- An increase of the trench depth for a layered soil indicates clear improvement of the isolation effect of the trench. Moreover, the optimum depth which provides the maximum isolation is given when the trench base is in contact with the surface bedrock base.

No more depth is needed since the trench effectiveness will not increase.

- Dense and stiff materials are the most suitable ones to be used for an in-filled trench since their function is based on the reflection of the surface Rayleigh waves.
- Open trenches are more effective than in-filled ones. A sheet piling trench avoids suffering from instability problems which an open trench may have. Moreover, it has been found that a sheet piling trench does not need to reach the bedrock base to achieve the maximum vibration isolation.

Acknowledgements

The authors would like to thank GTP for their permission to carry out measurements along the tram network of Alicante (Spain) and for providing the track cross sections. They would also like to thank the Spanish Ministry of Science and Innovation for their support given to the TRAVIESA project.

References

- [1] Gutowski T. G., Dym C. L. Propagation of ground vibration: A review. *Journal of Sound and Vibration*, Vol. 49, Issue 2, 1967, p. 179-193.
- [2] Verhas H. P. Prediction of the propagation of train-induced ground vibration. *Journal of Sound and Vibration*, Vol. 66, Issue 3, 1979, p. 371-376.
- [3] Kurweil L. Ground-borne noise and vibration from underground rail systems. *Journal of Sound and Vibration*, Vol. 66, Issue 3, 1979, p. 363-370.

- [4] Melke J. Noise and vibration from underground railway lines: Proposals for a prediction procedure. *Journal of Sound and Vibration*, Vol. 120, Issue 2, 1988, p. 391-404.
- [5] Metrikine A. V., Vrouwenvelder A. C. W. M. Surface ground vibration due to a moving train in a tunnel: two-dimensional model. *Journal of Sound and Vibration*, Vol. 234, Issue 1, 2000, p. 43-66.
- [6] Koziol P., Mares C., Esat I. Wavelet approach to vibratory analysis of surface due to a load moving in the layer. *International Journal of Solids and Structures*, Vol. 45, Issue 7-8, 2008, p. 2140-2159.
- [7] Sheng X., Jones C. J. C., Petyt M. Ground vibration generated by a harmonic load acting on a railway track. *Journal of Sound and Vibration*, Vol. 225, Issue 1, 1999, p. 3-28.
- [8] Zou J. H., Feng W. X., Jiang H. B. Dynamic response of an embedded railway track subjected to a moving load. *Journal of Vibroengineering*, Vol. 13, Issue 3, 2011, p. 544-551.
- [9] Cirianni F., Leonardi G., Scopelliti F. Study of the barriers for the mitigation of railway vibrations. *The Sixteenth International Congress on Sound and Vibration*, Kraków, 5-9 July 2009.
- [10] Wass G. Linear two-dimensional analysis of soil dynamic problems in semi-infinite layered media. Ph. D. Thesis, University of California, Berkeley, 1972.
- [11] Haupt W. A. Behaviour of Surface Waves in In-Homogeneous Half-Space with Special Consideration of Wave Isolation. Ph. D. Thesis, University of Karlsruhe, Karlsruhe, 1978.
- [12] Segol G., Lee P. C. Y., Abel J. F. Amplitude reduction of surface-waves by trenches. *Journal of the Engineering Mechanics Division-ASCE*, vol. 104, Issue 3, p. 621-641, 1978.

- [13] May T. W., Bolt B. A. The effectiveness of trenches in reducing seismic motion. *Earthquake Engineering & Structural Dynamics*, Vol. 10, Issue 2, 1982, p. 195-210.
- [14] Beskos D. E., Dasgupta B., Vardoulakis I. G. Vibration isolation using open or filled trenches. *Computational mechanics*, Vol. 7, Issue 2, 1989, p. 137-148.
- [15] Barkan D. D. *Dynamics of Bases and Foundations*. New York: McGraw-Hill, 1962.
- [16] Richart F. E., Hall J. R., Woods R. D. *Vibration of Soils and Foundations*. Englewood Cliffs: Prentice Hall, 1970.
- [17] Ahmad S., Al-Hussaini T. M. Simplified design for vibration screening by open and in-filled trenches. *Journal of Geotechnical Engineering-ASCE*, Vol. 117, Issue 1, 1991, p. 67-88.
- [18] Thompson D. *Railway Noise and Vibration*. Oxford: Elsevier, 2009.
- [19] Fuyuki M., Matsumoto Y. Finite difference analysis of Rayleigh wave scattering at a trench. *Bulletin of the Seismological Society of America*, Vol. 70, Issue 6, 1980, p. 2051-2069.
- [20] Woods R. D. *Screening of Elastic Surface Waves by Trenches*. Ph. D. Thesis, University of Michigan, Michigan, 1967.
- [21] Graff K. F. *Wave Motion in Elastic Solids*. Oxford: Dover, 1991.
- [22] Andersen L., Jones C. J. C. Three-dimensional elastodynamic analysis using multiple boundary element domains. ISVR Technical Memorandum, University of Southampton, 2001.
- [23] Anacleto S. *Modelización de la Interacción Vía-Tranvía*. M. Sc. Thesis, Universitat Politècnica de Catalunya, Barcelona, 2009.
- [24] Andersen L., Nielsen S. R. K. Reduction of ground vibration by means of barriers or soil improvement along a railway track. *Soil Dynamics and Earthquake Engineering*, Vol. 25, Issue 7-10, 2005, p. 701-716.

CHAPTER 3

STUDY OF RAILWAY GROUND VIBRATIONS CAUSED BY RAIL CORRUGATION AND WHEEL FLAT

J. I. Real, A. Galisteo, T. Asensio, L. Montalbán

*Vibroengineering. Journal of Vibroengineering, December 2012.
Volume14, Issue 4. ISSN 1392-8716*

Abstract

Over the last few years, railway has reached high relevance in cities causing trouble to citizens in form of noise and vibration in the surrounding buildings. Furthermore, these vibrations reach higher values when wheel-rail contact defects appear. The influence that two vibration sources derived from the wheel-rail contact have in their proximity is analyzed in this paper, particularly the defects of rail corrugation and wheel flats. Both defects are examined using the 3D finite element model discussed in a previous paper. The model has been developed and validated with real data and considers a train moving at subsonic speed. The analysis is carried out in the time domain, considering both the quasi-static and dynamic loads and applying dynamic loads to simulate the aforementioned defects. Conclusions are drawn based on the geometric characteristics of the imperfections. Thus, the results of this paper show that, concerning to the wheel flat, an important increase of acceleration peaks near the railway track is observed. Regarding corrugation, it is concluded that the lower corrugation wavelength, the higher vibration amplitude is reached. This work presents a validated method to relate wheel-rail defects to railway vibrations. It may be very useful in identifying the origin of vibrations and to determine which element needs maintenance works.

Keywords: ground vibration, railway track, corrugation, flat wheel, wavelength.

1. Introduction

Ground vibration from railway traffic is generated either by the static axle loads moving along the track or by the dynamic forces which arise in the presence of harmonic or non-harmonic wheel and rail irregularities. The most important frequency range of ground vibration considering human exposure is approximately 5-80 Hz. The excitation by the so called quasi-static axle loads primarily leads to low frequency vibrations. The frequency content of the dynamic excitation is determined by the speed of the vehicle and the wavelength content of the irregularities exciting the wheel-rail contact patch. On a given location, the vibration amplitudes are strongly influenced by the properties of the ground and hence the vibration problem must be seen as an interaction between vehicle, track and ground.

The importance of wheel and rail imperfections is clear when considering the dynamic excitation of ground-borne vibration. In presence of wheel and rail imperfections, the nominal contact forces are disturbed and a dynamic component is introduced into the excitation. In case the contact surface contains a discontinuity, e.g. a wheel flat or rail corrugation, the dynamic excitation is an impulse excitation. The dynamic excitation excites all propagating modes in the ground within the frequency range of the excitation.

Both wheel flat and rail corrugation defects result in an impact excitation on the rail which tends to grow with the size and/or depth of the discontinuity. In references [2-4], measured impact loads excited by wheel flats and long wavelength defects are presented. The results show that load increases with the length of the flatness and the depth of the periodic defect. Furthermore, influence of speed is understood clearly for periodic defects where higher speeds lead to higher forces.

However, regarding wheel flats, the speed dependence seems to be more complicated and varies for flats of different size. In [5] measured and simulated contact forces caused by a 100 mm long flatness show that the speed dependence varies with the axle load and the maximum contact force is excited in the 25-50 km/h speed range. The contact force excited by a long (0.5 m) local defect, on the other hand, shows a simpler speed dependence with a more or less linearly increasing contact load with increasing speed. The more complicated behaviour of the contact force generated by a wheel flat is caused by the potential loss of contact between wheel and rail, which is governed by the size and depth of the flat, the speed and the axle load [6, 7].

Previous studies on wheel-rail contact forces and the influence of wheel and rail defects have primarily focused on damage on rails and wheels and noise. When estimating the influence on ground vibration, the frequency content of the excitation needs to be known and compared with the track and ground response.

2. 3D FE model

A three-dimensional finite element model (FEM) has been developed for the study of ground vibrations caused by wheel-rail defects. The resulting model is based on the geometry and material characteristics of a specific railroad stretch of the tram network in Alicante (Spain), where real data for calibration and validation were measured and registered.

The FEM analysis was performed using ANSYS LAUNCHER software and Rayleigh Damping Theory was considered [1]. Since studied static loads are originated by trains self-weight and dynamic loads from wheel-rail defects, only vertical actions were considered.

The railway structure modelling is determined as a simplification of the real elements placed in the tram section selected for calibration and validation. A detailed view of the 3D model is represented in Figure 1, as a result of it.

In order to dimension the finite element model, a frequency range from 2 to 50 Hz has been set as the limiting parameter. This range includes large part of the frequency which is relevant to the whole internal body perception. Considering elastic vibration theory, the wavelength that restricts the minimum length of the entire model is approximately 50 m. Moreover, the length of elements is lower than 0.5 m. This length was calculated so that 6 nodes were present per wavelength of the Rayleigh waves at the highest frequency [8]. It is also remarkable the fact of using symmetry conditions to avoid the half of the total elements, thus reducing the computational time.

With respect to the sensitivity analysis, calibration and validation, an exposition can be found in [1].

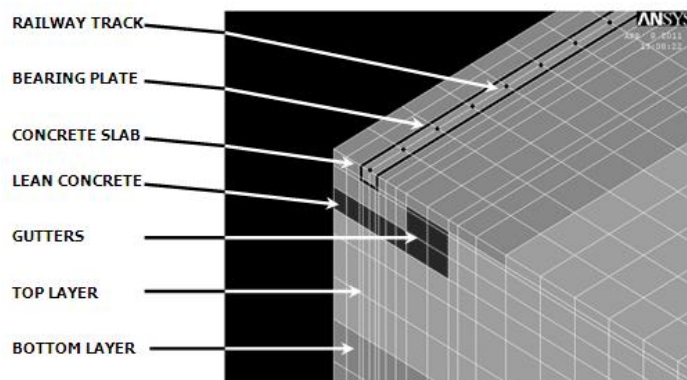


Fig. 1. Mesh and different zones of the simplified model.

3. Wheel flat modelling

3.1. Theoretical approach

One of the discrete defects which affects to railway wheels is the presence of wheel flats phenomenon. A wheel flat has its origin in high loads due to wheel-rail contact. These loads are continuously varying their module and position through the wheel path in curves, acceleration and braking zones or local railway track defects. These circumstances result in a modification of the wheel shape, often resulting in wheel flats, which cause an important increase over the static track loads.

As explained in [9], contact loads reach their maximum at speeds about 20-30 km/h, decreasing at higher speeds up to 100 km/h.

Wheel flats are an important vibration source whose dynamic effects are transmitted far away from the source, since they are a low frequency excitation. In their transmission they cause new problems activating vibration frequencies in the railway track and the soil and producing resonance effects if the new vibration modes match with some characteristic vibration mode of the railway system. The wheel flat frequency depends on the wheel shape and the train speed, as follows in equation (1):

$$f_{pr} = \frac{v}{2\pi r} \quad (1)$$

where v is the train speed and r is the wheel radius.

The wheel movement is assumed to be as shown in Figure 2. The wheel initially rolls around the first corner that contacts the rail, and then the second corner hits the rail, producing overloads.

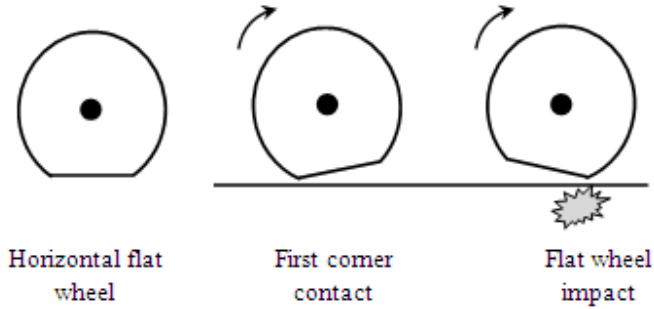


Fig. 2. Flat wheel movement.

Another significant parameter is the residence time t_R , which represents the time interval between the appearance of the first corner contact and the wheel flat impact. It is calculated according to equation (2).

$$t_R = \frac{d}{v} \tag{2}$$

where d is the horizontal wheel flat length.

3.2. Estimation of impact strength

Schramm formulation was used to solve the problem, determining the extra dynamic load produced by a wheel flat, commonly used in conventional railway track design. This dynamic overload has the expression shown in equation (3).

$$\Delta\sigma = \frac{15766 + 1.1Q\sqrt{f}}{W} \quad (3)$$

where Q is the load per wheel in N ($Q = 45.000$ N), f is the flat wheel depth in mm (a common value is $f = 2$ mm), and W is the resisting moment of the rail in cm^3 ($W = 438.22 \text{ cm}^3$). Applying to equation (2) the aforementioned parameters, a dynamic overload of $\Delta\sigma = 1.956 \cdot 10^8$ Pa was obtained.

In order to obtain the transmitted force by the wheel flat, it is necessary to estimate the wheel-rail contact area. It was achieved using the Hertzian contact model, which considers the contact region as a rectangle, calculated as follows.

The transversal size is directly $2b = 13$ mm.

The longitudinal size is calculated using equation (4):

$$2a = 2 \cdot 1.52 \sqrt{\frac{Qr}{2bE}} \quad (4)$$

where E is the wheel Young's modulus, in this case $E = 2.1 \cdot 10^7$ Pa. It results in a longitudinal dimension of $2a = 9.56 \cdot 10^{-3}$ m.

Hence, the contact area is given by equation (5):

$$S = 2a \cdot 2b = 1.243 \text{ cm}^2 \quad (5)$$

Finally, the total transmitted force per wheel due to the wheel flat is shown in equation (6):

$$F = S \Delta\sigma = 24309 \text{ N} \quad (6)$$

representing about the 50% of the static self-weight transmitted by the tram ($Q = 45.000 \text{ N}$).

3.3. Simulation and results

Before explaining the simulation process, it is important to consider the limitations of the model with regard to the wheel flats. Since loads can only be applied in the nodes of the track model, the phenomenon simulated must present a repetitive behaviour according to the distance between nodes. Specifically in this model, only wheels with a perimeter multiple of 0.5 could be studied.

Two different kinds of forces were modelled. On the one hand, static loads were modelled in every node belonging to the wheel-rail contact region. On the other hand, since a new effect is required to be considered in the model, an impulsive force was introduced simulating the wheel flat defect, according to equation (2). This new force had associated a short application time, considered as 0.001 s, and a module, calculated in the preceding subsection. A 1.50 m wheel perimeter has been supposed, making the dynamic load to actuate every 3 nodes.

The input loads are illustrated in Figure 3, which shows the force transmission diagrams of every node depending on time.

Furthermore, a new frequency appears because of the application of the dynamic force every 3 nodes. The new frequency, considering a tram speed of 30 km/h, is calculated in equation (7):

$$f_{pr} = \frac{v}{2\pi r} = \frac{30/3.6}{1.5} = 5.56 \text{ Hz} \quad (7)$$

This frequency was part of the response registers.

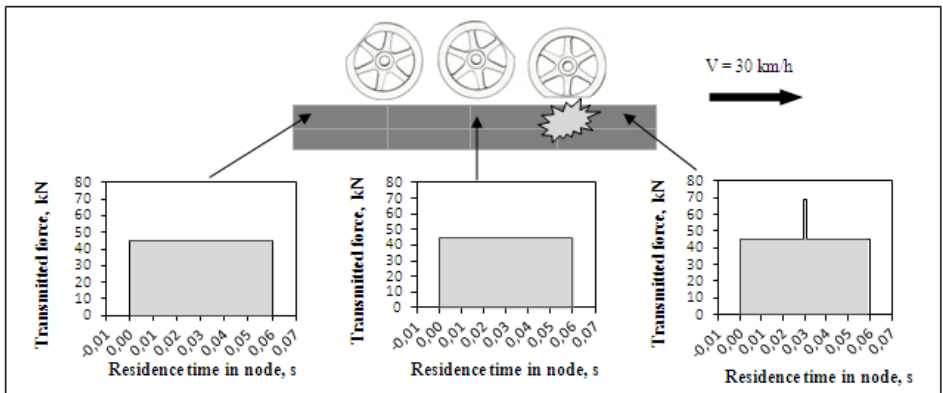


Fig. 3. Introduction process of different loads

The results of the developed model are given in Figure 4, where the model response for two different points is displayed. The locations of the points are 0.3 m from the track in the left graphic case, and 3 m from the track in the right one. Furthermore, the envelopes of the simulation without wheel flat defects are displayed in these graphics, so a comparison between the effects of two different wheel states in ground vibrations may be observed.

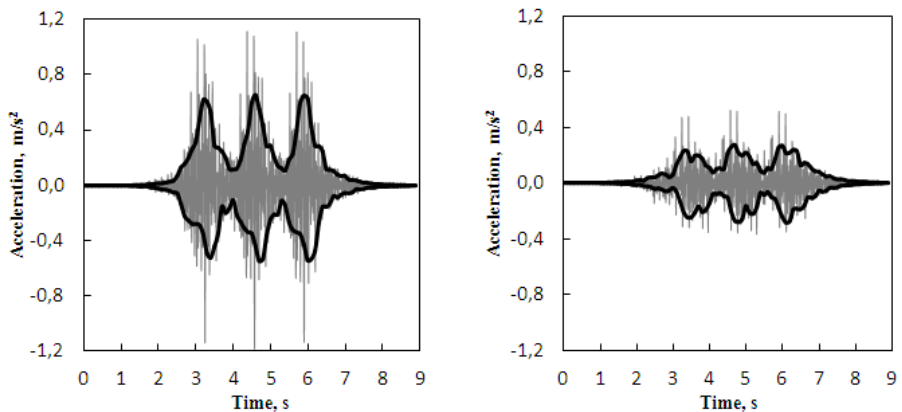


Fig. 4. Accelerations at 0.30 m (left) and 3m (right) from the railway track for different wheel states: Wheel flats (gray), wheel without defects (envelope black).

As can be noticed, wheel flats cause an increase in the magnitude response. Furthermore, the attenuation of the ground vibration as the distance from the track increases may be observed.

4. Railway corrugation modelling

4.1. Theoretical approach

Corrugation is a pathology which affects the top of the rail. It is visually identifiable and maintains a relatively constant wave geometry. The wavelength of rail corrugation varies from 25 mm to 1500 mm, but not all the wave lengths can be simulated by the proposed model. Since every wavelength has to be simulated at least by two consecutive nodes, the minimum wavelength L_m which can be simulated by the model is:

$$L_m = 2d \quad (8)$$

where d is the distance between two consecutive rail nodes.

The model was used to calculate two wavelengths: 1 m and 0.5 m, thus obeying the frequency precision requirement in 2-50 Hz range.

The residence time t_R must be also calculated according to equation (2).

4.2. Dynamic overloads calculation

Since a model that estimates the dynamic overloads because of corrugation is needed, the calculation has been based on an auxiliary quarter car model from [10], as shown in figure 5.

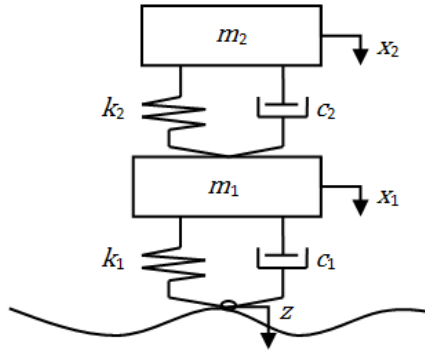


Fig. 5. Quarter car model based on model from [12]

The aforementioned model leads to the following equations of motion:

$$m_2 \ddot{x}_2 + c_2(\dot{x}_2 - \dot{x}_1) + k_2(x_2 - x_1) = 0 \quad (9)$$

$$m_1 \ddot{x}_1 + c_2 \dot{x}_2 + (c_1 + c_2) \dot{x}_1 - k_2 x_2 + (k_1 + k_2)x_1 - c_1 \dot{z} - k_1 z = 0 \quad (10)$$

where m_i , c_i and k_i correspond to the mass, viscous damping and stiffness of each i mass. x_i , \dot{x}_i and \ddot{x}_i correspond to position, velocity and acceleration of each i mass.

The above equations have been solved following indications in [10] with an algorithm implemented in the software *Mathematica*, whose inputs are the train velocity v , corrugation wavelength L and defects

amplitude A . In this way, the railway track is defined as a sinusoidal function.

The values of the parameters used in the model equations are given in table 1. They correspond to a tram configuration with a concrete mounted track.

Table 1. Parameters for characterization of system mass and vehicle damping

m_1 (kg)	k_1 (N/m)	c_1 (N·s/m)
500	32000000	0
m_2 (kg)	k_2 (N/m)	c_2 (N·s/m)
4000	501745	875

Depending on its corrugation wavelength, two different cases have been analyzed. Their input parameters and dynamic responses are shown in tables 2-3 and figures 6-7.

- Case 1: 0.5 m element size $\rightarrow L=2 \cdot 0.5=1$ m
- Case 2: 0.25 m element size $\rightarrow L=2 \cdot 0.25=0.5$ m

Table 2. Input parameters for case 1 solving

v (km/h)	L (m)	A (m)
30	1	0.0005

Table 3. Input parameters for case 2 solving

v (km/h)	L (m)	A (m)
30	0.5	0.0005

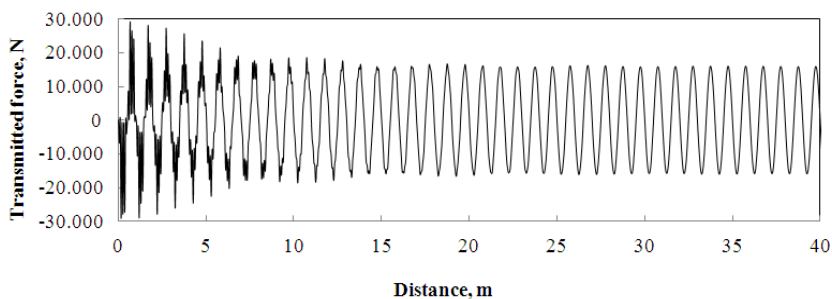


Fig. 6. Transmitted force to the track by a wheel in a track with corrugation defect of 1 m wavelength and $5 \cdot 10^{-4}$ m amplitude.

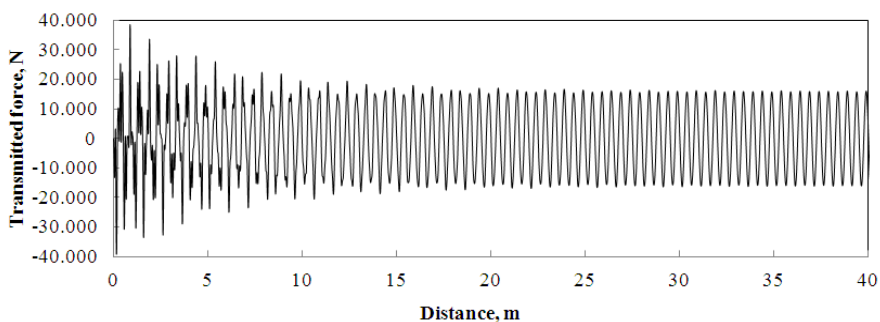


Fig. 7. Transmitted force to the track by a wheel in a track with corrugation defect of 0.5 m wavelength and $5 \cdot 10^{-4}$ m amplitude.

4.3. Simulation and results

In the present simulation two simultaneous loads were considered: dynamic loads due to imperfections, which are sinusoidal with a varying wavelength depending on the corrugation and an estimated magnitude of 16 kN, and static loads due to the tram self-weight, which are constant and equal to 45 kN. The superposition of both types of loads is illustrated in figure 8.

Moreover, a load step distribution was supposed in order to simplify the model. The force applied in every node is considered to be constant, with a value of 29 kN or 61 kN, depending on the node situation as figure 9 shows, based on superposition of figure 8.

The following figures show the model responses obtained with the 3D finite element model. The responses were measured in two different points, one of them in the concrete slab (located 0.30 m far from the track) and another one in the soil (located 3 m far from the track).

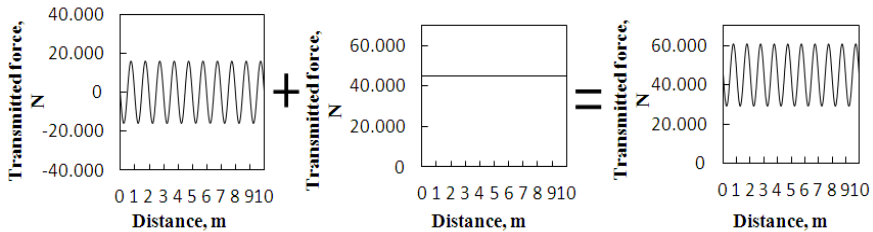


Fig. 8. Superposition of loads transmitted to the track. Dynamic and static loads

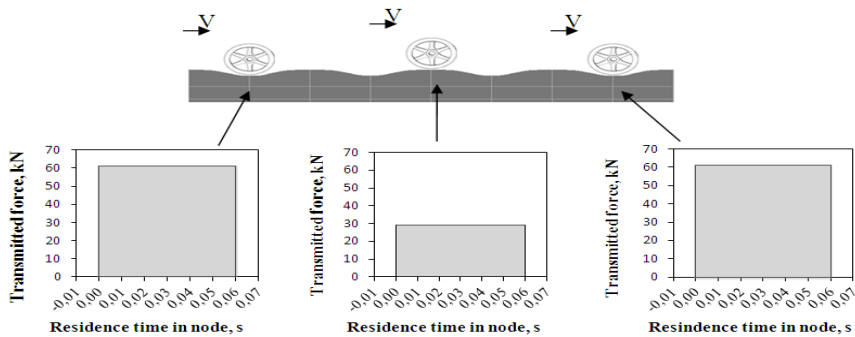


Fig. 9. Process of load introduction.

The solution is given for two cases depending on the wavelength of the defects.

- Case 1: Wavelength of defects = 1 m.
- Case 2: Wavelength of defects = 0.5 m.

As it may be seen in figures 10-11, higher acceleration values are obtained in the railway track model with imperfections. Furthermore, referring to the frequency of the acceleration peaks obtained, it is higher for lower wavelength defects.

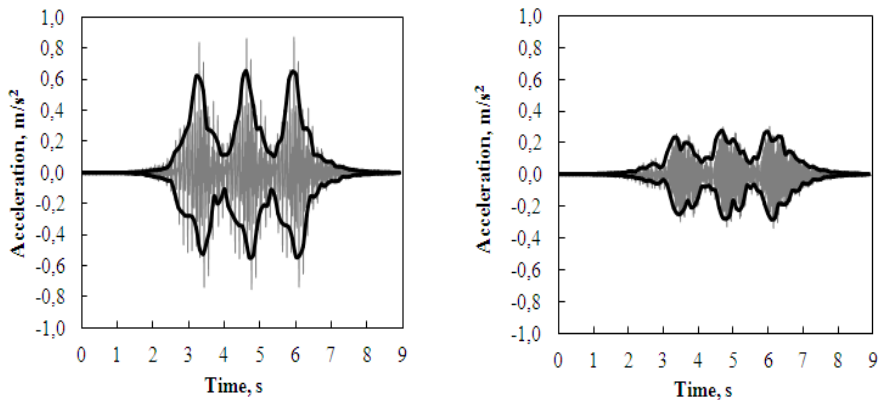


Fig. 10. Accelerations obtained at 0.30 m (left) and 3 m (right) from the track. Corrugation with a wavelength of 1 m and an amplitude of $5 \cdot 10^{-4}$ m (gray) is displayed beside the envelopes of a track in perfect conditions (black).

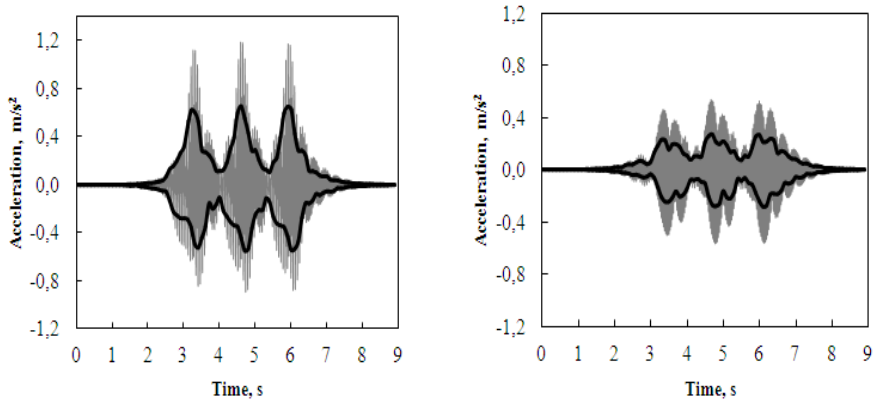


Fig. 11. Accelerations obtained at 0.30 m (left) and 3 m (right) from the track. Corrugation with a wavelength of 0.5 m and an amplitude of $5 \cdot 10^{-4}$ m (gray) is displayed beside the envelopes of a track in perfect conditions (black).

Regarding acceleration values, it has been proved that acceleration peaks are higher when corrugation wavelengths are lower. However, this fact (shown in figure 12) do not depend on the load values, as these values were the same from the wavelength of the defects.

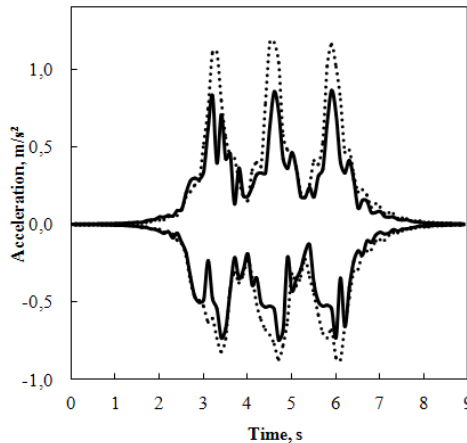


Fig. 12. Acceleration envelopes obtained at 0.3 m from the track for different wavelengths. Wavelength defect = 1 m (continuous line), wavelength defect=0.5 m (dashed line).

5. Conclusions

Wheel flats and rail corrugation have been analyzed with the developed finite element model. The results are valid for a frequency range from 2 to 50 Hz. The model considers static loads belonging to the train mass and different dynamics loads produced by both phenomena. From the analysis of the results, the following conclusions can be drawn:

1. The effect caused by wheel flats in railway ground vibrations has been evaluated using Schramm formulation. These defects produce an important increase in the magnitude response, producing high acceleration peaks when the flat wheel impacts on the rail.
2. The effect of rail corrugation in railway vibrations has been taken into account using a quarter car model. The frequency of the acceleration peaks becomes higher when the wavelength of corrugation decreases, since the acceleration peaks are closer.
3. In terms of magnitude, acceleration peaks in a corrugated railway are higher when corrugation wavelengths are lower. It could also be said that the acceleration peak increases with the track frequency of acceleration peaks.

References

- [1] J. I. Real, A. Galisteo, T. Real, C. Zamorano. Study of wave barriers design for the mitigation of railway ground vibrations. *Journal of Vibroengineering*, Vol. 14, Issue 1, 2012, p. 408-422.
- [2] M. Heckle et al. Structure-borne Sound and Vibration from Rail Traffic. *Journal of Sound and Vibration*, Vol. 193, Issue 1, 1996, p. 175-184.
- [3] X. Sheng, C.J.C. Jones, D.J. Thompson. A comparison of a theoretical model for quasi-statically and dynamically induced environmental vibration from trains with measurements. *Journal of Sound and Vibration*, Vol. 267, Issue 3, 2003, p. 621-635.
- [4] L. Auersch. The excitation of ground vibration by rail traffic: theory of vehicle-track-soil interaction and measurements on high-speed lines. *Journal of Sound and Vibration*, Vol. 284, Issue 1-2, 2005, p. 103-132.
- [5] Johansson. Out-of-Round Railway Wheels. Assessment of Wheel Tread Irregularities in Train Traffic. *Journal of Sound and Vibration*, Vol. 293, Issues 3-5, 2006, p.795-806.
- [6] J.C.O. Nielsen, A Igeland. Vertical dynamic interaction between train and track. Influence of wheel and track imperfections. *Journal of Sound and Vibration*, Vol.187, Issue 5, 1995, p. 825-839.
- [7] A. Johansson, J.C.O. Nielsen. Out-of-round railway wheels – wheel-rail contact forces and track response derived from field tests and numerical simulations. *Journal of Rail and Rapid Transit*, Vol. 217, Issue 2, 2003, p. 135-146.
- [8] Andersen L., Jones C. J. C. Three-Dimensional Elastodynamic Analysis Using Multiple Boundary Element Domains. ISVR Technical Memorandum, University of Southampton, 2001.
- [9] Hirano, M. (1972). Theoretical Analysis of Variation of Wheel Load. *Railway Technical Research Institute Quarterly Reports*, Vol. 13, Issue 1, 1972, p. 42-44.

- [10] M. Melis. Introduction to vertical dynamics of railway tracks and to digital signals in trains. School of Civil Engineering, Madrid, Spain, 2008.

GENERAL DISCUSSION

Discussion is divided in three points.

In the first point, devoted to the analytical modeling of the phenomenon of generation-transmission of vibration (which corresponds to the discussion in Chapter 1 of this Thesis), aspects related to the state of the art linked to the definition of the model are addressed. Additionally, the studied section and its modeling are presented; the governing equations of the phenomenon (equation of Timoshenko beam and vector wave equation) are introduced; boundary conditions are described; load implementation process developed in this chapter is extended and, finally, the resolution of the problem and the calibration and validation processes of the results using real data measured on track are presented.

The second point, devoted to the numerical modeling analysis of the phenomenon, is structured into two sub-points: the first one discusses the creation process of the numerical model (which would be comparable to what has been described in the analytical model, but deepening in specific aspects of the finite element method). The second one (with the model already developed, calibrated and validated), shows the simulations performed. In this regard, both extraordinary phenomena of vibrations generation caused by specific pathologies of the wheel or the rail as well as the mitigation effect of wave barriers in the propagation of railway vibrations are studied. The discussion included in this second point is applied to the cases studied in chapters 2 and 3 of the Thesis.

Finally, in a third point, reflections related to the main contributions of this PhD Thesis are stated. Moreover, the current and future work lines that are being followed by the workgroup, to which the author of this Thesis belongs, are presented.

Analytical Modelling of the Phenomenon.

In chapter 1 of the present work, the analytical study of the phenomenon of vibration generation and its transmission across the track is addressed.

This publication is the result of a research line whose first result was the paper “A procedure for the evaluation of vibrations induced by the passing of a train and its application to real railway traffic” (2010)

developed in a track section located in the high-speed line Madrid-Barcelona (KP 452+062). It is a ballasted track with international track width and UIC-60 rail mounted on monoblock concrete sleepers AI-99. The elastomeric railpad stiffness is 100 kN/mm and its thickness is 7mm. The railway superstructure rests on a subballast layer on the top of the embankment.

In 2011 the published paper “Modelling vibrations caused by tram movement on slab track line” worked on a track tram section of the line 1 of the TRAM network of Alicante. In this case, the studied section configuration was a concrete slab with Phoenix 37N rail embedded in dropped elastomer Edilon.

Finally, regarding to the work presented in chapter 1 of this Thesis, a metric track section located in Santander-Liérganes line of the extinct FEVE (whose infrastructure was integrated into ADIF's network in 2013) is used. Specifically, the studied section is located in the Orejo-Liérganes stretch, at the Solares station, 20 Km away from Santander. It is a metric-width ballasted track, with wooden sleepers and UIC-45 rail. The track has rigid fasteners, metal railpads and approximately has expansion joints every 36 m. Ballast layer rests directly on the foundation, without subballast intermediate layer.

Note that this investigation line is developed in very different scenarios. While the first case introduces a last generation track, in the second case a tram track is chosen. The tram track is more difficult to model and has been less studied but it has great importance given by the impact of the vibration as railway externality in urban environments. In the third case, an “old scenario” is chosen with a track in worse conditions (but not less important) because it represents the actual situation of lots of different tracks in Spain and all over the world.

When the section of study is chosen, it is necessary to model this reality to establish the governing equations of the generation and transmission phenomena of railway vibrations.

In chapter 1 of this Thesis as well as in previous publications, a bidimensional model is chosen in the vertical plane along the longitudinal track direction. This 2D domain is in which the different model equations are implemented. Regarding this simplification, the

different elements comprising the track structure have been modelled with a determined number of horizontal layers. In all models, the deepest layer is considered of infinite thickness and is modeled as a Boussinesq half-space. Hence, the bottom constraints have no influence in the model results. With the adopted coordinate system is not feasible to establish a 3D model. It would be possible if the equations in a cylindrical coordinate system were used, and it would permit the application to other type of infrastructure (e.g. a tunnel of circular cross section). In this case it could be possible to simultaneously study the three phenomena involved in the problem: generation-transmission and propagation of vibrations.

The importance of this publication in the compendium of this PhD Thesis is to stand out the little achievements that can be obtained with the analytical modeling. These achievements have been collected in the three publications listed in the preceding paragraphs and have justified its publication, following the same methodological approach.

Regarding the number of the layers of the model, the evolution along time and investigation advances play an important role. The studied section in the publication “A procedure for the evaluation of vibrations induced by the passing of a train and its application to real railway traffic” is modeled using two layers. The first one represents the track constituted of rail, rail pads, sleepers and ballast layer, with the same thickness as the ballast layer; while the second one accounts for the underlying terrain to the previous elements. This model is highly limited as consequence of the importance of considering all the track elements as a whole, being impossible to discern the vibration level in each one of the track elements.

The section studied and published in “Modelling vibrations caused by tram movement on slab track line” is modeled with three different layers. In this case, since it is a tram section, special attention has been paid to the model that represents the embedded rail into the slab together with the elastomeric material. In this manner, the first layer corresponds to the concrete slab; the second one is made of the same concrete as the first one but including the rail and the elastomeric element and the third one represents a lower strength concrete which rests on a lean concrete layer.

Although this publication provides a higher level of detail which is reached by incorporating more layers in the domain, there are still limitations. For example, the rail and elastomer have the same vibration level, which does not happen in reality.

In the publication of chapter 1 of this Thesis a more exhaustive model is performed. In figure 2 of this chapter, the layers to which the domain has been reduced are shown and its typology as well.

Note that in this case it is achieved to divide the domain into 5 different layers. The rail is located on the top of all of them. The first layer represents the railpads and the second one represents the wooden sleeper behavior. Now it is important to point out the fact that both elements are discrete elements and it has been necessary to transform the thickness of these layers to equate the vertical behavior of those elements to reality. The third layer corresponds to the ballast and the fourth one represents the first ground stratus, which is limited at the bottom by a second stratus of infinite thickness.

As can be easily observed, in chapter 1, the level of detail is higher than in previous publications. Obviously, this fact involves a major mathematical complexity but is able to determine the vibration level of the most important elements in the structure, differentiating between rail, railpad and sleepers.

Hitherto, the discussion has been focused on how to simplify the chosen domain. Then, the modeling of the rail is addressed. This point is especially important because it is on the rail where the vibration generation takes place.

Both Metrikine (2000) and Koziol (2008) decided to model the rail as an Euler-Bernouilli beam. One of the variations introduced in chapter 1 of this Thesis and in previous publications is the use of the beam of Timoshenko to model the rail. The main advantage of Timoshenko is that considers deformations caused by shear stresses, which can be important in secondary bending of the rail. However, the fact that the rail is considered continuously supported does not allow calculating the secondary bending. This problem has been overcome by calculating the secondary bending aside from the model and introducing it as an additional external excitation.

At this point it is convenient to reflect on the existence of possible interesting differences between both types of modeling. In this sense, Knothe and Grassie (1993) established that shear deformation can be neglected in analyses performed at frequencies below 500Hz. Subsequently, Dahlbert (1995) established that for frequencies below 500Hz, the theory of Euler-Bernoulli provides acceptable results, whereas for frequencies above 1000Hz, the differences between both theories become 30%.

Thus, in order to avoid the possibility of restricting the utility of the model to frequencies below 500Hz, it was decided to model the rail following the Timoshenko's beam theory. Although the frequencies studied in this article allow modeling the rail by the theory of Euler-Bernoulli, this decision was made in order to provide a proper application to demonstrate the accuracy of the model and to use it for future research.

Moreover, given the importance of this topic, it has already become a new investigation line in which many members of the Institute of Multidisciplinary Mathematics which includes the author of this Thesis are collaborating at the moment. This new research will focus on analyzing how affects the theory of beams used in the modeling to the results that can be obtained from the model.

Regarding the modeling of other layers which constitute the track, following the example of Metrikine (2000) and Koziol (2008), it is considered that the rest of the layers of the track have a visco-elastic behavior. In order to represent this fact, the movement equation used in every layer is the wave equation explained in chapter 1 of this Thesis in vector form.

The previous equation stands out that, in addition to the displacement vector (that in this case will only have two components as a consequence of the bidimensional domain adopted), the density of the material and the $\hat{\lambda}$ and $\hat{\mu}$ factors which describe the visco-elastic behavior of the material, play an important role in the wave equation.

Both $\hat{\lambda}$ and $\hat{\mu}$ factors are calculated/estimated using two mathematical expressions with two terms. The first term, known as the Lamé parameter, represents the elastic behavior of the material and is

calculated using the elasticity modulus and the Poisson ratio of the material. The second term, known as damping coefficient, simulates the viscous behavior of the material. In contrast to the first term, in the second term it does not exist any mathematical formulation to calculate its value. Those values must be calibrated along the mathematical process, and consulting experimental works to estimate an acceptable order of magnitude.

Any mathematical approach involves defining boundary conditions to satisfy, in addition to the own formulation of the problem. In this case, the following conditions are assumed:

Compatibility Conditions between layers: in the interfaces between the different layers which constitute the models, an equality of displacements and stresses (normal and shear) must exist, both in vertical and horizontal axis.

No displacements and no stresses (normal and shear) condition at the bottom boundary of the model. This condition is reached considering the bottom layer of the model as a Boussinesq semi-space of infinite thickness.

Once the premises for modeling the rail and track layers have been explained, it is convenient to point out the following: the rail is not modeled as an additional layer, but it is coupled to the modeled layers compatibilizing its boundary conditions. In this regard, the vertical stresses and displacements of the rail will be determined by the corresponding expressions of a Timoshenko beam. Moreover, a zero longitudinal displacement of the rail is imposed. This last assumption is in accordance with previous works of Metrikine (2000) and Koziol (2008) that have been followed in this chapter of the Thesis. The assumption of zero longitudinal displacement of the rail and the fact of coupled movements between rail and layers justify the reason why the longitudinal displacement is zero at $z = 0$.

At this point, it is important to think about the different track typologies described along this investigation and the influence of its characteristics in the model configuration. In chapter 1 it has been worked with a ballasted track. In these cases, the rail is located at the top of the model, resting over the first layer. The no-horizontal displacements condition will be accomplished at the top of the first

layer, and vertical displacements obtained will be equal to those calculated using the Timoshenko beam theory. At the rest of interfaces between layers, the compatibility conditions of displacements and stresses previously mentioned will be satisfied.

Different tracks lead to different models, for example in the case of tram tracks with embedded rail, the element representing the rail and the elastomer where it is embedded is placed in between the first and the second layer. In this manner, on the upper limit of the model, the no-stress condition of normal and shear stresses is accomplished. On the other hand, at the interface between the first and the second layer (which is where the element that models the rail will be located), the no horizontal displacements condition is also accomplished. Furthermore, vertical displacements are equal and will be determined by the deflection obtained from the Timoshenko beam equations.

The equations (16) of chapter 1 represent mathematically the boundary conditions previously described in these paragraphs.

When reflecting about the modelling of the applied loads (or those which may be applied) over the track, the possibilities are wide, as it is demonstrated following a “cronological order” of the developed investigation line. In the first publication about this topic “A procedure for the evaluation of vibrations induced by the passing of a train and its application to real railway traffic”, the following types of load (see the introduction of the Thesis in which the different loading mechanisms are classified) are taken into account: quasi-static load (corresponding to the passage of a load at a certain speed with a certain load axle and a certain constitution of axles and bogies, generically known as “physiological load due to vehicle”), load due to the secondary bending of the rail, caused by its discrete support (corresponding to one of the types of physiological load due to the track) and load caused by pathologies associated to the rail .

The so-called quasi-static load is introduced to the model using two mechanisms. On one hand, the static load (which is the axle load of the vehicle moving at a certain constant speed) is modeled by the method of Zimmermann and the theory of Pandolfo. On the other hand, the effect due to the configuration of axis and bogies of railway composition is represented by harmonic loads. By using this method,

those forces are simulated as $F_j(t) = P_j \cos(\bar{\omega}_j t)$, where F is the resultant load in the time for every load j ; P_j is the characteristic magnitude and $\bar{\omega}_j$ is the characteristic angular frequency for every load.

About the secondary bending, it cannot be reproduced using the model proposed (continuous rail resting on a layer) as it has been previously asserted, so it is necessary to introduce an additional strategy. It is assumed that the rail behaves as a Timoshenko beam and the study is particularized to an axle located in the middle of the span between two continuous sleepers. In this situation, neglecting the rotation of the adjacent sleepers, the deflection of the rail is theoretically calculated; which results in a harmonic function operated as in the previous case.

With regard to the load due to certain rail pathologies, this one is introduced in the model as a harmonic load represented by its characteristic magnitude and its characteristic angular frequency. It is important to consider that for an excitation repeated every wavelength λ , the characteristic angular frequency is calculated as $\omega = 2\pi V / \lambda$. In case of induced loads due to rail corrugation, if the profile is already known, this one is transformed to the frequency domain thanks to the Fourier Transform. From this moment, it is possible to detect the principal wavenumbers which origin the excitations and their corresponding amplitudes. Both phenomena (rail pathologies and generated harmonic forces) can be plotted in time and frequency domain, being possible to clearly identify the predominant frequencies for each one.

By doing so for every load, the response of the layers which idealize the rail pad, sleepers, ballast and subballast is analyzed, and the global system response will be the result of the sum of response obtained of every excitation. This procedure agrees with the superposition principle, which has also been adopted in this PhD Thesis.

In the second article published, previous to the work exposed in chapter 1 of the present Thesis, which is titled "Modelling vibrations caused by tram movement on slab track line", only the physiological loads due to the vehicle and pathological loads associated to the track

have been considered. It is because in concrete slab track (tram in this case) there is no secondary bending, as it has been previously explained. The formulation followed to model these loads is similar to the first publication formulation.

In the studied case of chapter 1 of the present Thesis, the different loads mentioned in the first publication have been considered again but an important advance on its processing has been achieved. To begin inserting the loads, the harmonic method described is used to introduce the static and dynamic loads in the model. Thus, for the case of static loads, the Zimmerman and Pandolfo formulations have been omitted, supposing the quasi-static load as harmonic with the same amplitude as the axle vehicle load and zero frequency (to the case of sinus-harmonic). It has been done in order to represent the invariability of the force amplitude over time, since it is a constant and permanent load. By proceeding this way, five harmonics have been obtained, four of them corresponding to dynamic loads with amplitudes ranging between 4.7 and 13.3 kN and frequencies between 5.7 and 21 Hz.

After the analysis of the processing of the different loads, the resolution of the analytical problem outlined is performed. As it has been exposed in previous paragraphs, the rector equations of the problem are the Timoshenko's beam theory to model the rail and the vector waves equation to represent the other layers behavior.

The analytical solution of the problem is addressed following to Koziol (2008). To do so, different mathematical operations are implemented to introduce an algebraic equation system which can be easily solved using the Kraemer's theory. This theory allows obtaining the displacements and stresses for every point of the structure and for every material layer in the frequency domain and in the wavenumber.

The next step is to apply the inverse Fourier Transform to the obtained expressions, but the complexity of these equations requires to assume several simplifier hypothesis that allow obtaining the solution in the time and space domain. The simplifications adopted are the following:

To fix $x=0$, in this manner the transient part of the resolution is neglected and it is assumed that the stationary solution is the one which defines the problem.

The z coordinate is fixed depending on the point desired to obtain the results. In such problems, the most interesting solution is for the surface and consequently, for this situation, $z=0$ is taken.

With these simplifications it is possible to obtain the vertical displacement of the ground surface. Deriving twice the mathematical expression of the vertical displacement respect to time, vertical accelerations are obtained.

After the analytical resolution of the introduced problem, the next step is to calibrate and validate the model.

The calibration consist of assigning different values to the unknown parameters, either by nature (for example, the visco-elastic damping coefficients of the different layers that constitute the model) or simply because it is not possible to have reliable data.

Nevertheless, prior to the calibration, it is necessary to know which parameters from the unreliable data are relevant for the model, namely, which ones have a real influence on the results calculated by the model. This task of the work is known as "Sensitivity Analysis of the Model".

In the case studied in chapter 1, it would be necessary to perform a wide sensitivity analysis. On the one hand, given that the domain has been divided into five different layers, it would be necessary to estimate the damping coefficients for each one. This work would involve ten different sensibility analyses, which is not viable, so the decision to assign the same damping coefficient to all layers is taken. It is important to consider that although these values are not specific to each layer, the assumption of equal values will represent the global model behavior due to the model will be calibrated and validated depending on these parameters.

On the other hand, as a consequence of the absence of recent tests in the track, the values of some mechanical characteristics of materials are unknown. Additionally, due to the poor conditions of the track, it is hard to estimate these values properly. To overcome this problem, the elasticity modulus and the Poisson's ratio of the ballast and the two ground layers are incorporated to the process.

In short, the sensitivity analysis of eight variables is done, which is considered as an appropriate approach to the problem, concluding that the relevant parameters are the damping coefficients (especially μ , which governs the vertical displacements) and the modulus of elasticity of the ballast and the upper layer of the ground.

After the sensitivity analysis used to identify the parameters that must be calibrated, the calibration process begins.

Basically, calibration includes the comparison of the results obtained by the model, fixing a value of the parameter to be calibrated, with the values measured by the device at the same point of the domain.

This comparison process has been developed in a qualitative manner. In chapter 1, the comparison is showed based on the following values:

- The maximum and minimum values of the acceleration peaks must be similar.
- The time measured between peaks must be similar
- The time between the beginning of the signal and the first peak must be close enough
- The attenuation time of the last peak must be similar in both cases

The model results are compared with measured vibration values in the rail, selecting data sets which were not significantly affected by background noise and those in which the train speed did not differ significantly from the average speed. Background noise is understood as all those vibrating components which are recorded during measurements in absence of railway traffic by the study section. This background signal can be caused by actions external to the railway which are close to the track, so that the sensors detect certain levels of unsuitable vibration. Therefore, the procedure is to measure several data series without railway traffic to obtain a signal representative of the background noise, and finally to separate this signal in the subsequent measurements made with railway traffic.

After this process, the previously unknown values of the four relevant parameters are set. These are: elasticity modulus of the ballast layer (calibrated value: $2 \cdot 10^7$ Pa), elasticity modulus of the upper ground layer (calibrated value: $5 \cdot 10^5$ Pa), visco-elastic parameter μ

(calibrated value: $5 \cdot 10^5$) and visco-elastic parameter λ (calibrated value: $4 \cdot 10^4$).

The next step is to validate the model. Again, the results of the model (with the values of the four parameters previously determined) are compared with another data series, different from the previous used to the calibration process. This can be found in Figure 6 of chapter 1, where the results obtained by the model are overlapped with the data measured on the track.

Note how satisfactory the adjustment is. The values of the positive acceleration peaks are practically the same, while the values of the negative acceleration peaks are overestimated by the model. The times of growth and attenuation of accelerations are very similar. Based on the previous comments, it is concluded that the analytical model is a suitable tool for predicting vibrations given that, in the worst case, the model always yields results on the safe side.

At this stage, we can affirm that the defined model is capable to reproduce the vibrations in the studied track. This is useful for predicting, for example, the vibrational behavior of the track considering a replacement of sleepers or railpads. The replacement of wooden sleepers for concrete sleepers leads to a considerable increase in vibration amplitudes, probably due to the increment of the vertical stiffness of the track. Then, the railpads replacement by others more elastic can be analyzed. This fact involves a very significant decrease of the amplitudes obtained.

Notice how it is only possible to model changes in the existing elements/layers. Nevertheless, if it would be necessary to analyze, for example, the influence of a layer of bituminous subballast in the vibrations attenuation, a new model should be created due to this element has not previously been taken into account. This is one of the most important limitations of this kind of models: only a few types of simulations are allowed.

Numerical Modeling of the Phenomenon.

This second part of the discussion will be divided into two clearly differentiated parts: at the first point of the discussion, the process followed to "create" a numerical model able of reproducing the phenomenon will be shown, and at the second one, several applications of the model are presented.

Creation of the Numerical Model.

In contrast to the analytical model analyzed in chapter 1 of the Thesis, the numerical modeling allows studying the phenomena of generation of vibrations in the wheel-rail contact, transmission of the same across the track section and propagation through the adjacent ground to the track at the same time.

One of the basic aspects to consider when modeling a track section with finite element models is to find the right balance between the computing time criteria and the required accuracy. Both are antagonistic and the relationship between them is not linear, which stands out the importance of considering this aspect. Usually, and this has been done in the present study, some "artifices" are tried to apply. Some examples of these "artifices" are to study only a part of the domain based on the application of symmetry respect to a specific axis or to apply different types of mesh according to the accuracy required in each area of the model. Thus, it would be carried out a "dense mesh" in the most requested areas and a "coarse mesh" in the less relevant, always making a smooth transition from one case to another and to prioritize the study of the vertical dynamics of the track to the detriment of the longitudinal and transverse dynamics according to the work object.

The first task to carry out in the process of creating a numerical model is the definition of the domain and mesh_of its elements.

In this regard, the work presented in chapters 2 and 3 of the Thesis has followed, as much as possible, the document "Recommendations for the project of railway platforms", written by the Ministerio de Fomento (1999). The different elements of the railway superstructure have been modeled replacing them by simpler figures but with identical mechanical behavior. In this context, the two most

complicated elements have been the rail (Phoenix 37N of 65 kilograms per linear meter) and the rail pad (model Edilon of 15mm thickness).

In the case of the rail, it is important to find a simple shape that faithfully represents its flexural strength. It is chosen a parallelepiped whose width matches with the width of the rail foot and whose vertical dimension is calculated by equating the moment of inertia, about the horizontal axis, of the original rail with the simplified parallelepiped.

With respect to the railpad (mechanically defined by its Young's modulus, Poisson's ratio and density), although the geometry is relatively simple, it has been necessary to modify its size in order to avoid introducing in the model elements with very different dimensions (this fact causes problems of numerical convergence). The criterion used to this substitution is to equal the stiffness values between the real and the modeled pad. This consideration forces to modify the elasticity modulus of the modeled pad (the rigidity of an element depends on its area, elasticity modulus and thickness). In short, a parallelepiped element of 50 mm thickness and with a fictitious elasticity modulus is employed.

The modeling of the concrete slab where the rails lies is relatively simple. It is a reinforced concrete HA-25 slab, with known values of Young's modulus, Poisson's ratio and density. A similar situation occurs with the layers of lean concrete and mass concrete located under the concrete slab.

About the modeling of the existing ground under the track, data obtained from the relevant geotechnical tests in the trace and geological map of the area are available. It is concluded that the ground is composed of an upper stratum of sand, with 2 m thickness, under which a wide layer of calcarenites is located. Nevertheless, to begin with the modeling process, a lower limit to the model must be fixed. Combining again the computing time criteria and accurate representation of the phenomenon to study, and following the Recommendations for the project of railway platforms written by the Ministerio de Fomento, the thicknesses of the lower stratus was set to 3.5 meters.

Note how the physical phenomenon of vibration generation and transmission through track package is, until this moment, the one which “leads” both the establishment of the vertical domain and the modeling process of the different elements that constitute the track section and the ground beneath the track (vertical dynamics of the track). Then, the propagation of vibrations in the adjacent ground occurs. In that moment, according to this physical phenomenon, the size of the domain is fixed in longitudinal and transversal directions from the track.

At this point, the first thing to consider is the frequency range to be studied. Since the main goal is to analyze how the railway vibrations affects people who live/work/transit in the track vicinity, the range from 2 Hz to 80 Hz should be the range chosen. It is documented that, in this environment, the human health is altered. Authors as Griffin (1990) make statements about this topic, even affirming that the most damaging vibrations are those between 2 and 50 Hz, being the vibrations from 50 to 80 Hz less harmful than the previous.

The lower value of the frequency considered, in this case 2 Hz, influences the parallel and perpendicular dimensions of the track’s model, because a full wavelength must be developed in these directions. As it has already been discussed in the introduction of this Thesis, the predominant mechanism of transmission of railway vibrations is the Rayleigh waves, whose speed depends on the ground characteristics trough which the waves are propagated. In the present case, the propagation speed is 110 m/s. Knowing that the maximum wavelength is given by the quotient of the propagation speed and the minimum frequency to be studied, it is obtained a maximum value of wavelength of 55 meters.

At this stage, it is convenient to reflect on the dimensions of the considered domain. Certainly, there is no clear consensus in this regard. As evidence, there are discrepancies among authors as Ekevid and Wiberg (2002), Connolly et al. (2013) and Hall (2003). Nevertheless, in the various publications studied, the location of the point where the results are obtained is particularly important because the dimensions of the domain are set depending on this location. It is done in order to avoid the influence of the domain dimensions on the results obtained in the point considered.

Given the interest of this specific point of the discussion, this aspect has been studied in depth modifying the original dimensions of the model and analyzing the results in different points of the domain in order to obtain a "minimum dimension".

The transversal dimension of the model (which original value was 50 meters) has been reduced to 40 meters and 30 meters, analyzing the influence of this reduction in the different points of model: in the rail and at several distances from it (1.20 m, 9.50 m, 14.50 m, 20 m and 29 m). It is verified that the domain size has no influence on the first cases (in the rail, at 1.20 m from the rail, at 9.50 m from the rail and at 14.50 m from the rail), given that the results are similar in all cases. The difference is perceptible when the results are obtained at 20 m and 29 m from the rail, since the accelerations obtained are amplified as the model size is decreased due to the existence of reflective phenomena.

In short, in this case, the models carried out allow supporting that, for points located below 14.5 m from rail, it would be sufficient to develop a model of 30 meters in transversal dimension. However, if it would be necessary to obtain results in further points, it would be also necessary to resort to models with 50 meters in transversal dimension. We must consider that this fact will increment the computational cost.

Regarding the longitudinal dimension of the model, it is contemplated, besides the original 50 meters, a length of 70 meters. The results obtained in the center of the model have been analyzed and it has been concluded that there are no differences in both cases, so it makes no sense to increase this length.

In terms of depth, we have analyzed three different models: 5.50 m (the original), 25 m and 50 m, obtaining results at 0.30 m depth. In all three cases the results are identical, but the calculation times vary considerably. Thus, the lightest case has spent 4 hours, while the deeper model has spent 40 hours. Therefore, it is sufficient to consider a model of 5.50 meters depth.

According to the frequency range chosen, the upper value (50 Hz in this case) determines the maximum size of the elements of the meshed model. According to Andersen and Jones (2001) "the

smallest wavelength which is expected to represent, has to cover at least 6 nodes of the model". Continuing with the example proposed to the previous case and assuming a propagation velocity of Rayleigh waves in the terrain analyzed of 110 m/s, a lower limit of 2.2 meters length is obtained. Therefore, the size of the elements must be, at most, 0.5 m.

The rule proposed by Andersen and Jones is generally accepted by many authors. It is possible to find explicit reflections about it in Marburg (2002). In this regard, in Real et al. (2014) the possibility of reducing the mesh size below the values obtained by that rule is discussed, and it is concluded that there are no significant differences in the cases studied. Nevertheless, a substantial increase in computing time occurs.

Regarding the boundary conditions adopted, the document "Recomendaciones para el proyecto de plataformas ferroviarias" (Ministerio de Fomento, 1999, in Spanish) has been followed. This document is signed by several authors and collected in different publications. As example, the works of Santos Areias et al. (2007) and Gallego et al. (2012) can be mentioned.

The boundary conditions set in that document are:

- ✓ In transversal vertical boundaries of the track, it has been decided to impose its perpendicular movement. ($U_z = 0$)
- ✓ In longitudinal vertical boundaries of the track, as in the previous case, the boundary condition set is to impose the zero movement on its perpendicular direction ($U_x = 0$)
- ✓ In the lower limit of the model, it has been set no vertical movement ($U_y = 0$).

With the first two conditions the effect of confined terrain is simulated, allowing only vertical deformation of the model. The stiffness of the material located in the lower boundary is supposed to be much higher than the stiffness of the upper materials. This allows introducing this type of condition without affecting the results of the points located on the surface of the model.

Once defined and meshed the domain of work, the next step is to choose the model element.

This is a very important aspect in the process since the possibility of representing or not certain phenomena depends on the accurate choice of the computation element (type and sizes). This point can be verified through this discussion.

As several authors as Prat et al. (1995) reveal in their publications, the 20-node hexahedron is the ideal element for three-dimensional modeling of structures and ground. Overall, according to these authors, prismatic elements are the most suitable for this kind of problems.

In ANSYS v11, the discretization of three-dimensional elements is carried out with elements type "SOLID". The most used are the SOLID95 with 20 nodes and the SOLID45 with 8 nodes. In both cases, each node has three degrees of freedom. In this sense, the document "Recommendations for the project of railway platforms" recommends to use SOLID95 in those finite element analyses that are going to be subjected to bending.

Despite the previous comments, in the modeling carried out in Chapter 2 of this Thesis, it has been used the SOLID45 element. The large size of the model and its heterogeneities, involve a very high computing time if SOLID95 element is chosen. Specifically, for the SOLID95 element, each one of the conventional models takes 16:30 hours, in contrast to the 1:48 hours used up by the SOLID45 element for a model of identical complexity. The analysis of the results obtained for both simulations, concludes that in points close to the track (accelerations in the rail and at points located at a distance of 1.20 meters) the results are substantially similar. At the same time that the location of the furthest points of the track are compared, the modeling with SOLID45 provides positive and negative peaks, slightly higher to the modeling conducted with SOLID95. Both arguments (less calculation time and acceptable results) have made the decision to use the SOLID45 instead of SOLID95.

The next step is to define the constitutive model of the different materials involved in the problem.

ANSYS, like other commercial finite element programs available in the market, has implemented all constitutive models, from the simplest (linear-elastic model) to more complexes (visco-elastoplastic model).

The models proposed in Chapters 2 and 3 assume an elastic, linear and isotropic behavior for all materials involved. Indeed, the ground is an exceptional "material" in this respect, due to it follows an elastoplastic behavior with yielding criterion of Drucker-Prager. In order to justify this simplification, two models have been calculated: the first one, assuming elastic behavior for the ground and the second one assuming an elastoplastic behavior. In the first case, each one of the models took 2 hours; but assuming an elastoplastic behavior, calculation the time is increased up to 6 hours and 45 minutes. The analysis of calculation results obtained from both simulations concludes that the results for the rail are slightly higher considering an elastic model than in the case of the elastoplastic model (the positive peaks are 14% higher in the first case compared to the second). However, when far field data (from the rail) are compared, the differences in terms of the absolute value of peak acceleration diminish. Thereby, comparing data at a distance of 9 meters from the track, there are little differences between the two proposals. Both arguments (less calculation time and acceptable results) entail the decision to choose the linear elastic model for the ground instead of the elastoplastic model. In short, with small loads, as in the case of the vehicle under investigation, the yielding stress of the material is not exceeded. Note that these simplifications might not be valid in other scenarios, and therefore it must be analyzed.

The fourth step is to "load the model", which consists in the process of load definition, establishment of the load implementation criterion and introduction in the software.

With regard to the load implementation process, the ideal manner to perform it would have been the "launch" of a set of loads which represents the axles of the railway vehicle moving at the same speed as the train. This approach would involve the modification of the dimensions of the elements which represent the rail. In this case, it would be necessary to match the application points of each load with the nodes of the mesh, and this is not always possible, especially when there is not any clear relationship between separation distance between axles of a bogie and the distance between adjacent bogies. This could be solved with a "denser" mesh.

Definitively, it was decided to launch a single load and overlap the results as many times as axles the vehicle has, taking into account the time interval between them. This approach is only possible if a linear behavior of materials has been previously assumed, as is the case of this Thesis.

At this point it should be stood out the close relationship between size and type of calculation element (which determines the points of application of the load); the speed at which the rail vehicle moves; the time that the maximum load remains on each node; the time periods in which every load step is divided and the maximum vibration frequency which is desired to model. The definition of these parameters is not a trivial topic, and a mistake planning them will lead to a considerable rise on the calculation time.

The calculation element chosen is a SOLID45 (characterized, among other things, by having only nodes at the vertices) with an edge length of 0.5 meters. These considerations imply that loads can be only applied every 0.5 meters. Moreover, the real operating speed of the line used in the model is 30 km/h. This fact, combined with the previous, assumes that the residence time of each load in each node (which is known as "load step") is 0.06 seconds (the time is obtained as the quotient of the distance between nodes and speed).

The relationship between the highest frequency vibration to study (in this case 50 Hz) and the time periods in which each loadstep is divided is defined by the Nyquist-Shannon Theorem, which says that "if FMAX is the highest frequency contained in an analog signal X(t), in order to represent that signal from one of its samples, it is necessary that the sampling frequency of these exceeds twice the maximum frequency of the signal". Therefore, the minimum number of records that must be obtained is set to 100 per second. Thus, each loadstep, whose duration is 0.06 seconds, has to provide six records, that is to say that each load step is divided into six periods of 0.01 second duration.

Once the loads are applied, the "Time-History Postprocessor" of ANSYS allows obtaining, for each node, values of displacement, velocity and acceleration in time domain. These data are transformed to the frequency domain applying the discrete Fourier transform, with

"Wolfram Mathematica" software. At this point, it can be stated that a numerical model capable of representing the physical phenomenon described, is already available.

The last step is to perform the calibration and validation of the model. This process is carried out comparing the model results with real data from the data gathering campaign.

At this point, it should be noted that the measured data on the track probably corresponds to a deformed track geometry and/or vehicle. This aspect was not considered in the modeling. To overcome this problem, the project entitled "Modelización de la interacción vía-tranvía" of S. Anacleto (2009) is consulted. According to this project, in tram way operations, the values of the dynamic overloads account for 33% of the static load. This assumption is not exempt from discussion, given the great variability that may occur.

In this context, as it is reflected in the PhD Thesis of P. Teixeira (2003), the different criteria that exist to increase static loads clearly depend on the train speed among others. Hence, it is not acceptable to extrapolate the data proposed by S. Anacleto to other operations.

Previous to the model calibration, it is necessary to identify the variables of the model that have a clear influence on the results; in the case of being unknown, there are incorporated to the calibration process. This mechanism is commonly known as "Sensitivity Analysis". In the case of this PhD Thesis, there are three unknown parameters whose influence on the model results is not known a priori, and they are: Young's modulus of sands, Poisson's ratio of sands and β coefficient of Rayleigh. Three modeling sets are conducted in order to analyze the influence of each of the three parameters in the final results. As can be seen in Figures 5 and 6 of Chapter 2 in this Thesis, only the Young's modulus of sands and Rayleigh β coefficient have been demonstrated to be significant. Hence, both parameters will be introduced in the calibration process in order to estimate their values in this case.

The calibration is performed by comparing certain measured data at specific points on the track with the data calculated by the model at the same points. Specifically, in chapter 2 of this Thesis, the following values have been compared: average value of positive acceleration

peaks, average value of negative acceleration peaks, decay ratio at the beginning of the accelerogram and decay ratio at the end of the accelerogram. The results of this calibration process are the values of Young's modulus of sands (70MPa) and Rayleigh β coefficient (0.001).

Once the calibration process is finished, the model validation begins with another data set obtained from the data gathering campaign. In this case, the same process is carried out. Thus, a qualitative validation process is performed with identical magnitudes. In this regard, it is convenient to note that the model results are always higher than those measured in the data campaign. Regarding the value of the acceleration positive peaks, the excess add up to 5% of the value (which is perfectly acceptable), while in the case of negative peaks the excess is higher (a 9% of the value).

From the previous results, it can be stated that a numerical model capable of representing the generation of vibrations on the wheel-rail contact, transmission across the track and propagation throughout the adjacent ground is now available.

Applications of the numerical model.

Using the model developed in chapter 2 of the Thesis discussed in the previous epigraph, the influence of certain pathologies of wheel and rail in the genesis of vibrations as well as the role of certain solutions in the minimization of the propagation of railway vibrations, specifically wave barriers, can be analyzed.

This section is divided in two sub-points: the first one corresponds to the discussion of chapter 3 of the Thesis, and aspects related to the vibrations generation-transmission-propagation in cases where certain pathologies exist are considered. The second part is identified with the discussion of the effectiveness of wave barriers in the propagation of railway vibrations (chapter 2 of the Thesis).

With regard to the first sub-point, as it was mentioned, in chapter 3 of the PhD Thesis the modeling of two pathologies that frequently appear in the railway wheel and on the rail is addressed. These pathologies are known as "wheel flat "and "rail corrugation ", respectively.

Now, it is convenient to reflect on the general limitations of numerical models when certain pathologies are represented. As has previously said in this discussion, loads can only be applied at the nodes of the elements used for the rail modeling. In the present case, nodes are separated a distance of 0.5 meters, so any phenomenon expected to be modeled must have a multiple periodicity of 0.5 meters. For the wheel flat, it is only possible to work with those wheels whose perimeter is a multiple of 0.5 meters (in this case, it has been chosen a wheel whose perimeter is 1.5 meters) and with regard to the rail corrugation, due to the fact that in every cases there are two situations (crest and trough), only wavelengths that are multiples of 1 m will be able to be represented (twice the distance between nodes).

Certainly, this limitation would be greatly improved by reducing the size of the model elements, although it would imply a considerable increase on calculation time. Again, as has already been mentioned throughout this discussion, it is necessary to find a balance between accuracy and calculation time.

As far as “Wheel Flat” is concerned, it is defined by its length (which can reach values up to 50 mm) and its depth (which typical value is 2 mm).

The existence of a wheel flat involves two clear situations:

- Activation of certain vibration frequencies.
- Increase of dynamic overloads.

With regard to the first point, the dynamic effects generated by the wheel flat will be transmitted from the point of wheel-rail contact (which is where dynamic overloads are generated) across the track and then will be propagated through the adjacent ground. As a consequence of this, some vibration frequencies that did not exist will be activated. The danger of this is that these new frequencies may coincide with the natural vibration modes of the systems existent on the track. If it happens, some systems can vibrate in resonance, with the resulting consequences that it would imply.

The frequency at which the defect appears depends on the train speed and on the wheel perimeter. In the case presented in Chapter 3 of the Thesis, the frequency reached a value of 5.56 Hz (which is the

quotient of the speed between the train speed -30 km/h- and perimeter of the wheel -1.5m-).

For the second point (increase of dynamic overloads), this phenomenon was revealed by Hirano (1972) demonstrating how the train speed affects the magnitude of the maximum stress. López Pita (2006) shows the effect of train speed and flat length on the generated overload. In Chapter 3 of this Thesis, the value of this overload is estimated according to the theory of Schramm (1961) according to which, the tensional increase due to wheel flat depends on the static load, mechanical parameters of the rail and wheel flat depth. Knowing the stresses and estimating the area of the wheel-rail contact, the transmitted force to the rail due to the existence of the wheel flat is obtained.

About the estimation of wheel-rail contact area, the railway literature talks about a standard contact surface of 2 cm². Schramm provides an experimental expression to calculate this area as a function of static load, the radius of the wheel and some mechanical parameters of the wheel.

Assuming the theory of Schramm, it has been obtained a force of 24000 N, approximately, which represents more than 50% of the static load (which had been set to 45000 N). Note that the hypothesis from S. Anacleto (2009) are not too accurate, compared to the result obtained in Chapter 3. This fact corroborates that there is a great variability among the dynamic loading factors because, besides the speed factor, there are other inputs such as track and vehicle quality which greatly influence this increase. This circumstance was emphasized by P. Teixeira in his doctoral Thesis, as it has been discussed in previous paragraphs.

One of the most notorious deficits of the formulation of Schramm is that it does not consider the vertical stiffness of the track. Given the importance of this input in the generated dynamic overloads, and in order to be aware of the order of magnitude of the difference, a dynamic model of vehicle-track interaction has been developed. Thus, a wheel flat is simulated by modifying the rail profile, matching this profile with the wheel profile at the points where the flat appears in the contact zone. Thus, a rail profile which simulates the equivalent

geometry of the wheel-rail contact area is obtained. Using this methodology, the maximum load value is a 13% higher than the obtained using the experimental expression of Schramm. Indeed, it would be possible to think that the difference is not relevant, but the conceptual error committed by not taking into account factors such as track stiffness, is remarkable.

Once all the values related to the frequency and overload due to the wheel flat are estimated/calculated, a procedure to incorporate them to the model developed in chapter 2 has to be implemented. The way to do this is represented in figure 3 of chapter 3 of this work.

Before the appearance of the wheel flat, the application of the static load had a constant value of 45000 N applied during a time (estimated in 0.06 seconds) in each node of the rail. Nevertheless, when a wheel flat appears, these load values have to be incremented with an impulsive force of magnitude equal to the calculated force (24000 N) acting for a infinitesimal period of time (0.001 seconds in this case; which mainly depends on the elasticity of the shocking elements) in some specific nodes (in the case of this Thesis, as a wheel perimeter of 1.5 meters is assumed, the load is applied to one of every three nodes).

Once the process of loads application in the numerical model developed in Chapter 2 has been described, the model is run and representations of accelerations are obtained as a function of time in several points more or less separated from the track. The results obtained are shown in Figure 4 of chapter 3.

The figure clearly shows how the presence of wheel flats causes significant variations in the response with the growth of positive and negative acceleration peaks. This response is appreciated with total clarity, although in a different magnitude, at points located from 0.3 to 3 meters from the rail.

Regarding the "Rail Corrugation", this is a pathology which affects the rail and which corresponds to relatively constant wave geometry. It is represented by its wavelength and amplitude.

The estimation of the dynamic overloads due to the rail corrugation is performed using the auxiliary model of two masses (M. Melis, 2008).

The mathematical formulation of this model allows obtaining the forces transmitted to the rail depending on the point where the wheel is located. To do so, the mechanical characteristics of various systems of the railway vehicle and rail profile must be known.

In chapter 3 of the present work, the approach of the auxiliary model aforementioned based on the mechanical data of the vehicle (sprung and unsprung masses, stiffness of the primary and secondary suspension and damping of the primary and secondary suspension) is shown. Moreover, a circulation speed of 30 Km/h is set and two wavelengths defects have been supposed: $L_1 = 1$ m. and $L_2 = 0.5$ m. In both cases, it has been assumed amplitudes of 0.5 mm for the defects. These values have been adopted in order to consider the long wave corrugation rail defects ($L = 1$ m) and medium wave corrugation rail defects ($L = 0.5$ m). The value of 0.5 mm, taken as amplitude of the defects, represents in both cases a defect in full development phase, which therefore would require maintenance tasks. These considerations about wheel corrugation can be consulted and expanded in the dissertation of S. Anacleto (2009).

At this point it is necessary to reflect on the influence of the wavelength and amplitude of rail corrugation as well as the train speed on the numerical value and frequency of the dynamic overloads obtained.

Thus, for fixed amplitude and constant speed, the decreasing of the wavelength involves a considerable increase in the value of the dynamic overload and an increase of the excitation frequency (which is in accordance with the wavelength of the defect and the train speed).

Given a particular rail corrugation (defined by its wavelength and amplitude), as the train speed grows, the frequency and the numerical value of the dynamic overload are also increased.

Finally, if the amplitude of the rail corrugation is modified, keeping constant the wavelength and speed, a variation of the same magnitude in the value of the dynamic overload takes place. However, the frequency of dynamic overload is not affected by changes in the amplitude of the defect.

In short, the numerical value of the exciting force increases with the growth of the circulation speed, with the growth of the amplitude of the corrugation and with the decrease of the wavelength of the defect. In contrast, the frequency of the exciting force increases with the growth of the circulation speed and with the decrease of the wavelength of the defect; not being affected by its amplitude.

Before introducing the dynamic overloads to the model created in Chapter 2, it is important to think again about the mesh. As the numerical model is originally defined, only the first case analyzed could be simulated (1 meter wavelength), as has been explained in previous paragraphs. In order to analyze the second case it is necessary to vary the dimension of the elements of the model. For this reason, the rail is meshed again using 0.25 m elements instead of the previous 0.50 m elements. It is necessary to mention how computing time has been increased: in the original case (0.50 m elements) a computation time of 4:30 hours has been required and in the second case (0.25 m elements) an 18 hours calculation time has been required.

Once the premises are established, the next step is to use (and modify if necessary) the numerical model created to reproduce the phenomenon. To do so, it is needed to introduce in the model the dynamic overloads calculated by the auxiliary model.

Both static and dynamic loads due to the wheel corrugation must be simultaneously considered in the simulation. Just as in the previous study case (wheel flats) the static load is constant and has a value of 45000 N. Regarding the dynamic overload, this presents a sinusoidal profile which wavelength matches with the wavelength of the defects that generated the overloads, given that the speed remains constant and with a value calculated in accordance with the auxiliary model of two masses.

After the process of load application, the model presents the accelerations obtained at two points: at 0.30 m and 3 m from the rail, and does it under the hypothesis of 1 m wavelength, 0.5 m wavelength and track without defects. The results are shown in Figures 10 and 11 of chapter 3 of the Thesis. In this regard, it is convenient to mention how these higher accelerations magnitudes are

obtained (both positive and negative) in those cases in which rail corrugation was considered. Moreover, this fact takes place in the vicinity of the track (namely to 0.30 meters from it) as well as at a certain distance from there (3 meters). Moreover, an interesting finding is that as the wavelength analyzed decreases, the magnitude of the acceleration significantly increases, both close to the rail as at a certain distance from this.

In the second part of this section, the work included in chapter 2 of the Thesis (effectiveness of different types of wave barriers in the propagation of railway vibrations) is discussed.

Certainly, the wave barriers parallel to the track have emerged as an effective way to minimize the propagation of vibrations from the track to the adjacent buildings. It is a solution of special interest to be implemented on active railway lines, since it does not involve any work in the track.

The operating mechanism of wave barriers is based on the theory of refraction of the incident energy, which is mainly transported as Rayleigh waves. Thus, the presence of an in-filled trench in the propagation path of waves implies some discontinuity in the medium motivated by an impedance variation, fact that causes reflections and refractions of the incident wave.

In order to evaluate the capacity of the filling of a trench to mitigate waves, it is convenient to arrange trenches with low waves refraction coefficient. This fact ensures to the amplitude of the refracted wave to be lower than the amplitude of the incident wave. In the studied case, two simplifications that provide higher values of the refracted wave amplitudes are taken into account. In any case, they are on the safe side:

- It is considered that the incident wave is perpendicular to the interface of the two media.
- The mode conversion between P and SV waves (constituents of Rayleigh waves, as stated in the introduction of this PhD Thesis) is not considered.

In case of an open trench, in addition to the effect described for in-filled trenches, it is achieved to place an obstacle against the wave progression. This is the reason why it is traditionally assumed that open trenches are more efficient than in-filled trenches to minimize the propagation of vibrations. However, it is important to consider that only a few terrains are capable to support vertical slopes. In addition, certain authors have demonstrated that the vertical slopes of open trenches present instability phenomena against low frequency waves.

Regarding the optimal location of trenches, most authors advocate to place them "as close as possible to track trace" (F. E. Richardt, 1970). Indeed, the closer they are to the trace of the track, the greater the energy to which they are exposed. Nevertheless, this fact will involve that its design will be more demanding, but also its efficiency will be superior.

Another aspect traditionally studied has been the analysis of the effectiveness of trenches in homogeneous terrains vs. multi-layered terrains. In case of homogeneous areas, wave barriers only work properly when the depth of the trench is greater than the wavelength of the incident vibration (F. E. Richardt, 1970). Furthermore this "suitable operation", which is equivalent to decreasing the incident wave amplitude of 50%, only remains in a certain distance behind the trench known as a "shadow zone". This is caused by the diffraction suffered by the waves at the base of the trench. However, in a multi-layered terrain, the effectiveness of the wave barrier is greater because the energy is transmitted through surface waves moving through this layer. In these cases, the optimum depth of a trench is that which corresponds to the depth of the upper layer.

Following these assumptions, the application concerning to the study of the effectiveness of trenches in minimizing the propagation of railway vibrations, analyzed in chapter 2 of this Thesis, is discussed below.

The analysis is focused, as it has been done in the model development, in the studied section of the line 4 of the tram in Alicante. The section is formed of a multi-layered soil formed by a 2 meters thick sand layer supported on a bedrock base.

Moreover, the application will only consider the characteristics of railway operations (track and vehicle type, speed, etc) modeled.

The discussion of this part will be structured as follows: based on data and assumptions extracted from the scientific literature about the characteristics of wave barriers (width, depth, in-filled material...) a number of specific cases are introduced for each one of the characteristics presented calculated using the developed model. Then, the results which respond to the questions arisen are presented.

Firstly, the width of the wave barrier is analyzed independently.

Several authors, including L. Andersen et al. (2005) showed the poor efficiency of the width of the trench to mitigate the propagation of vibrations. Furthermore, for trench widths greater than 25% of the Rayleigh wavelength of the predominant vibration, the effect of the width is zero. Hence, from this point it is not logical to dig a wider trench.

Knowing that the Rayleigh wavelength is obtained as the quotient between the wave speed in the ground (which in the case presented in Chapter 2 of the Thesis are sands, and assuming its mechanics characteristics, a value of 106 m/s is obtained) and the predominant vibration frequency (which in the case study, and in agreement with the model is 16.6 Hz). In addition, a wavelength value of 6.3 meters is used.

Hence, following the previous hypothesis, an open trench of 1.50 m depth and variable width (coinciding with the standards of conventional machinery) is introduced in the model.

In Figure 7 of Chapter 2, the vibrational patterns corresponding to the three studied widths are represented. Note how the variations are so small that there is no reason to consider wider trenches.

Thus, effectively, the hypothesis stated by L. Andersen et al. has been corroborated in the studied case.

Secondly, on the basis of the analysis of several works among which Al- Hussaini and Ahmad (1991), Yang and Hung (1997), Takemiya

(2001), Hung et al. (2004) and the aforementioned study by Andersen et al. (2005) stand out, the following variables can be outlined:

- Depth of the trench in a multi-layered terrain
- Mechanical properties of the in-filled materials
- Wave barrier typology: Open trench versus in-filled trench.

Then, in order to analyze the influence of the variables outlined, 16 cases of a wide casuistry are studied: four depths (from 1 meter to 2.5 meters) and four types of trenches (filled with concrete, filled with polyurethane, open trench and open trench with sheet piling). Furthermore a 0.45 meters width is set for all the cases studied.

With this approach, in order to cover all the cases studied and analyze the results obtained from the model, the features of the trench are modified. However, in the case of the sheet piling open trench, it is necessary to modify the boundary conditions in the model to incorporate the mechanical role of the sheet piles.

After calculating all the cases, it is concluded that the optimal depth of trench coincides with the depth of the upper layer, as the scientific literature evidenced (F. E. Richardt, 1970).

Regarding mechanical and physical properties of the constituent materials of the trench, the influence of the elastic modulus, Poisson's ratio and the density of different fillers have been analyzed. It is demonstrated that the density and Poisson's ratio are not significant, as Adam et al. (2005) showed. However it is significant the influence of the modulus of elasticity of the filler, but it is not in a single direction. Thus, if the difference between the modulus of elasticity of the soil and the modulus of elasticity of the filler increases, the effectiveness of the wave barrier in attenuating vibrations also increases. This conclusion is obtained from the modeling of the four types of filler materials: concrete-1 (30000 MPa), concrete-2 (40000MPa), polyurethane-1 (20 MPa) and polyurethane-2 (2 MPa). Certainly in the study case, the attenuation due to the concrete-1 is higher than that the attenuation due to the polyurethane-1 (which are the data shown in the paper), but also notes that the attenuation due to concrete-2 is greater than

the attenuation due to the concrete-1 (identical situation occurs between the polyurethane-2 and polyurethane-1).

Finally, the assertion about the greater efficiency of open trenches against trenches in-filled with concrete-1 has been evidenced obtaining accelerations at different points located between the rail and the trench and behind the trench. It is possible to state that, according to the results obtained, the open trenches attenuate better than the trenches in-filled with concrete-1 (due to the accelerations calculated behind the trench are lower). On the contrary, the acceleration value between the rail and the trench is significantly higher in the case of open trenches than in the case of trenches in-filled with concrete-1.

Main contributions and research lines

The main contributions of this Thesis are identified with the small advances that each one of the publications supposes with regard to the previous state of the art. Furthermore, the study of these contributions allows to outline future investigation lines about this topic.

Related to the **analytical modeling** of generation-transmission phenomenon of vibrations through the track, contained in chapter 1 of the this PhD Thesis, the following *contributions* are discussed:

The first of them, already present in the previous papers of this chapter, is related to the modeling of the rail as a Timoshenko beam. Usually the rail was modeled as an Euler-Bernoulli beam, however, this modeling made impossible to consider the deformations caused by shear stresses, which can be important in secondary bending rail phenomena.

Regarding the treatment of secondary bending of the rail, the study has been particularized for the case of an axle located in the middle of the span between two adjacent sleepers. The deflection of the rail, theoretically calculated and appropriately treated, is introduced as "an extra load to the model". Hence, in those track typologies where the rail rests on discrete sleepers, an additional load is introduced to the

model, which is precisely the load caused by the secondary bending of the rail.

A useful contribution for future works deals with the homogeneous treatment of the different loads that can appear in a railway operation. Usually it is talk about the quasi-static load, a load due to the dynamic overload and loads due to the secondary bending of the rail. Traditionally, the static load was modeled by the Zimmermann's method and the theory of Pandolfo. In Chapter 1 of this Thesis, this load is treated as another harmonic whose amplitude matches with to the axle load of the vehicle with zero frequency.

Finally, the publication included in Chapter 1 shows, in contrast to previous publications, a modeling of the domain into five layers. Certainly, this fact does not involve a substantial advance in the field, but allows obtaining independent results in each layer (although it involves more complex calculations).

Regarding to the investigation lines that are considered of interest, linked to the work presented in Chapter 1 of the Thesis and previous publications, it should be noted the approach of an analytical three-dimensional model of generation-transmission-propagation of vibrations in tunnels of circular section, using in this case a cylindrical coordinates system. Additionally, the analysis of the validity of the analytical model to certain frequency ranges, depending on the modeling of the rail (according to Timoshenko or assuming the theory of Euler-Bernoulli) is, without a doubt, very interesting.

In the **numerical modeling** of the phenomenon of generation-transmission-propagation of railway vibrations contained in Chapter 2 of this PhD Thesis, it is emphasized the search of a balance between computation time and accuracy of results. In this context, the main methodological contributions are the following:

In the context of the use of a commercial software for the modeling of the considered phenomenon, one of the treated problems is the definition of the limits of the model. As chapter 2 and previous paragraphs of this discussion demonstrate, these limits depend largely on the frequency range to be analyzed. An interesting methodological contribution in this field is to analyze how the boundary limits of the

model influence on the phenomenon to analyze and how, if any, certain aspects have to be varied to avoid these influences. As reflected in figure 3 of chapter 2, the vertical stiffness of the model decreases in the boundaries vicinities. According to this circumstance, in order to prevent the influence of this on the final results, it is proposed to modify the value of the applied loads.

A verification which can be interesting for future works is to analyze the possibility of replace some elements of meshing and calculation to simpler ones. In the discussion of the Thesis, it has been outlined the results and calculation time of the model by using the SOLID45 element in front of SOLID95. It demonstrates that, despite the scientific literature encourages the use of SOLID95, the use of SOLID45 produces satisfactory results with much less computation time.

In this context, different points in which is needed to delve into are emphasized in order to solve those facts that have not been considered, at least with the desirable extension, in this Thesis.

One of these reflections refers to the influence of the constitutive model of materials in the model results; particularly in the case of the ground. This has to be modeled with an elastoplastic behavior with Drucker -Prager yielding criterion. However, the numerical model presented in chapter 2 assumes that the terrain behavior is linear elastic due to the fact that in the case of small loads transmitted, as is the case of a tram line, the elastic limit of the material is not exceeded. The suitability of this simplification has been demonstrated in previous paragraphs of this discussion. At this point, it is proposed to perform the analysis of different railway systems in which the axle load, speed or other aspects determine the accuracy of this simplification.

Another methodological aspect which should be more deeply investigated is in the procedure of the load application in an undeformed track. In this work, this process has been carried out similar to the most consulted publications: passing a load and adding together the results as many times as axles the vehicle has. However, in order to check the validity of the simplification that has been assumed, a test with the following features has been made: a section of ballasted track is modeled by applying symmetry. The dimensions

of the model are: 46 meters length, 20 meters width and 4.5 meters depth. The mesh size, in longitudinally direction, is 20 cm and an element known as SOLID45 has been set. A load of 49 kN is applied to each wheel, circulating at 28 Km/h speed. The results obtained by passing a single load and applying superimposed loads and passing the whole train simultaneously, are compared. Acceleration values on sleepers are obtained, and the differences of magnitude and form of the acceleration graphics hardly differ from each other. However the computational time varies (in case of a single load step applying superposition takes 2 hours and 10 minutes and in the case of full load step, 5 hours and 45 minutes are consumed). The computer used has a 4-core processor to 3.6 GHz and 32 GB RAM memory.

The numerical modeling presented in Chapter 2 of this Thesis has been developed in a very basic design: a straight line without ramps or gradients. Several authors have evidenced the considerable differences in other types of designs. In this context, it is considered very interesting to obtain a robust and simple model of the phenomenon of generation-transmission-propagation in these scenarios, in order to deepen in the analysis of the influence of the design in the genesis of railway vibrations.

In chapter 2 of this PhD Thesis, the study of the **effectiveness of wave barriers** in the attenuation of railway vibrations propagation using the model created, is also collected. In this regard, the main contribution of this analysis lies in demonstrating the utility of the model in the simulation of the phenomena of refraction and reflection experienced by the waves in their propagation through a certain type of terrain. This has allowed comparing the effectiveness of different types of trenches (width, depth, in-fill materials...) in a multi-layered ground, showing the accuracy of the assumptions contained in the scientific literature.

In this context it should be mentioned, as a methodological contribution, the modeling of sheet piles in an open trench supported by this mechanism. Indeed, as evidenced in Chapter 2, the open trenches are more effective than any other trench, but have the disadvantage of its low mechanical stability in granular soils, hence the analysis of this type of trenches but stabilized with sheet piles.

Related to this fact, given the effectiveness and simplicity of the "trench" as attenuator element of the propagation of vibrations in consolidated railway environments, it has been decided to go further in this investigation line, as in multi-layered terrains (chapter 2 of this Thesis) as in non-layered terrains, in which the casuistry to consider is much larger than in the first case.

As well as trenches, there are "less invasive" alternatives beginning to be implemented as satisfactory attenuation elements of vibration propagation. These are usually known as "vibration glasses", in analogy with the sound glasses. The study of the type of materials, arrangement of cylinders and location relative to the track is one of the most interesting investigation lines outlined in this point.

In Chapter 3 of this PhD Thesis, using the model developed, calibrated and validated in the previous chapter, two classic pathologies of railway transport are simulated: **wheel flat and rail corrugation**.

The main contribution of this chapter deals with the easiness of implementation of these phenomena in the proposed model. After calculating the excitation frequencies and dynamic overloads, two different procedures have been designed to incorporate these dynamic overloads to the model created in Chapter 2. The obtained results show the accuracy of the method.

According to the results obtained in this chapter, the intention is to go more deeply into already existing investigation lines from other authors, such as:

Reflect on the effects of short-wave rail corrugation. Certainly, this condition gives rise, keeping constant the other factors, to a higher acceleration values and longer duration of the transient effects of the response. These facts justify its importance. However, as it has been stated in the discussion of this phenomenon, the smaller the wavelength of the rail corrugation is, the smaller the mesh and calculation element of the rail must be. This circumstance requires searching again the balance between size/type of element and coherent results.

To go more deeply into the existing methods in scientific literature (experimental, analytical, numerical...) focused on calculating/estimating/approximating the value of the dynamic overload due to different vehicle and track pathologies. It is also considered if there are important differences between them and how these, if any, would affect the final results of the model globally considered. This approach should be applied to different types of railway operations.

Finally, and considering the subject of this Thesis from a global point of view, the author has been working on it over the last two years (the last paper that contains the Thesis was accepted on 4th December 2012), publishing four additional papers:

The first one is an experimental study that allows comparing the damping capability of different tramway superstructures. Note how this work can be a useful contribution to the design of new railway superstructures, considering the vibratory phenomenon. Nevertheless, it is not valid for analyzing the vibration damping in operating tracks (aspect in which solutions such as trenches and/or vibration glasses are useful). This paper is "Study of the mitigation of tram-induced vibrations on different track typologies", Journal of Vibroengineering (ISSN 1392-8716). Volume 15. Pages: 2057 - 2075. 2013. Index JCR 2013. (Impact factor 0.660). Q3.

The second one contains interesting reflections when both formulations are compared. The comparison considers aspects such work domain, 2D versus 3D modeling, calculation of the solution in the whole domain or only in some specific nodes, load application formulation and frequency range under study. This work is "Railway traffic induced vibrations: comparison of analytical and finite element models". Journal of Vibroengineering (ISSN 1392-8716). Volume 15. Pages: 1701-1710. 2013. Index JCR 2013. (Impact factor 0.660). Q3.

The third contains the methodological concerns that have arisen during the numerical modeling of the phenomenon globally considered, such as influence of the mesh size in the accuracy of the results and computation time, validity of the load step method (isolated load superimposed against the passage of the whole train), influence of the type of mesh element and considerations of constitutive model

of materials. It is titled as "Computational considerations of 3-D finite element method models of vibration prediction in ballasted railway tracks", and is published in Journal of Vibroengineering (ISSN 1392-8716). Volume 16. Pages: 1709-1722. 2014. Index JCR 2013. (Impact Factor 0.660). Q3.

The latest work shows the influence of the type of sleeper in the generation and transmission of vibrations of a ballasted track in an curved track area, and it is titled as "Comparison of the effect of different typologies and sleeper railway track layout on vibrations" having been published in Latin American Journal of Solids and Structures (ISSN 1679-7817). Volume 11. Issue 12. Pages: 2241-2254. 2014. Index JCR 2013. (Impact Factor 1.254). Q2

Parallel to the study of vibrations as a railway externality and given the importance of knowing the deformed geometry of the track (as for the analysis of vibrations as for the establishment of maintenance procedures, among others) some years ago, it was decided to begin a new investigation line in order to obtain the deformed track profile. It was achieved by placing triaxial accelerometers on the unsprung masses of commercial railway vehicles. The results of this research are found in the following publications:

"Determination of Rail Vertical profile through inertial methods" (2011), "Development of a system to obtain vertical track geometry measuring axle-box accelerations from in-service trains" (2012) and "Design and validation of a railway inspection system to detect lateral track geometry defects based on axle-box accelerations registered from in-service trains" (2014)

References

- Ahmad, S., & Al-Hussaini, T. M. (1991). Simplified design for vibration screening by open and in-filled trenches. *Journal of Geotechnical Engineering* , 117 (1), 67-88.
- Anacleto, S. (2009). Modelización de la interacción vía-tranvía. *PhD Thesis. Universitat Politècnica de Catalunya. Escola Tècnica Superior d'Enginyers de Camins, Canals i Ports de Barcelona. Departamento de Infraestructura del Transporte y del Territorio.*
- Andersen, L., & Jones, C. J. (2001). Three-Dimensional Elastodynamic Analysis Using Multiple Boundary Element Domains. *ISVR Technical Memorandum.*
- Andersen, L., & Nielsen, S. R. (2005). Reduction of ground vibration by means of barriers or soil improvement along a railway track. *Soil Dynamics and Earthquake Engineering* , 25 (7), 701-716.
- Areias, A. S. (2007). Design of high-speed track bed with granular and bituminous layers using elastoplastic finite elements models.
- Arslan, Y. Z., Adli, M. A., Akan, A., & Baslo, M. B. (2010). Prediction of externally applied forces to human hands using frequency content of surface EMG signals. *Computer methods and programs in biomedicine* , 98 (1), 36-44.
- Auersch, L. (2005). The excitation of ground vibration by rail traffic: theory of vehicle track soil interaction and measurements on high speed lines. *Journal of Sound and Vibration* , 284 (1), 103-132.
- Barkan, D. D. (1962). Dynamics of Bases and Foundations. *New York: McGraw-Hill.*
- Beskos, D. E., Dasgupta, B., & Vardoulakis, I. G. (1986). Vibration isolation using open or filled trenches. *Computational Mechanics* , 1 (1), 43-63.
- Çelebi, E., Firat, S., Beyhan, G., Çankaya, I., Vural, I., & Kirtel, O. (2009). Field experiments on wave propagation and vibration isolation

by using wave barriers. *Soil Dynamics and Earthquake Engineering* , 29 (5), 824-833.

Cirianni, F., Leonardi, G., Scopelliti, F., & Buonsanti, M. (2009). Study of the barriers for the mitigation of railway vibrations. *The Sixteenth International Congress on Sound and Vibration*, (págs. 5-9). Kraków.

Connolly, D., Giannopoulos, A., & Forde, M. C. (2013). Numerical modelling of ground borne vibrations from high speed rail lines on embankments. *Soil Dynamics and Earthquake Engineering* , 46, 13-19.

Dahlberg, T. (1995). Vertical dynamic train/track interaction-verifying a theoretical model by full-scale experiments. *Vehicle System Dynamics* , 24 (sup1), 45-57.

Ekevid, T., & Wiberg, N. E. (2002). Wave propagation related to high-speed train: a scaled boundary FE-approach for unbounded domains. *Computer Methods in Applied Mechanics and Engineering* , 191 (36), 3947-3964.

Fomento, M. d. (1999). Recomendaciones para el proyecto de plataformas ferroviarias. *Madrid: Servicio de publicaciones del Ministerio de Fomento*.

Fonseca Teixeira, P. (2003). Contribución a la reducción de los costes de mantenimiento de vías de alta velocidad mediante la optimización de su rigidez vertical. *PhD Thesis. Universitat Politècnica de Catalunya. Escola Tècnica d'Enginyers de Camins, Canals y Ports de Barcelona*.

Fuyuki, M., & Matsumoto, Y. (1980). Finite difference analysis of Rayleigh wave scattering at a trench. *Bulletin of the Seismological Society of America* , 70 (6), 2051-2069.

Gallego, I., Sánchez-Cambronero, S., & Rivas, A. (2012). Criteria for Improving the Embankment-Structure Transition Design in Railway Lines. *InTech*.

Graff, K. F. (1975). *Wave Motion in Elastic Solids*. Oxford: Courier Dover Publications.

Griffin, M. J. (1990). Handbook of Human Vibration. San Diego: Academic Press INC.

Gutowski, T. G., & Dym, C. L. Propagation of ground vibration: A review. *Journal of Sound and Vibration* , 49 (2), 179-193.

Hall, L. (2003). Simulations and analyses of train-induced ground vibrations in finite element models. *Soil Dynamics and Earthquake Engineering* , 23 (5), 403-413.

Heckl, M., Hauck, G., & Wettschureck, R. (1996). Structure borne sound and vibration from rail traffic. *Journal of sound and vibration* , 193 (1), 175-184.

Hertz, H. (1896). On the contact of elastic solids. *Hertz's Miscellaneous Papers*.

Hirano, M. (1972). Theoretical analysis of variation of wheel load. *Railway Technical Research Institute, Quarterly Reports* , 13 (1), 42-44.

Hung, H. H., Yang, Y. B., & Chang, D. W. (2004). Wave barriers for reduction of train induced vibrations in soils. *Journal of geotechnical and geoenvironmental engineering* , 130 (12), 1283-1291.

Johansson, A. (2006). Out-of-round railway wheels - assessment of wheel tread irregularities in train traffic. *Journal of Sound and Vibration* , 293 (3-5), 795-806.

Johansson, A., & Nielsen, J. C. (2003). Out-of-round railway wheels - wheel-rail contact forces and track response numerical simulations. *Journal of Rail and Rapid Transit* , 217 (2), 135-146.

Jones, C. J., Sheng, X., & Petyt, M. (2000). Simulations of ground vibration from a moving harmonic load on a railway track. *Journal of Sound and Vibration* , 231 (3), 739-751.

Ju, S. H. (2004). Three-Dimensional Analyses of Wave Barriers for Reduction of Train-Induced Vibrations. *Journal of geotechnical and geoenvironmental engineering* , 130 (7), 740-748.

Kalker, J. J. (1990). Three Dimensional Elastic Bodies in Rolling Contact. *Dordrecht: Kluwer Academic Publishers*.

Knothe, K. L., & Grassie, S. L. (1993). Modelling of railway track and vehicle-track interaction at high frequencies. *Vehicle system dynamics* , 22 (3-4), 209-262.

Koziol, P., Mares, C., & Esat, I. (2008). Wavelet approach to vibratory analysis of surface due to a load moving in the layer. *International Journal of Solids and Structures* , 45 (7), 2140-2159.

Kurzweil, L. G. (1979). Ground-borne noise and vibration from underground rail systems. *Journal of sound and vibration* , 66 (3), 363-370.

López Pita, A. (2006). Infraestructuras Ferroviarias. *Ediciones UPC*.

Marburg, S. (2002). Six boundary elements per wavelength: is that enough? *Journal of Computational Acoustics* , 10 (01), 25-51.

May, T. W., & Bolt, B. A. (1982). The effectiveness of trenches in reducing seismic motion. *Earthquake Engineering & Structural Dynamics* , 10 (2), 195-210.

Melis, M. (2008). Introduction to vertical dynamics of railway tracks and to digital signals in trains. *Madrid: Universidad Politécnica de Madrid*.

Melke, J. (1988). Noise and vibration from underground railway lines: Proposals for a prediction procedure. *Journal of Sound and Vibration* , 120 (2), 391-406.

Metrikine, A. V., & Vrouwenvelder, A. C. (2000). Surface ground vibration due to a moving train in a tunnel: two-dimensional model. *Journal of Sound and vibration* , 234 (1), 43-66.

Murillo, C., Thorel, L., & Caicedo, B. (2009). Ground vibration isolation with geofoam barriers: Centrifuge modeling. *Geotextiles and Geomembranes* , 27 (6), 423-434.

Nielsen, J. C., & Igeland, A. (1995). Vertical dynamic interaction between train and track influence of wheel and track imperfections. *Journal of Sound and Vibration* , 187 (5), 825-839.

Otero, J. (2009). Study of rail vehicle dynamics in curved tracks. Part I: Wheel-rail contact analysis. *Revista Colombiana de Tecnologías de Avanzada* , 2 (14), 48-53.

Polach, O. (2000). A fast wheel-rail forces calculation computer code. *Vehicle System Dynamics* , 33, 728-739.

Real, J. I., Zamorano, C., Hernández, C., Comendador, R., & Real, T. (2014). Computational considerations of 3-D finite element method models of railway vibration prediction in ballasted tracks. *Journal of Vibroengineering* , 16, 1709-1722.

Real, J., Martínez, P., Montalbán, L., & Villanueva, A. (2011). Modeling vibrations caused by tram movement on slab track line. *Mathematical and Computer Modelling* , 54 (1), 280-291.

Richart, F. E., Hall, J. R., & Woods, R. D. (1970). *Vibration of Soils and Foundations*. Berkshire: Prentice-hall.

Salvador, P., Real, J., Zamorano, C., & Villanueva, A. (2011). A procedure for the evaluation of vibrations induced by the passing of a train and its application to real railway traffic. *Mathematical and Computer Modelling* , 53 (1), 42-54.

Schramm, G. (1961). *Permanent way technique and permanent way engineering*. Darmstadt, Germany: Otto Elsner Verlag.

Segol, G., Abel, J. F., & Lee, P. C. (1978). Amplitude reduction of surface-waves by trenches. *Journal of the Engineering Mechanics Division* , 104 (3), 621-641.

Sheng, X., Jones, C. J., & Petyt, M. (1999). Ground vibration generated by a harmonic load acting on a railway track. *Journal of Sound and Vibration* , 225 (1), 3-28.

Sheng, X., Jones, C. J., & Thompson, D. J. (2003). A comparison of a theoretical model for quasi-statically and dynamically induced

environmental vibration from trains with measurements. *Journal of Sound and Vibration* , 267 (3), 621-635.

Sheng, X., Jones, C. J., & Thompson, D. J. (2006). Prediction of ground vibration from trains using the wavenumber finite and boundary element methods. *Journal of Sound and Vibration* , 293 (3), 575-586.

Takemiya, H. (2001). Ground vibrations alongside tracks induced by high-speed trains: prediction and mitigation, in Noise and Vibration from High-Speed Trains. *Noise and vibration from high-speed trains* , 347.

Thompson, D. (2009). Railway noise and vibration: mechanisms, modelling and means of control.

Timoshenko, S. P. (1981). *Teoría de las Estructuras. Madrid: Urmo Ediciones.*

Verhas, H. P. (1979). Prediction of the propagation of train-induced ground vibration. *Journal of Sound and Vibration* , 66 (3), 371-376.

Wass, G. (1972). *Linear Two-Dimensional Analysis of Soil Dynamic Problems in Semi-Infinite Layered Media. University of California, Berkeley.*

Woods, R. D. (1967). Screening of Elastic Surface Waves by Trenches. *Journal of Soil Mechanics Division* , 951-979.

Yan, W., & Fischer, F. D. (2000). Applicability of the Hertz contact theory to rail-wheel contact problems. *Archive of applied mechanics* , 255-268.

Yang, J., Wang, K., & Chen, H. (2012). Characteristics of wheel-rail vibration of the vertical section in high-speed railways. *Journal of Modern Transportation* , 20 (1), 10-15.

Yang, Y. B., & Hung, H. H. (1997). A parametric study of wave barriers for reduction of train-induced vibrations. *International Journal for Numerical Methods in Engineering* , 40 (20), 3729-3747.

Yang, Y. B., & Hung, H. H. (2008). Soil vibrations caused by underground moving trains. *Journal of geotechnical and geoenvironmental engineering* , 134 (11), 1633-1644.

Zou, J. H., Feng, W. X., & Jiang, H. B. (2011). Dynamic response of an embedded railway track subjected to a moving load. *Journal of Vibroengineering* , 13 (3), 544-551.

CONCLUSIONS

Next, the most relevant conclusions of this PhD Thesis are introduced, which deal with the behavior of the different modeling of the physical phenomenon under study.

The uniform treatment of different types of loads presented in chapter 1 of this Thesis provides a great versatility to the analytical models concerned, due to almost all types of loads can be expressed as a harmonic function defined by a characteristic magnitude and a particular angular frequency.

The implementation of the analytical and numerical models throughout this Thesis, allows emphasizing the strengths and weaknesses of each one. Thus, the study of wave barriers introduced is only possible with a numerical model that considers the phenomenon of vibrations propagation through the ground. Instead, the study of rail corrugation and wheel flats can be carried out as with a numerical model (this has been presented in Chapter 3 of the Thesis) as with an analytical model, using the uniform treatment of loads exposed in the first conclusion.

The frequency range to study is a very limiting aspect if a numerical model is considered, due to it affects to the longitudinal dimension of the model and to the elements size. Thus, a wide range would imply a considerable longitudinal dimension of the model and a minimum dimension of the elements, which would suppose a high computation time. In the studied case proposed in this Thesis, a frequency range from 2 Hz to 50 Hz has been set, knowing that the real range of human disease includes a range from 0.5 Hz to 80 Hz. This limitation does not exist in the analytical models.

The consideration of the train speed involves different complexity depending on the model type. Thus, in case of analytical models, the speed is an input and its consideration is immediate. Nevertheless, in the case of numerical models, due to each one is configured for a specific circulation speed, the models must be readjusted as during the meshing process as during the loads implementation process. In this Thesis, the circulation speed adopted in chapter 2 is 30 km/h. Hence, if it was necessary to study a higher speed, the residence time of each force on each node (loadstep) would have to be decreased.

Furthermore, it would be also necessary to modify the number of substeps for each load step.

APPENDIX 1

This appendix contains three aspects related to the analytical modeling of the physical phenomenon of generation and transmission of vibrations, contained in chapter 1 of the Doctoral Thesis.

Firstly, the Inverse Fourier Transform development referenced in chapter 1 of the Thesis is outlined; then, several parameters that have been used in the modeling and partially shown at the end of chapter 1 of the Doctoral Thesis are collected, and finally, two spectra obtained as intermediate or final results of the mathematical process are shown.

1. Inverse Fourier Transform

Given the complexity of solving the problem in space and time domain, it is transformed to the wavenumber and frequency domain by the Fourier Transform:

$$\tilde{f}(k, \omega) = \int_{-\infty}^{+\infty} \int_{-\infty}^{+\infty} f(x, t) e^{i(\omega t - kx)} dx dt \quad (1)$$

Once the problem has been solved and displacements have been obtained in each one of the layers of the domain, these are returned to the space and time domain by the Inverse Fourier Transform:

$$f(x, t) = \frac{1}{4\pi^2} \int_{-\infty}^{+\infty} \int_{-\infty}^{+\infty} \tilde{f}(k, \omega) e^{i(kx - \omega t)} d\omega dk \quad (2)$$

Moreover, expressing the Inverse Fourier Transform based on cosines and performing some calculations (see Koziol (2008)) the double integral can be transformed as follows:

$$v_j(0, t) = \frac{F_i}{4\pi} \int_{-\infty}^{+\infty} [\tilde{v}_j(k, kV - \Omega) e^{-i(kV - \Omega)t} + \tilde{v}_j(k, kV + \Omega) e^{-i(kV + \Omega)t}] dk \quad (3)$$

Where Ω is the frequency considered for each of the harmonics in which the dynamic forces have been decomposed and V is the train speed.

Discretizing the variable k , the above integral can be converted into a sum as follows:

$$v_j(0,0,t) = \frac{P_i}{4VT} \sum_{n=1}^N [\tilde{v}_j(k(n), k(n)V - \Omega)e^{-i(k(n)V - \Omega)t} + \tilde{v}_j(k(n), k(n)V + \Omega)e^{-i(k(n)V + \Omega)t}] \quad (4)$$

The discretization of k requires enough resolution to avoid the loss of relevant information of the Fourier spectrum. The values of k should be ranged between 10^{-3} and 300 m^{-1} because of small values can generate singularities in the problem when it is calculated with commercial software, whereas if the values of the wave number are too large, the solution can present convergence problems.

2. Parameters

2.1. Track Modeling

The mechanical properties adopted for each layer of the model are:

Layer	E (Pa)	ν	ρ (kg/m ³)
Rail pad	$3,4125 \cdot 10^{10}$	0,3	7850
Sleeper	$3,0625 \cdot 10^8$	0,35	690
Ballast	$2 \cdot 10^7$ Pa	0,2	1900
Upper layer	$5 \cdot 10^6$ Pa	0,3	1800
Bottom layer	$2 \cdot 10^9$	0,25	1830

Table 1. Mechanical properties

2.2. Ground stiffness

The track stiffness has been calculated as follows:

$$\frac{1}{k_1} = \frac{1}{k_{W-R \text{ contact}}} + \frac{1}{k_{\text{rail}}} + \frac{1}{k_{\text{railpad}}} + \frac{1}{k_{\text{sleeper}}} + \frac{1}{k_{\text{ballast}}} + \frac{1}{k_{\text{ground}}} \quad (5)$$

Assuming Hertzian contact, the wheel-rail contact stiffness can be obtained as follows:

$$K_{W-R \text{ contact}} = \frac{4E'}{3} \sqrt{\frac{2}{\alpha \xi^3}} \quad (6)$$

Where:

α is the effective radius of curvature

ξ is a dimensionless parameter which depends on the inclination existing between the plane which contains the main curvature of the rail and the plane which contains the main curvature of the wheel

E' is the coefficient that defines the elastic behavior of the material.

The stiffness values of all elements are shown in table 2.

2.3. Layers' stiffness

The table that contains the stiffness values of each layer is shown below:

Element	Value (kN/m)
Wheel-rail contact	$1.675 \cdot 10^8$
Rail	$7.35 \cdot 10^6$
Rail pad	$6.56 \cdot 10^5$
Sleeper	$6.5 \cdot 10^5$
Ballast	$2 \cdot 10^5$
Ground	$1 \cdot 10^5$

Table 2. Layers stiffness

3. Time history and spectrum of irregularities and forces

3.1. Time history (or rail profile) and spectrum (in third octave) of the irregularities.

Below, in Figure 1 (left), the rail profile and its irregularities are shown. Moreover, in Figure 1 (right), the spectrum of the mentioned irregularities in third octave is shown. The model heeds the effect of these irregularities by the introduction of dynamic overloads.

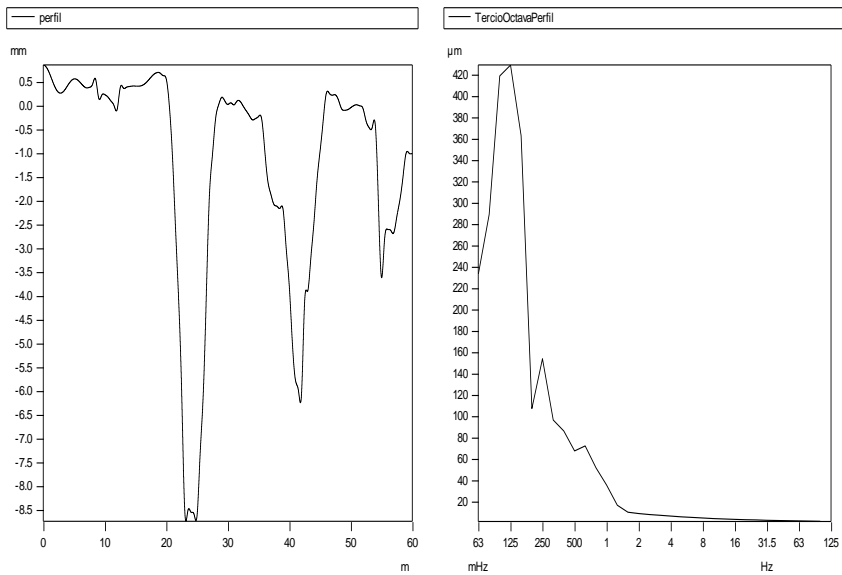


Fig. 1. Profile (left) and spectrum (right) of irregularities

3.2. Time history and spectrum (in third octave) of the forces.

The forces that excite the model in time domain (left) and its spectrum in third octave (right) are shown below in figure 2.

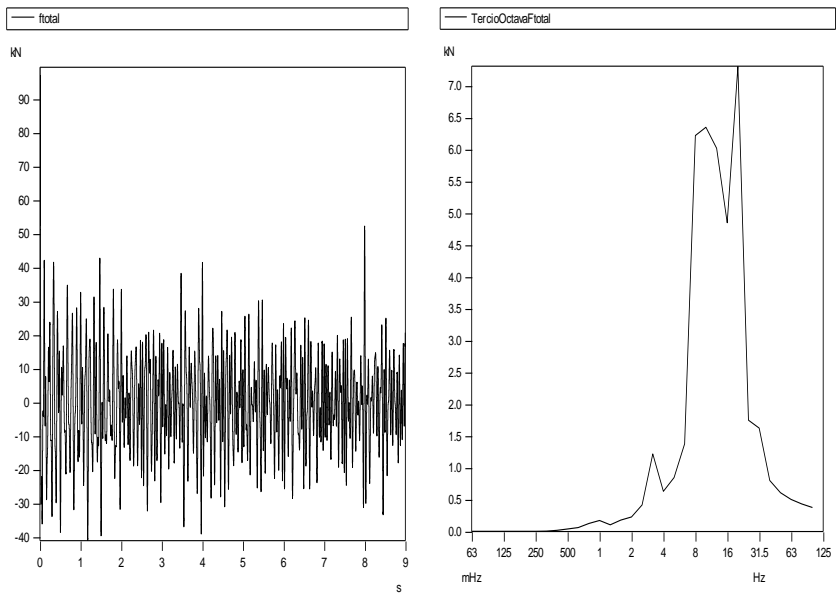


Fig. 2. Excitation forces (left) and its spectrum (right)

APPENDIX 2

This appendix contains three aspects related to the modeling of different types of trenches, which are considered as attenuator elements of the propagation of railway vibrations.

Thus, the first reflection alludes to the sheet pile figure. Then, two vibration accelerations spectra with and without trenches are presented and, finally, the attenuation of vibration amplitude versus distance is represented.

1. Acceleration spectra with and without different wave barriers

The accelerograms obtained from the numerical models have been shown in time domain until this moment. These accelerograms can be represented in frequency domain by the Fourier Transform (FFT) using the commercial software Mathematica, which allows observing the dominant frequencies.

The spectra of the data calculated in 2 points with the model of an open trench of 2 meters depth are shown below. The first one is located at 0.3 meters from the rail (before the trench) and the other one is located at 2.5 meters from the rail, once the wave has traversed the trench.

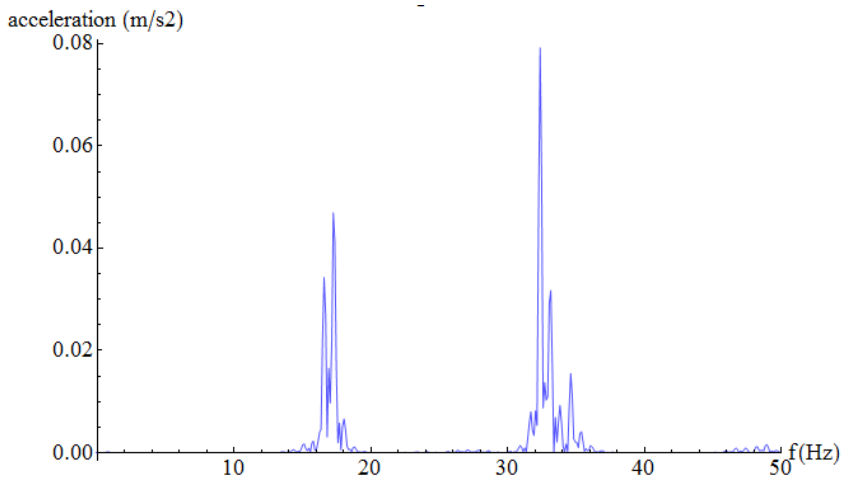


Fig. 1. Acceleration spectrum at 0.3 meters from the rail

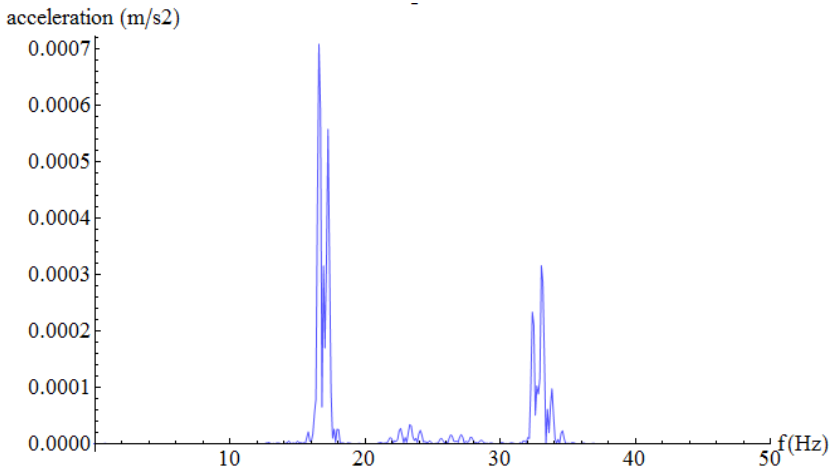


Fig. 2. Acceleration spectrum at 2.5 meters from the rail

Note that the maximum frequency is set around 16 Hz, which is due to the discrete load advance throughout the rail. This value depends on the distance between two consecutive nodes and on the load speed, and is determined by the following expression:

$$f_{ind} = \frac{\textit{Load speed}}{\textit{Distance between nodes}} = 16,67 \text{ Hz} \quad (1)$$

Where f_{ind} is the frequency induced by the discrete load step. This frequency is fictitious and intrinsic to the resolution method employed. Therefore, its presence is inevitable and its value will be higher or lower depending on the parameters mentioned above.

2. Amplitudes attenuation versus distance

The following figures show an example of the maximum peaks attenuation versus the distance to the external side of the elastomer. These charts are calculated for two different types of trenches, an in-filled trench and an open trench. Specifically, it is represented the open trench fixed with sheet piles and the concrete in-filled trench. In both cases, the depth is set to two meters.

It is observed higher values for the case of an open trench with sheet piling in the stretch between rail and trench. Zero slope is observed, even a slight increase as we approach to the trench, due to the rebound of waves on the walls of the trench. But once the trench is traversed, the vibrations are close to zero. In contrast, for the trench filled with concrete, the values near the rail are much lower than in the previous case, even more than 50%, with a progressive attenuation. However, once the trench is exceeded, the values, although being small, are greater than in the case of an open trench.

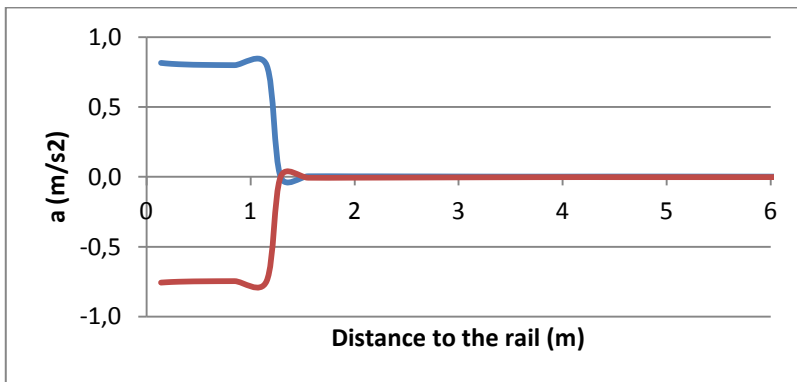


Fig. 3. Attenuation with a sheet piling trench

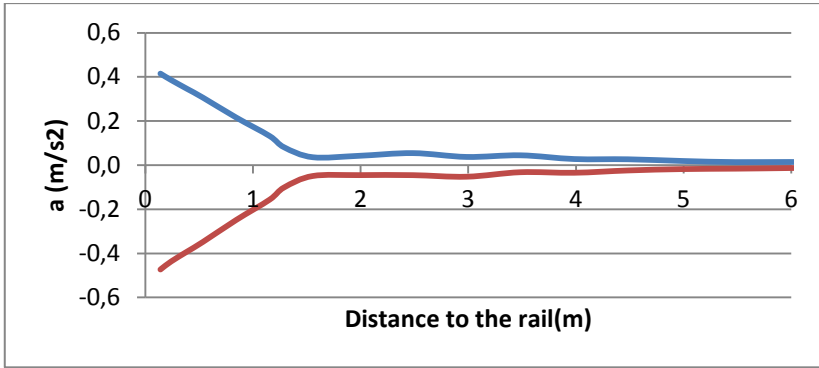


Fig. 4. Attenuation with a trench filled with concrete

3. The figure of a sheet pile

3.1 Definition

Sheet piles are thin structures that, affixed to its bottom, provide the necessary support to the natural ground when its natural mechanical properties cannot ensure the structural stability.

These elements are made of different materials, among which steel, wood and concrete stand out. The choice of the material and construction method varies depending on the necessities in each case.

3.2 Relation with the Thesis

The main problem existing during the construction of an open trench is the structural stability of the excavation walls. The possible existence of low cohesive materials, coupled with the necessity to provide a durable structure in time, makes absolutely necessary the use of a structure that provides support.

This paper applies the theoretical development of finite element model to a real case such as the attenuation of railway vibrations by wave barriers. For this reason, not only a theoretical solution is performed, but also, from knowledge of the art, a feasible solution that allows implementing an open trench in both model and reality is provided.

3.3 Justification

The influence of the sheet piles material on the vibrations propagation has not been considered. Its low thickness and its contiguity to the free surface make irrelevant the internal damping (which is determined by its mechanical properties) that may provide compared to the rest of the parameters studied (depth and width of trench).

To take into account the effect that the sheet pile has on the propagation of vibrations, it has been restricted the horizontal movement of all nodes located on the walls of the open trench in the finite element model. Thus, the boundary conditions provided by the sheet piles are simulated, no being necessary to include this element in the model.

APPENDIX 3

This appendix contains three aspects related to the chapter 3 of this Doctoral Thesis. The first one is aimed to explain the concept of "residence time" used in the modeling of wheel flat phenomenon; the second shows some spectra obtained in the mathematical development of the problem and, finally, the third point shows a correction of the modeling of the dynamic forces generated by both rail corrugations shown in the cited chapter.

1. Residence time

It is considered that a wheel flat has two corners. When the first corner contacts the rail, the contact area is reduced because of it is a corner. By reducing the contact area, the force transmitted to the rail increases and appears a first peak in a graph of transmitted force vs. time. From this point, the wheel begins to swing on the first corner. When the second corner of the wheel flat contacts the rail, a second peak in the graph force transmitted vs. time appears. The magnitude of this peak will be greater because of it is an impact.

Due to the wheel flat, a new frequency generated by the repetitive impact will appear. This frequency is calculated as the inverse of the time interval between impacts, which matches with the quotient of the train speed and the wheel perimeter. In addition, another frequency associated with phenomenon due to the time elapsed between the first and second peak appears, which is the inverse of the so called "residence time".

2. Spectra representation

The accelerations obtained from numerical models until this point are represented in time domain. These accelerations may also be represented in frequency domain by discrete Fourier transform in order to identify the dominant frequencies. To do so, the algorithm for calculation of the fast Fourier transform (FFT) implemented in the commercial software Mathematica is used.

On this occasion, it has been calculated the spectra accelerations resulting from the wheel flat obtained in points located at 0.3 and 3 m from the rail. These spectra are shown in Figures (1) - (2). The distribution of excitation frequencies shows again the discrete passage of the quasi-static load. Moreover, other peaks appear as consequence of the wheel flats. This excitation shows a cadence corresponding to the wheel perimeter (1.5 m). That is to say that the excitement caused by the wheel passage will be added to the quasi-static load every 3 nodes.

The frequency associated with the dynamic load due to the wheel flat is 5.56 Hz (see eq. (7) paper 3). This is just the elemental gap observed in the spectrum respect to the loads caused by the quasi-static load passage (16.67 Hz). Therefore, in the range studied will appear impulsive excitations at frequencies of 16.67 Hz; 11.11 Hz; 22.23 Hz and so on.

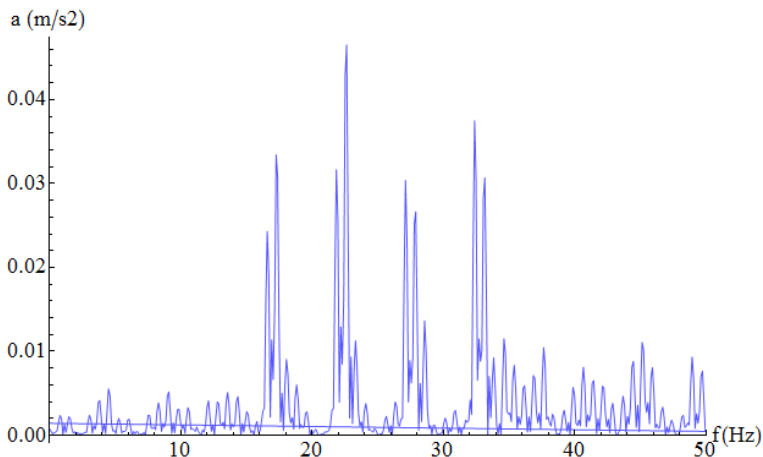


Fig. 1. Accelerations in frequency domain obtained at 0.3 meters from the rail

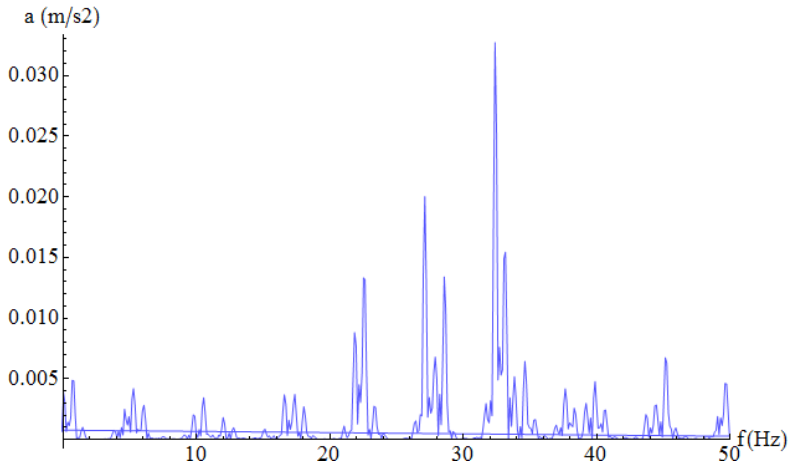


Fig. 2. Accelerations in frequency domain obtained at 3 meters from the rail

Figures (3) and (4) show, respectively, the accelerations spectra generated by a rail corrugation of 1 meter wavelength and 0.5 meters wavelength. Since the loads associated with the peaks and valleys of the corrugation are introduced, at any time, overlapped to the quasi-static load, the frequencies at which excitation is registered are related to the passage of the load through the nodes (as happened in the model of waves barrier studied in paper 2).

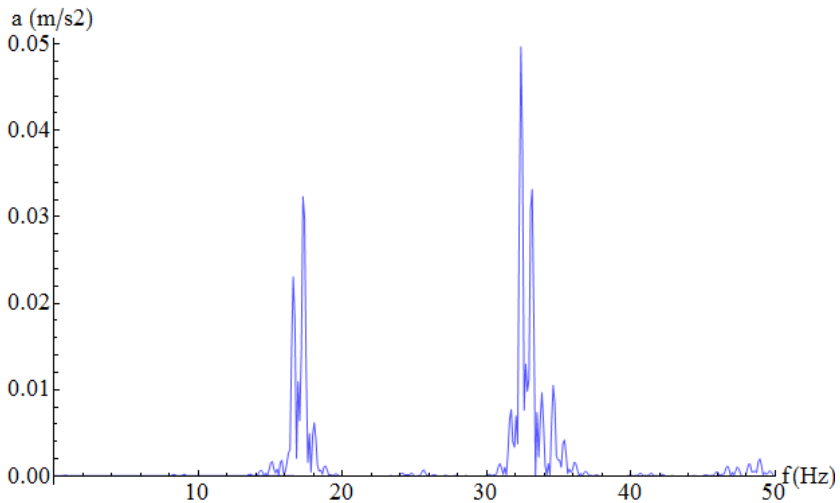


Fig. 3. Accelerations in frequency domain obtained for a 1 meter wavelength

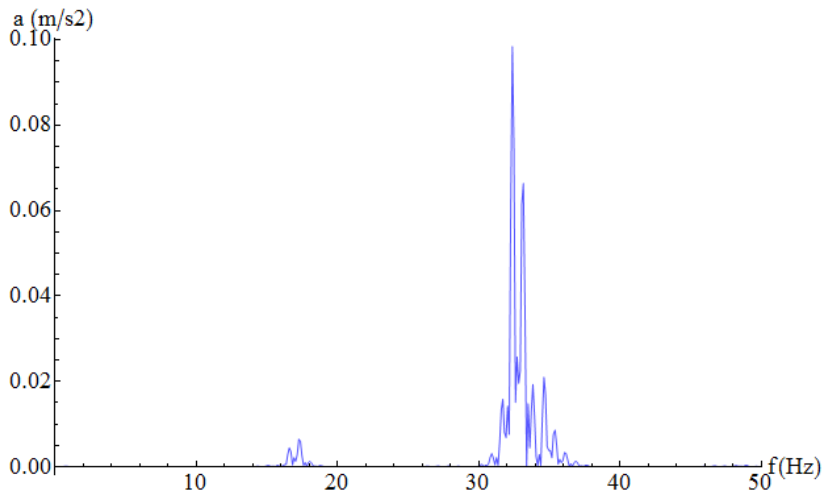


Fig. 4. Accelerations in frequency domain obtained for a 0.5 meters wavelength

3. Dynamic forces due to rail corrugation

In chapter 3 of the Thesis, two cases of rail corrugation are shown. Both are characterized by an amplitude of 0.0005 meters and in both cases it is assumed that the railway vehicle is circulating at a speed of 30 km / h. The difference between them lies in the value of the wavelength: a wavelength of 1 meter is set in the first case and 0.5 meters is set in the second case.

Any track or vehicle defect generates a dynamic overload (defined by its magnitude and frequency) that must be taken into account during the loads application to the model. The calculation of this overload has been conducted with the model of quarter car (shown in figure 5 of chapter 3 of the Thesis).

The figure 6 of chapter 3 of the Thesis aims to represent the dynamic overload in the first case studied (corrugation wavelength of 1 meter, amplitude of 0.0005 meters and 30 km/h speed). The figure must be replaced by the following graphic:

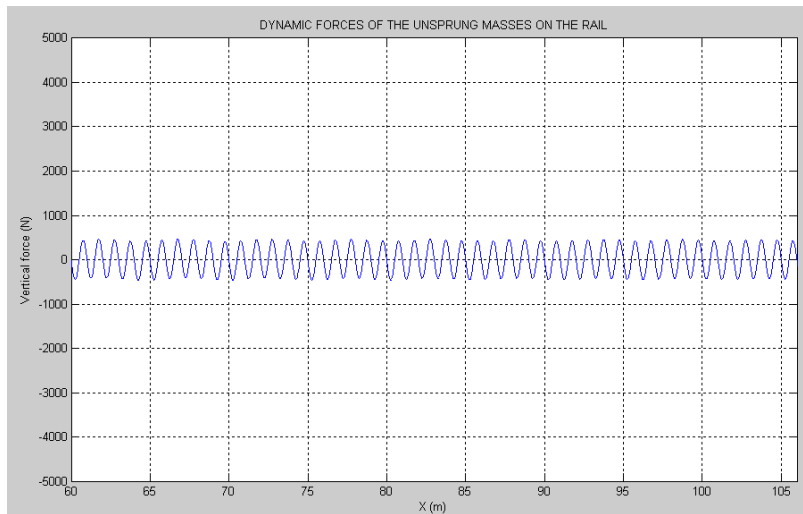


Fig. 5. Dynamic forces on the rail due to a rail corrugation of $\lambda=1\text{m}$

Analogously, figure 7 of chapter 3 of the Thesis aims to represent the dynamic overload in the second case studied (corrugation wavelength

of 0.5 meters, amplitude of 0.0005 meters and 30 km/h speed). The figure must be replaced by the following graphic:

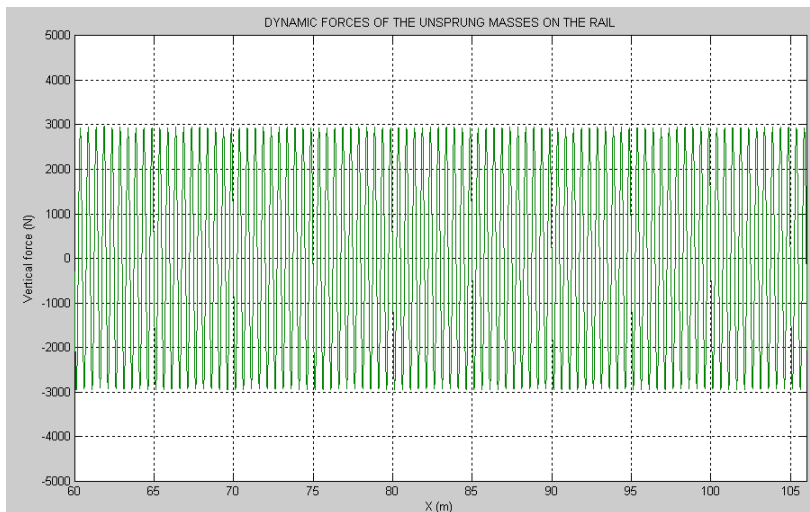


Fig. 6. Dynamic forces on the rail due to a rail corrugation of $\lambda=0.5\text{m}$.

At this point it is necessary to reflect on the influence of the wavelength and amplitude of rail corrugation as well as the train speed on the numerical value and frequency of the dynamic overloads obtained.

Thus, for fixed amplitude and constant speed, the decreasing of the wavelength involves a considerable increase in the value of the dynamic overload and an increase of the excitation frequency (which is in accordance with the wavelength of the defect and the train speed).

Given a particular rail corrugation (defined by its wavelength and amplitude), as the train speed grows, the frequency and the numerical value of the dynamic overload are also increased.

Finally, if the amplitude of the rail corrugation is modified, keeping constant the wavelength and speed, a variation of the same magnitude in the value of the dynamic overload takes place. However,

the frequency of dynamic overload is not affected by changes in the amplitude of the defect.

In short, the numerical value of the exciting force increases with the growth of the circulation speed, with the growth of the amplitude of the corrugation and with the decrease of the wavelength of the defect. In contrast, the frequency of the exciting force increases with the growth of the circulation speed and with the decrease of the wavelength of the defect; not being affected by its amplitude.

Since the dynamic overloads generated by the rail corrugations studied have been modified, each of the new situations must be simulated again. The final load that must be applied to the model is the composition of the static load and the dynamic overload due to each case. The accelerograms calculated by the model, for both studied cases and at different distances from the rail, are:

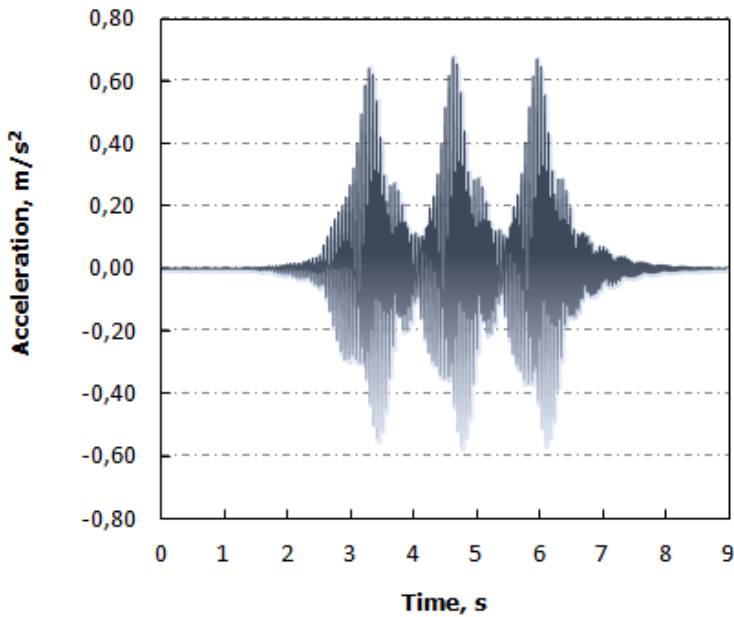


Fig. 7. Accelerogram calculated in a track with no defects (black) and in a track with rail corrugation of $\lambda=1\text{m}$ (blue) at 0.3 meters from the external side of the rail.

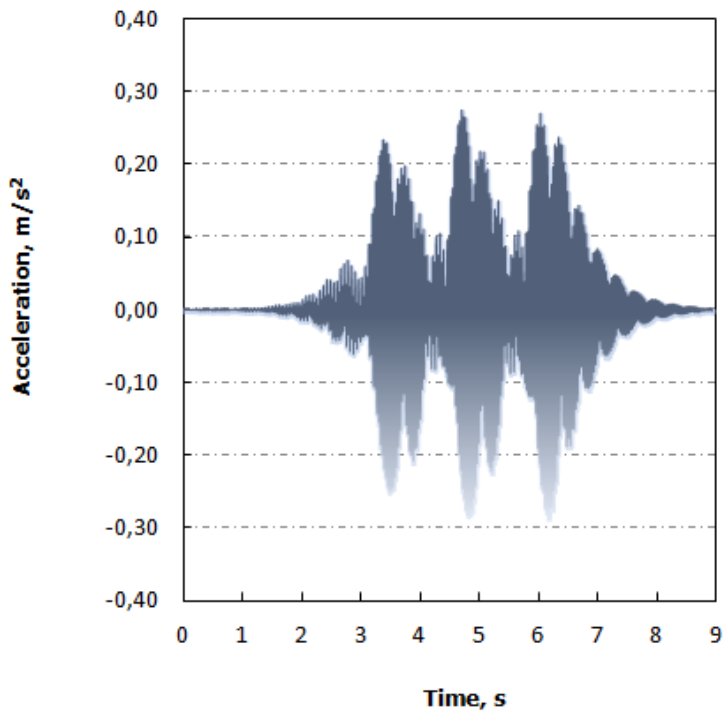


Fig. 8. Accelerogram calculated in a track with no defects (black) and in a track with rail corrugation of $\lambda=1\text{m}$ (blue) at 3 meters from the external side of the rail.

The two figures above have to replace the figure 10 of chapter 3 of the Thesis.

Proceeding similarly with the second case study, the following results are obtained.

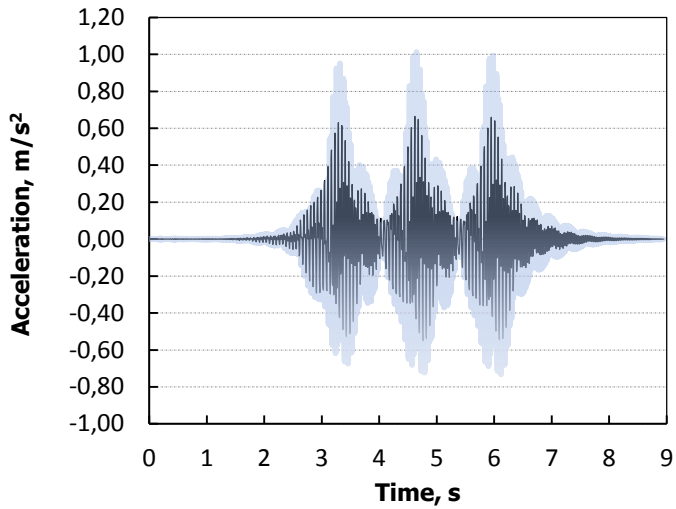


Fig. 9. Accelerogram calculated in a track with no defects (black) and in a track with rail corrugation of $\lambda=0.5\text{m}$ (blue) at 0.3 meters from the external side of the rail.

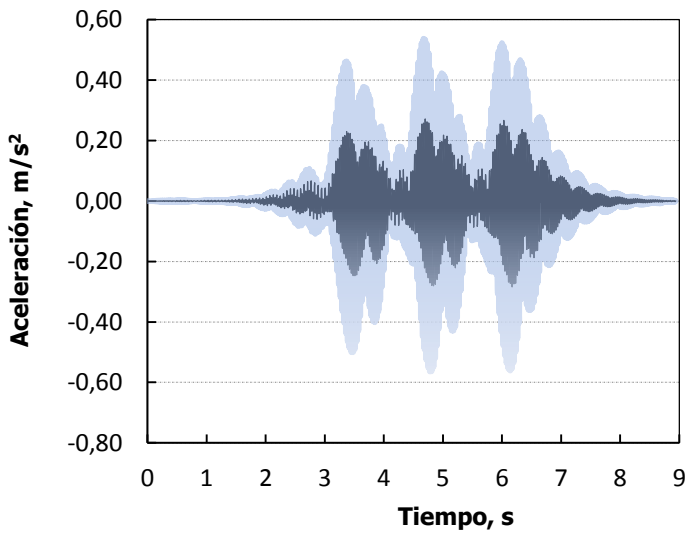


Fig. 10. Accelerogram calculated in a track with no defects (black) and in a track with rail corrugation of $\lambda=0.5\text{m}$ (blue) at 3 meters from the external side of the rail.

Analogously, the two figures above have to replace the figure 11 of chapter 3 of the Thesis.

Note that if the wavelength is 0.5 meters, the accelerations calculated at 0.3 meters from the rail (maximum peak = 1 m/s^2) are higher than those obtained for a wavelength of 1 meter (maximum peak = 0.7 m/s^2). In both cases, obviously, the maximum peak accelerations calculated at 3 meters from the rail are lower due to the attenuation capability of ground existing in the vicinities of the track.